SCIENCES FORCE
International Academic Publisher

NEUTROSOPHIC SYSTEMS WITH APPLICATIONS

AN INTERNATIONAL JOURNAL ON INFORMATICS, DECISION SCIENCE, INTELLIGENT SYSTEMS APPLICATIONS

ISSN (ONLINE): 2993-7159
ISSN (PRINT): 2993-7140

VOLUME 16
2024

https://sciencesforce.com
nswa@sciencesforce.com

Neutrosophic Systems with Applications

An International Journal on Informatics, Decision Science, Intelligent Systems Applications

Information for Authors and Subscribers

Neutrosophic Systems with Applications (NSWA) is an international academic journal, published monthly online and on paper by the Sciences Force publisher, Five Greentree Centre, 525 Route 73 North, STE 104 Marlton, New Jersey 08053, United States, that has been created for publications of advanced studies in neutrosophy, neutrosophic set, neutrosophic logic, neutrosophic probability, neutrosophic statistics that started in 1995 and their applications in any field, such as Informatics, Decision Science, Computer Science, Intelligent Systems Applications, etc.

The submitted papers should be professional, and in good English, containing a brief review of a problem and obtained results.

Neutrosophy is a new branch of philosophy that studies the origin, nature, and scope of neutralities, as well as their interactions with different ideational spectra.

This theory considers every notion or idea <A> together with its opposite or negation <antiA> and with their spectrum of neutralities <neutA> in between them (i.e., notions or ideas supporting neither <A> nor <antiA>). The <neutA> and <antiA> ideas together are referred to as <nonA>.

Neutrosophy is a generalization of Hegel's dialectics (the last one is based on <A> and <antiA> only). According to this theory, every idea <A> tends to be neutralized and balanced by <antiA> and <nonA> ideas - as a state of equilibrium.

In a classical way <A>, <neutA>, <antiA> are disjointed two by two. But, since in many cases, the borders between notions are vague, imprecise, Sorites, it is possible that <A>, <neutA>, <antiA> (and <nonA> of course) have common parts two by two, or even all three of them as well.

Neutrosophic Set and Logic are generalizations of the fuzzy set and respectively fuzzy logic (especially of intuitionistic fuzzy set and intuitionistic fuzzy logic). In neutrosophic logic, a proposition has a degree of truth (*T*), a degree of indeterminacy (*I*), and a degree of falsity (*F*), where *T, I, F* are standard or non-standard subsets of *]-0, 1+[.*

Neutrosophic Probability is a generalization of the classical probability and imprecise probability.

Neutrosophic Statistics is a generalization of classical statistics.

What distinguishes neutrosophic from other fields is the <neutA>, which means neither <A> nor <antiA>.

<neutA>, which of course depends on <A>, can be indeterminacy, neutrality, tie game, unknown, contradiction, ignorance, imprecision, etc.

All submissions should be designed in MS Word format using our template file on the journal website.

A variety of scientific books in many languages can be downloaded freely from the Digital Library of Science:

To submit a paper, mail the file to the Editor-in-Chief on this email nswa@sciencesforce.com. To order printed issues, contact the Editor-in-Chief on this email nswa@sciencesforce.com.

Journal of Neutrosophic Systems with Applications is also supported by:

University of New Mexico and Zagazig University, Computer Science Department.

This journal is a non-commercial, academic edition. It is printed from private donations.

Publisher's Name: Sciences Force

The home page of the publisher is accessed on. https://sciencesforce.com/

The home page of the journal is accessed on. https://sciencesforce.com/nswa

Publisher's Address: Five Greentree Centre, 525 Route 73 North, STE 104 Marlton, New Jersey 08053.

Tel: +1 (509) 768-2249 Email: nswa@sciencesforce.com

Contents

Neutrosophic Systems with Applications, Vol. 16, 2024
https://doi.org/10.61356/j.nswa.2024.16203

CT Image Segmentation Using Optimization Techniques under Neutrosophic Domain

Doaa El-Shahat [1,*], Nourhan Talal [1], Jun Ye [2,3], and Wen-Hua Cui [3]

[1] Department of Computer Science, Faculty of Computers and Informatics, Zagazig University, Zagazig 44519, Egypt; Emails: doaazidan@zu.edu.eg; N.Talal22@fci.zu.edu.eg.

[2] School of Civil and Environmental Engineering, Ningbo University, Ningbo, Zhejiang, China; yejun1@nbu.edu.cn.

[3] Department of Electrical Engineering and Automation, Shaoxing University, Shaoxing, Zhejiang, China; wenhuacui@usx.edu.cn.

* Correspondence: doaazidan@zu.edu.eg

Abstract: In this paper, we introduce a hybrid technique between optimization algorithms and neutrosophic theory. This new hybridization can deal with uncertainties in brain computed tomography (CT) images in three different memberships very effectively. To prove the real-time application of this theory, a new segmentation method for brain CT medical images is presented. The grayscale medical image suffers from uncertainties and inconsistencies in the gray levels due to their bad luminance. The proposed technique addressed this problem by performing neutrosophic operations on gray levels based on the S membership function.

Keywords: Neutrosophic Set; CT Image Segmentation; Medical Images; Optimization Algorithms.

1. Introduction

The segmentation process in medicine aims to extract the region of interest (ROI) object (organ) from a medical image (2D or 3D). It separates an image into regions according to a given outline, for example, segmenting human tissues or organs in medical applications for border detection, tumor detection/segmentation, and mass detection [1]. Furthermore, computed tomography (CT) medical imaging suffers from different uncertainty problems that affect the process of image segmentation. A CT is a gray-level image with large amounts of noise and a low level of intensity. Additionally, CT has poor edge representation and contrast regions. With so little data and low-quality images. These problems pose a challenge in the segmentation process because they can degrade the efficiency of the whole image processing operation. So, it's important to use methods that can handle and deal with uncertain information within images [2]

The fuzzy set (FS), intuitionistic fuzzy set (IFS), and neutrosophic set (NS) were developed to deal with uncertainties. FS theory was introduced by Zadeh to deal with uncertainty based on the degree of membership [3]. The FS theory is used widely in medical image segmentation. Zhang et al. [4] proposed the Reference-guided Fuzzy Integral GAN (RFI-GAN) generating ultrasound images by combining feature fusion between samples and reference sets. It generalizes feature additivity to non-additivity using fuzzy integral. Two Fuzzy Integral Modules are proposed for the nonlinear fusion of texture and structure features. Another contribution by Zhao et al. [5] presents a BLS surrogate-assisted evolutionary framework for improving time efficiency in clustering-based image segmentation. The BLS-MOEFC algorithm uses two fuzzy clustering objective functions, a BLS surrogate model-assisted multi-objective evolutionary framework, adaptive parameter updating, and a novel fuzzy clustering validity index. Also, Kumar et al. [6] introduced a new CoMHisP framework using a fuzzy support vector machine (SVM) with within-class density information. It extracts image micropatterns and computes the center of mass for each pixel. The framework performs well on a CMT dataset of histopathological images of canine mammary tumors and human breast cancer. It achieves a classification accuracy of 97.25%, outperforming traditional ML and deep FE-VGGNET16-based feature descriptors.

In 1986, Atanassov introduced the IFS, which links each attribute in the universe with membership (M) and non-membership (non-M) degrees [7]. Kumar et al. [8] proposed an optimization problem for the IFCM with spatial neighborhood information (IFCMSNI) method, incorporating intuitionistic fuzzy set theory and spatial regularization to handle noise in medical images. The method uses IFS and Sugeno's negation function. Also, Namburu et al. [9] proposed a simplified clustering method for melanoma detection, using the triangular membership function (TMF) to identify initial regions and intuitionistic fuzzy c-means clustering, achieving an average accuracy of 90%. Dahiya and Anjana Gosain [10] introduced a novel Type-II intuitionistic fuzzy C means clustering algorithm, combining Type-II membership with a hesitation degree. This algorithm offers advantages such as clear cluster definition, robustness to noise and outliers, and improved centroids' desired position. Compared to other fuzzy clustering algorithms, it outperforms others in accurately identifying lump shape and size in mammograms. The algorithm reduces the average error by 84% on synthetic data sets.

The segmentation methods goal under the FS, and IFS environment is to deal with the uncertainties within an image, but they suffer from some problems such as:

- The segmentation approaches under the FS environment handle uncertainty by taking into consideration only the membership degree for image pixel values between$[0,1]$.
- The segmentation approaches under the FS environment handle uncertainty by taking into consideration only a hesitant degree in conditions of 'Membership' and "Non-Membership" degrees of image pixel values.

Smarandache [11] proposed NS to associate each element with a {truth membership, Indeterminacy membership, and falsity membership} function independently. The NS has values ranging $]^{-}0,1^{+}[$on real standard or non-standard subsets. Many applications can deal with the interval $[0,1]$ because dealing with $]^{-}0,1^{+}[$ in real situations is difficult [12].

On the other hand, a variety of segmentation approaches have been developed to address CT image segmentation, ranging from conventional methods to swarm intelligence techniques and metaheuristics. Anter et al. [13] proposed a dynamic approach to improve the fuzzy c-means clustering algorithm for automatic localization and segmentation of liver and hepatic lesions from CT scans. The approach uses fast-FCM, chaos theory, and bio-inspired ant lion optimizer (ALO) to determine optimal cluster centroids. Another contribution presented a novel multi-disease diagnosis model using chest X-ray images using deep learning approaches. The model uses standard datasets, pre-processing, segmentation, and classification using Optimized DeepLabv3, optimized by the Mutation Rate-based Lion Algorithm (MR-LA). The model improves sensitivity, precision, and specificity, achieving higher classification and detection accuracy. The recommended method outperforms other models in relative analysis [14]. Chouksey et al. [15] investigated the effectiveness of antlion optimization (ALO) and multiverse optimization (MVO), two nature-inspired algorithms, in detecting tumors in medical images. ALO mimics antlion hunting behavior, while MVO is based on multiverse theory. The proposed algorithm outperforms other evolutionary algorithms and is faster than MVO. The results are analyzed using a Wilcoxon test.

The previous studies have outlined some challenges in CT brain segmentation:

- The segmentation technique is complicated by bias areas and inconsistent borders present in CT images.
- Unfortunately, several factors make the segmentation of CT images difficult, including the patient's condition, and operator error.
- The increasing dimension of membership functions may pose challenges for high precision in addressing uncertainty.

These problems highlight the critical need for a more thorough method in medical image segmentation to effectively handle fuzziness and uncertainty in CT brain images. This study presented a segmentation strategy based on optimization techniques under the NS domain. A comparison between Differential Evolution (DE), Spider Wasp Optimization (SWO), Grey Wolf Optimizer (GWO), Particle Swarm Optimization (PSO), and Whale Optimization Algorithm (WOA) optimization algorithm under the NS domain was implemented.

Consequently, the following are this paper's main contributions:

- Propose a segmentation approach based on NS that can deal with uncertainty by presenting a degree of indeterminacy.
- Compare five optimization algorithms under the NS domain.
- The NS image is obtained from the image guided by a DE, SWO, GWO, PSO, and WOA for optimized clustering for segmenting the medical images with reduced time consumption and efficient accuracy.

The remainder of the paper is divided as follows. Section 2 provides the background needed for this study. Section 3 presents preliminaries for neutrosophic theory and optimization algorithms. Section 4 presents the steps of the proposed approach. Section 5 presents experimental results. Section 6 illustrates the conclusion and future directions of this proposal.

2. Related Work

Many studies aim to integrate NS with optimization and metaheuristics methods. Palanisamy et al. [16] proposed a method using NS combined with fuzzy c-means clustering (FCM) and modified particle swarm optimization (PSO) for brain tumor segmentation, achieving superior sensitivity, specificity, Jaccard, and dice values compared to FCM alone and FCM with NS. Ashour et al. [17] introduced a skin lesion detection method called optimized neutrosophic k-means (ONKM), based on genetic algorithms. The method optimizes the neutrosophic set operation to reduce indeterminacy in dermoscopy images. The Jaccard index is used as the fitness function. The ONKM method is applied to segment dermoscopy images, and its performance is evaluated using metrics like Dice coefficient, specificity, sensitivity, and accuracy. The ONKM method outperforms k-means and y-k-means methods in accuracy.

Another contribution by Anter et al. [18] proposed a segmentation approach for abdominal CT liver tumors using neutrosophic sets, PSO, and fast fuzzy C-mean algorithm (FFCM). The method involves removing intensity values and high frequencies, transforming the image to the NS domain, optimizing FFCM using PSO, and clustering the livers using PSOFCM. The results showed neutrosophic sets offer accurate, less time-consuming, and noise-sensitive segmentation on non-uniform CT images.

Sayed et al. [19] presented an automatic mitosis detection approach for histopathology slide imaging using NS and moth-flame optimization (MFO). The approach involves two phases: candidate extraction and classification. The Gaussian filter is applied to the image, and morphological operations are applied to enhance it. The best features are selected using the meta-heuristic MFO algorithm. The approach is tested on a benchmark dataset of 50 histopathological images, including breast pathology slides. The results show the MFO feature selection algorithm maximizes classification performance, with high accuracy, recall, precision, and f-score.

Hanbay and Talu [20] introduces a novel SAR image segmentation algorithm based on the neutrosophic set and an improved artificial bee colony (I-ABC) algorithm. The algorithm uses threshold value estimation to search for a proper value in grayscale intervals. The I-ABC optimization algorithm is used to find the optimal threshold value. The paper contributes to SAR image segmentation by introducing a hybrid model with two feature extraction methods and demonstrating its effectiveness in real SAR images.

Another study introduced a new methodology for license plate (LP) recognition using image processing algorithms and an optimized neutrosophic set (NS) based on genetic algorithm (GA). The methodology uses edge detection, morphological operations, and a new methodology using GA to optimize NS operations. The k-means clustering algorithm and connected components labeling analysis (CCLA) algorithm are used to segment characters. The proposed methodology is suitable for both Arabic-Egyptian and English LP, achieving high recognition accuracy in high-resolution Egyptian and low-resolution-corrupted English. The system also achieves 92.5% accuracy in image disturbances [21].

From previous studies, we conclude that

- No studies are comparing different optimization techniques under the neutrosophic domain.
- Few studies investigate the results of hybrid NS and optimization in medical images.

3. Neutrosophic Sets

The NS can deal with uncertainty and fuzziness within any data by describing the attribute with three components such as the True (T), Indeterminate(I), False (F) subsets. The CT images are mapped into the NS domain. Where a pixel P in the image is defined as P(T, I, F) where t, i, and f are the true, indeterminate, and false in the set, respectively, as t diverges in T, i diverges in I, and f diverges in F. Then, the pixel P(x, y)in the image space is transformed into the NS space PNS (x, y) = {T(x, y), I(x, y), F(x, y)}. T(x, y), I(x, y) and F(x, y)are the corresponding probabilities which are given by [27]:

$$T(x,y) = \frac{\overline{g}(x,y) - \overline{g}_{min}}{\overline{g}_{max} - \overline{g}_{min}} \tag{1}$$

$$\overline{g}\,(x,y) = \left(\frac{1}{w \times w}\right) \sum_{m=a-\frac{w}{2}}^{a+\frac{w}{2}} \sum_{m=i-\frac{w}{2}}^{i+\frac{w}{2}} g(m,n) \tag{2}$$

$$F(x,y) = 1 - T(x,y) \tag{3}$$

$$\delta(x,y) = abs(g(x,y) - \overline{g}(x,y) \tag{4}$$

$$I(x,y) = \frac{\delta(x,y) - \delta_{min}}{\delta_{max} - \delta_{min}} \tag{5}$$

where the pixels in the window have$\overline{g}\,(x,y)$ local mean, and $\delta(x,y)$ implies the absolute value of difference among intensity $g(x,y)$ and its $\overline{g}\,(x,y)$.

The entropy is computed for a grayscale image to evaluate the distribution of gray levels. When the intensities have a uniform distribution and equal probability, maximum entropy occurs. When intensities have nonuniform distribution and varying probabilities, little entropy arises. The totality of the T, I, and F entropies is referred to as the entropy in the neutrosophic image, and it is used to calculate the element distribution in the NS domain [27]. The entropy can be donated by the following

$$Entropy_{NS} = Entropy_T + Entropy_I + Entropy_F \tag{6}$$

$$Entropy_T = -\sum_{j=min\{T\}}^{max\{T\}} P_T\,(K)\ \ln P_T(k) \tag{7}$$

$$Entropy_I = -\sum_{j=min\{I\}}^{max\{I\}} P_I\,(K)\ \ln P_I(k) \tag{8}$$

$$Entropy_F = -\sum_{j=min\{F\}}^{max\{F\}} P_F(K) \ \ln P_F(k) \quad (9)$$

where the entropies are $Entropy_T$, $Entropy_I$, and $Entropy_F$ for T, I, and F, respectively. Furthermore, the probabilities of the element k are $P_T(K), P_I(K), and\ P_F(K)$ in T, I, and F, respectively.

4. Proposed Algorithm

The neutrosophic set theory allows us to handle uncertainties, imprecision, and vagueness in image data. By combining optimization algorithms with neutrosophic image segmentation, we can improve the adaptability of the segmentation process to different image types and conditions. Optimization algorithms can also help refine the segmentation process by iteratively adjusting the parameters of some membership functions to maximize the entropy, thereby aiding in segmenting the images more accurately. In this study, we employ the S membership function to generate both T and F domains in NS theory. This function is mathematically defined as follows:

$$T(\overline{g}(x,y),a,b,c) = \begin{cases} 0, & \overline{g}(x,y) \le a \\ \frac{(\overline{g}(x,y)-a)^2}{(b-a)(c-a)}, & a \le \overline{g}(x,y) \le b \\ 1-\frac{(\overline{g}(x,y)-c)^2}{(c-b)(c-a)}, & b \le \overline{g}(x,y) \le c \\ 1, & \overline{g}(x,y) \ge c \end{cases} \quad (10)$$

where a, b, and c are three parameters that need to be accurately estimated to better separate the true and false NS domains. $Entropy_T$ is used as an objective function to be optimized for reaching the near-optimal values for those parameters. To perform this optimization process, the DE algorithm is herein employed due to its high performance and stability for several optimization problems [22].

5. Results and Discussion

This section assesses the performance of the DE algorithm when applied to search for the near-optimal intervals of the S membership function that could accurately segment the true (object) and false (background) NS domains from eight brain tumor MRI images. The MRI images used in our experiments are shown in Table 1. The performance of this algorithm is compared to four metaheuristic algorithms, such as spider wasp optimizer (SWO) [23], grey wolf optimizer (GWO) [24], particle swarm optimization (PSO) [25], and whale optimization algorithm (WOA) [26] in terms of four performance metrics, such as best entropy, worst entropy, average (Avg) entropy, and standard deviation (SD). All algorithms are executed 25 independent times, and those performance metrics are computed under the estimated outcomes and reported in Table 2. Inspecting this table shows that DE is the highest-performing algorithm because it could achieve the best outcomes for all test images. To show those findings more clearly, Figure 1 is presented to compute the average entropy obtained by each algorithm on all test images. From this figure, DE is the best, WOA is the second best, and PSO is the worst algorithm. Table 3 displays the NS domains for three test images obtained by the intervals optimized by DE. Finally, Figure 2 shows the convergence curves of various algorithms on three test images, showing the superiority of DE.

Table 1. Brain tumor MRI images used in this study.

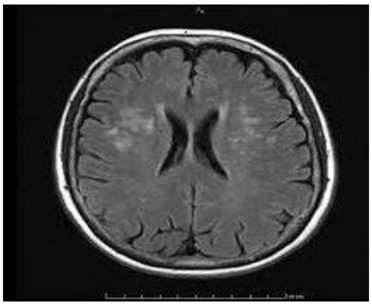

Im1

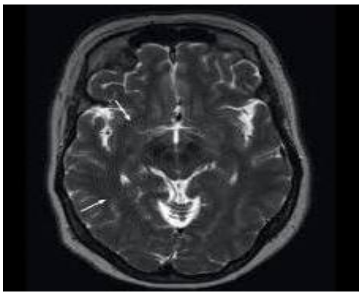

Im2

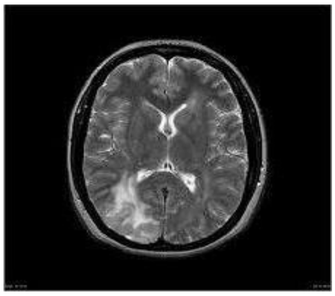

Im3

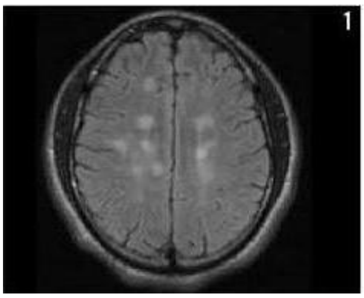

Im4

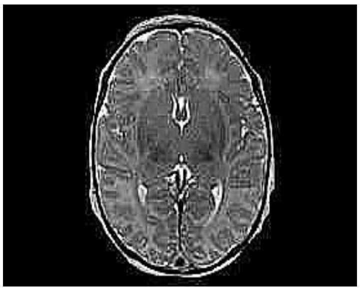

Im5

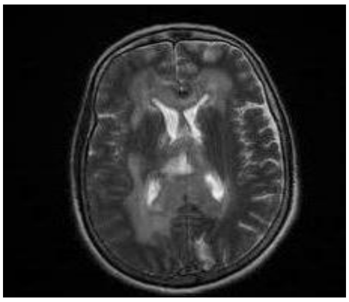

Im6

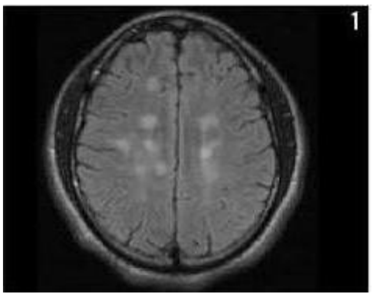

Im7

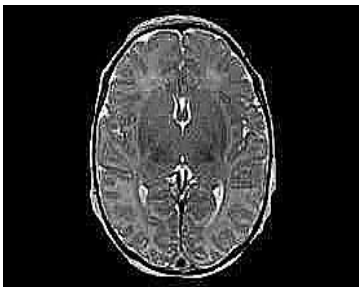

Im8

Table 2. Comparison among algorithms under various performance indicators.

		DE	GWO	SWO	PSO	WOA
Im1	**Worst**	**0.620686**	0.415060	0.444266	0.398349	0.471238
	Avg	**0.677270**	0.574949	0.490833	0.488476	0.627003
	Best	**0.680248**	0.680248	0.539082	0.647501	0.680248
	SD	**0.013318**	0.071869	0.026369	0.050946	0.077810
Im2	**Worst**	**0.642074**	0.493266	0.442960	0.030411	0.457366
	Avg	**0.654727**	0.596860	0.501641	0.462250	0.624038
	Best	**0.661597**	0.661484	0.563887	0.659975	0.661602
	SD	**0.007790**	0.050992	0.033069	0.188853	0.055873
Im3	**Worst**	**0.402475**	0.276877	0.292270	0.295417	0.318098
	Avg	**0.402475**	0.354111	0.342486	0.324730	0.368765
	Best	**0.402475**	0.393584	0.387712	0.384954	0.402475
	SD	**0.000000**	0.033357	0.026493	0.021967	0.031272
Im4	**Worst**	**0.550052**	0.395324	0.432564	0.356642	0.458786
	Avg	**0.593570**	0.508910	0.481033	0.468366	0.560984
	Best	**0.598151**	0.582767	0.565751	0.568650	0.598151
	SD	**0.014121**	0.048259	0.036770	0.042583	0.048622
Im5	**Worst**	**0.369277**	0.300446	0.351128	0.340329	0.350936
	Avg	**0.389828**	0.371943	0.372858	0.366689	0.374335
	Best	**0.391531**	0.391531	0.386141	0.387104	0.391531
	SD	**0.005029**	0.019334	0.010194	0.012415	0.013341
Im6	**Worst**	**0.533367**	0.394530	0.338283	0.037360	0.380744
	Avg	**0.535418**	0.480866	0.432992	0.399207	0.488436
	Best	**0.536576**	0.529927	0.490044	0.528113	0.536576
	SD	**0.001156**	0.042239	0.032867	0.105190	0.060838
Im7	**Worst**	**0.320014**	0.256615	0.244669	0.205086	0.264061
	Avg	**0.336299**	0.292112	0.274215	0.262058	0.300279
	Best	**0.337156**	0.337156	0.308615	0.305846	0.337156
	SD	**0.003833**	0.024531	0.017462	0.025219	0.023771
Im8	**Worst**	**0.589639**	0.428177	0.360343	0.334022	0.481198
	Avg	**0.630500**	0.526989	0.424768	0.403364	0.601137
	Best	**0.635223**	0.635223	0.503232	0.478930	0.635223
	SD	**0.012705**	0.052780	0.040396	0.033492	0.057329

Bold values indicate the best findings.

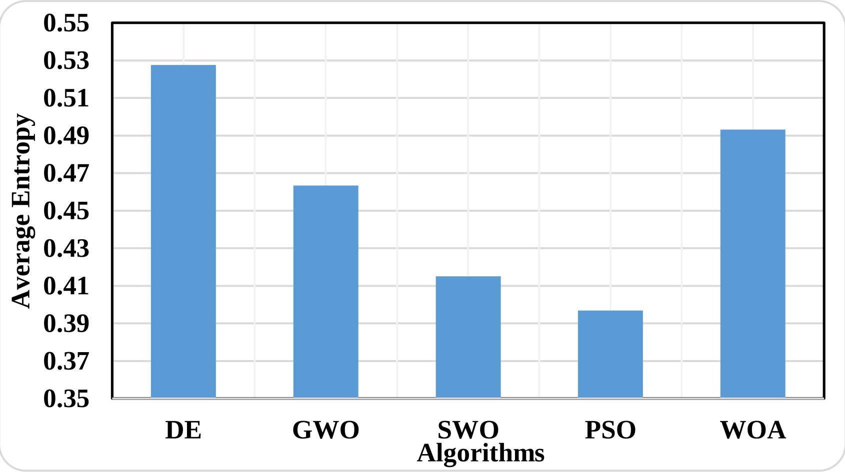

Figure 1. Average entropy obtained by each algorithm on all test images.

Table 3. Depiction of NS domains for four test images obtained after applying the DE algorithm.

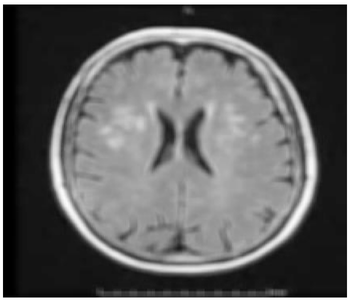
T-domain for im1

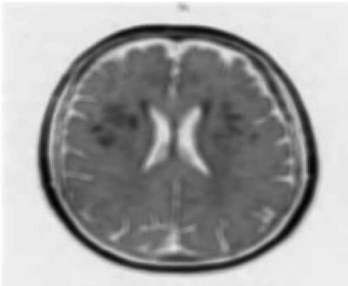
F-domain for im1

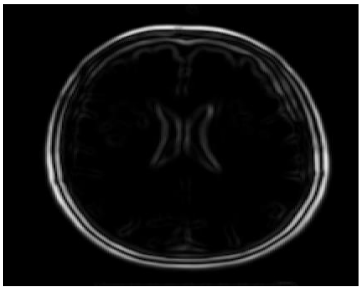
I-domain for im1

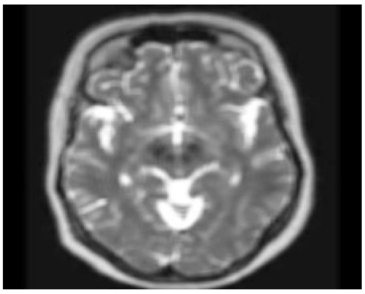
T-domain for im2

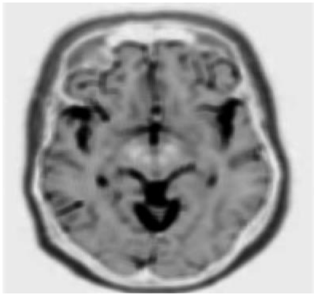
F-domain for im2

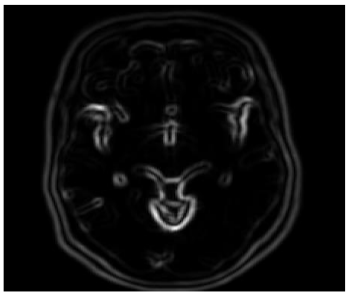
I-domain for im2

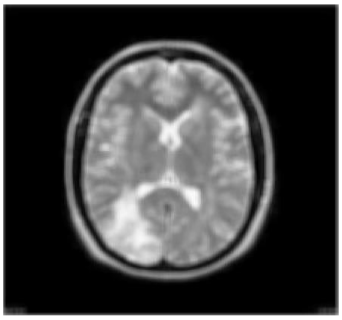
T-domain for im3


F-domain for im3

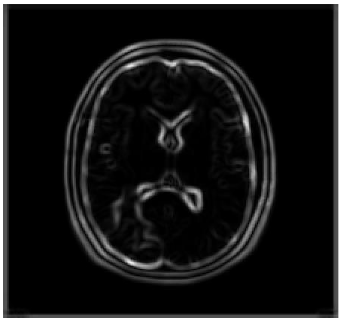
I-domain for im3

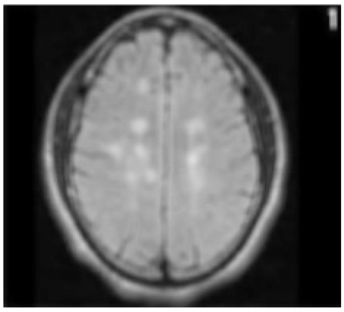
T-domain for im4

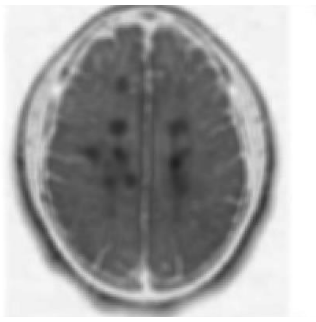
F-domain for im4

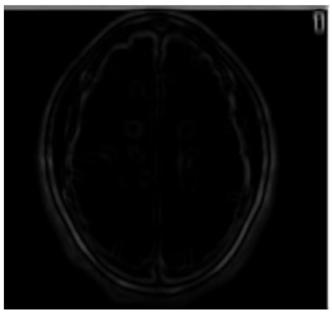
I-domain for im4

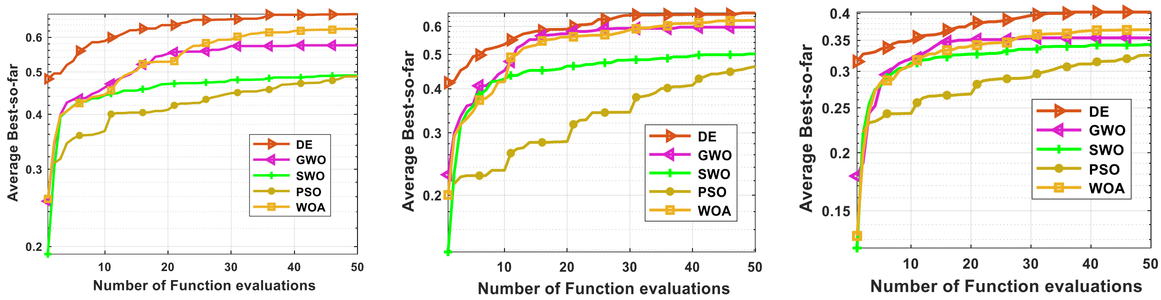

a) Im1 b) Im2 c) Im3

Figure 2. Convergence curves obtained by various algorithms on three test images.

6. Conclusion and Future Work

In this paper, a novel segmentation algorithm based on a Neutrosophic set and optimization techniques has been introduced. The applicability of the image segmentation under the neutrosophic domain was demonstrated on CT images. In our approach, Neutrosophic was obtained to transform the grayscale CT image to the NS domain and measure uncertainties using Neutrosophic entropy. The experiments were presented on 8 CT images.

Acknowledgments

The author is grateful to the editorial and reviewers, as well as the correspondent author, who offered assistance in the form of advice, assessment, and checking during the study period.

Author Contributions

All authors contributed equally to this research.

Data availability

The datasets generated during and/or analyzed during the current study are not publicly available due to the privacy-preserving nature of the data but are available from the corresponding author upon reasonable request.

Funding

This research was not supported by any funding agency or institute.

Conflict of interest

The authors declare that there is no conflict of interest in the research.

References

1. Yan, L., Zhao, H., Lin, Y., & Sun, Y. (2023). Basic Theory of Remote Sensing Digital Image Pixel Processing II: Time–Frequency Fourier Transform from Convolution to Multiplication. In Math Physics Foundation of Advanced Remote Sensing Digital Image Processing (pp. 157-187). Singapore: Springer Nature Singapore. https://doi.org/10.1007/978-981-99-1778-5_6
2. Baumgartner, C. F., Tezcan, K. C., Chaitanya, K., Hötker, A. M., Muehlematter, U. J., Schawkat, K., & Konukoglu, E. (2019). Phiseg: Capturing uncertainty in medical image segmentation. In Medical Image Computing and Computer Assisted Intervention–MICCAI 2019: 22nd International Conference, Shenzhen, China, October 13–17, 2019, Proceedings, Part II 22 (pp. 119-127). Springer International Publishing. https://doi.org/10.1007/978-3-030-32245-8_14
3. Zadeh, L. A. (1978). Fuzzy sets as a basis for a theory of possibility. Fuzzy sets and systems, 1(1), 3-28. https://doi.org/10.1016/0165-0114(78)90029-5
4. Zhang, R., Lu, W., Gao, J., Tian, Y., Wei, X., Wang, C., & Yu, M. (2023). RFI-GAN: A reference-guided fuzzy integral network for ultrasound image augmentation. Information Sciences, 623, 709-728. https://doi.org/10.1016/j.ins.2022.12.026

5. Zhao, F., Liu, Y., Liu, H., & Fan, J. (2022). Broad learning approach to Surrogate-Assisted Multi-Objective evolutionary fuzzy clustering algorithm based on reference points for color image segmentation. Expert Systems with Applications, 200, 117015. https://doi.org/10.1016/j.eswa.2022.117015
6. Kumar, A., Singh, S. K., Saxena, S., Singh, A. K., Shrivastava, S., Lakshmanan, K., & Singh, R. K. (2020). CoMHisP: A novel feature extractor for histopathological image classification based on fuzzy SVM with within-class relative density. IEEE Transactions on Fuzzy Systems, 29(1), 103-117. https://doi.org/10.1109/TFUZZ.2020.2995968
7. Atanassov, K. T. (1999). Intuitionistic fuzzy sets (pp. 1-137). Springer, Physica-Verlag HD.
8. Kumar, D., Agrawal, R. K., & Kirar, J. S. (2019, June). Intuitionistic fuzzy clustering method with spatial information for mri image segmentation. In 2019 IEEE international conference on fuzzy systems (FUZZ-IEEE) (pp. 1-7). IEEE. https://doi.org/10.1109/FUZZ-IEEE.2019.8858865
9. Namburu, A., Mohan, S., Chakkaravarthy, S., & Selvaraj, P. (2023). Skin Cancer Segmentation Based on Triangular Intuitionistic Fuzzy Sets. SN Computer Science, 4(3), 228. https://doi.org/10.1007/s42979-023-01701-8
10. Dahiya, S., & Gosain, A. (2023). A novel type-II intuitionistic fuzzy clustering algorithm for mammograms segmentation. Journal of Ambient Intelligence and Humanized Computing, 14(4), 3793-3808. https://doi.org/10.1007/s12652-022-04022-5
11. Smarandache, F. (2002, January). Preface: an introduction to neutrosophy, neutrosophic logic, neutrosophic net, and neutrosophic probability and statistics. In Proceedings of the first international conference on Neutrosophy, neutrosophic logic, neutrosophic set, neutrosophic probability and statistics (pp. 5-21).
12. Mohan, J., Krishnaveni, V., & Guo, Y. (2013). A new neutrosophic approach of Wiener filtering for MRI denoising. Measurement Science Review, 13(4), 177-186.
13. Anter, A. M., Bhattacharyya, S., & Zhang, Z. (2020). Multi-stage fuzzy swarm intelligence for automatic hepatic lesion segmentation from CT scans. Applied Soft Computing, 96, 106677. https://doi.org/10.1016/j.asoc.2020.106677
14. Balmuri, K. R., Konda, S., kumar Mamidala, K., & Gunda, M. (2024). Automated and reliable detection of multi-diseases on chest X-ray images using optimized ensemble transfer learning. Expert Systems with Applications, 246, 122810. https://doi.org/10.1016/j.eswa.2023.122810
15. Chouksey, M., Jha, R. K., & Sharma, R. (2020). A fast technique for image segmentation based on two meta-heuristic algorithms. Multimedia tools and applications, 79(27), 19075-19127. https://doi.org/10.1007/s11042-019-08138-3
16. Palanisamy, T. S. C. A., Jayaraman, M., Vellingiri, K., & Guo, Y. (2019). Optimization-based neutrosophic set for medical image processing. In Neutrosophic set in medical image analysis (pp. 189-206). Academic Press. https://doi.org/10.1016/B978-0-12-818148-5.00009-6
17. Ashour, A. S., Hawas, A. R., Guo, Y., & Wahba, M. A. (2018). A novel optimized neutrosophic k-means using genetic algorithm for skin lesion detection in dermoscopy images. Signal, Image and Video Processing, 12(7), 1311-1318. https://doi.org/10.1007/s11760-018-1284-y
18. Anter, A. M., & Hassenian, A. E. (2018). Computational intelligence optimization approach based on particle swarm optimizer and neutrosophic set for abdominal CT liver tumor segmentation. Journal of Computational Science, 25, 376-387. https://doi.org/10.1016/j.jocs.2018.01.003
19. Sayed, G. I., & Hassanien, A. E. (2017). Moth-flame swarm optimization with neutrosophic sets for automatic mitosis detection in breast cancer histology images. Applied Intelligence, 47, 397-408. https://doi.org/10.1007/s10489-017-0897-0
20. Hanbay, K., & Talu, M. F. (2014). Segmentation of SAR images using improved artificial bee colony algorithm and neutrosophic set. Applied Soft Computing, 21, 433-443. https://doi.org/10.1016/j.asoc.2014.04.008
21. Yousif, B. B., Ata, M. M., Fawzy, N., & Obaya, M. (2020). Toward an optimized neutrosophic K-means with genetic algorithm for automatic vehicle license plate recognition (ONKM-AVLPR). IEEE Access, 8, 49285-49312. https://doi.org/10.1109/ACCESS.2020.2979185
22. Price, K. V., Storn, R. M., & Lampinen, J. A. (2005). The differential evolution algorithm. Differential evolution: a practical approach to global optimization, 37-134.

23. Abdel-Basset, M., Mohamed, R., Jameel, M., & Abouhawwash, M. (2023). Spider wasp optimizer: A novel meta-heuristic optimization algorithm. Artificial Intelligence Review, 56(10), 11675-11738. https://doi.org/10.1007/s10462-023-10446-y
24. Faris, H., Aljarah, I., Al-Betar, M. A., & Mirjalili, S. (2018). Grey wolf optimizer: a review of recent variants and applications. Neural computing and applications, 30, 413-435. https://doi.org/10.1007/s00521-017-3272-5
25. Aje, O. F., & Josephat, A. A. (2020). The particle swarm optimization (PSO) algorithm application–A review. Global Journal of Engineering and Technology Advances, 3(3), 001-006. https://doi.org/10.30574/gjeta.2020.3.3.0033
26. Mirjalili, S., & Lewis, A. (2016). The whale optimization algorithm. Advances in engineering software, 95, 51-67. https://doi.org/10.1016/j.advengsoft.2016.01.008
27. Guo, Y., Cheng, H. D., & Zhang, Y. (2009). A new neutrosophic approach to image denoising. New Mathematics and Natural Computation, 5(03), 653-662. https://doi.org/10.1142/S1793005709001490

Received: 02 Dec 2023, **Revised:** 01 Mar 2024,

Accepted: 27 Mar 2024, **Available online:** 01 Apr 2024.

Disclaimer/Publisher's Note: The perspectives, opinions, and data shared in all publications are the sole responsibility of the individual authors and contributors, and do not necessarily reflect the views of Sciences Force or the editorial team. Sciences Force and the editorial team disclaim any liability for potential harm to individuals or property resulting from the ideas, methods, instructions, or products referenced in the content.

Neutrosophic Systems with Applications, Vol. 16, 2024
https://doi.org/10.61356/j.nswa.2024.16204

Modeling Metaverse Perceptions for Bolstering Traffic Safety using Novel TrSS-Based OWCM-RAM MCDM Techniques: Purposes and Strategies

Mona Mohamed [1,*], Asmaa Elsayed [2], and Marwa Sharawi [3]

[1] Higher Technological Institute, 10th of Ramadan City 44629, Egypt; mona.fouad@hti.edu.eg.
[2] Faculty of computers and informatics, Zagazig University, Egypt; aa.ahmed023@eng.zu.edu.eg.
[3] College of Engineering and Applied Sciences, American University of Kuwait, Safat, Kuwait; mamostafa@auk.edu.kw.

* Correspondence: mona.fouad@hti.edu.eg

Abstract: The Metaverse has the potential to revolutionize various aspects of human life, including transportation systems. The integration of the Metaverse into intelligent transportation systems has the potential to significantly improve traffic safety in smart cities. By creating a virtual replica of the physical world, the Metaverse can provide a platform for testing new traffic management systems, road designs, and vehicle technologies in a controlled and safe environment before implementing them in the real world. One way to integrate the Metaverse into intelligent transportation systems (ITS) is by enhancing traffic safety. This can be achieved by developing an evaluation model that considers both safety and traffic efficiency. The proposed evaluation methodology encompasses three phases. Firstly, the obligations/criteria, and subsidiary obligations are modeled into nodes within levels based on Tree Soft Sets (TrSSs). Secondly, the Opinion Weight Criteria Method (OWCM) is utilized for generating the weights for obligations and subsidiary obligations. Finally, the Root Assessment Method (RAM) harnesses the generated weights for assessing and ranking alternative approaches to improving traffic safety in smart cities. The utilized techniques are working under the authority of neutrosophic theory to support these techniques in uncertain and ambiguous circumstances. Subsequently, the proposed methodology is tested in a case study that considers three alternative approaches to improving traffic safety in a smart city. The criteria for evaluation include safety and traffic aspects. The results of the case study indicate that the proposed evaluation model effectively ranks the alternative approaches based on their safety and traffic efficiency. This suggests that the Metaverse can be effectively integrated to enhance traffic safety and improve overall transportation efficiency. Overall, the results of the case study suggest that the proposed evaluation model effectively ranks the alternative approaches based on their safety and traffic efficiency. This indicates that the integration of the Metaverse can indeed enhance traffic safety and improve overall transportation efficiency in smart cities.

Keywords: Intelligent Transportation Systems; Opinion Weight Criteria Method; Tree Soft Sets; Root Assessment Method; Metaverse; Neutrosophic Theory.

1. Introduction

Among the most horrifying and deadly incidents in the world are traffic accidents. For instance, statistics according to [1] on fatal collisions in the US demonstrate the sharp rise in single-vehicle, run-off-road incidents. Evidence of this [2] indicated that around 1.3 million individuals worldwide lose their lives in road accidents each year, while 20 to 50 million more have non-fatal injuries and impairments. There are several explanations for this high frequency of accidents, which are covered in [3], which are situated in blunders made by humans such as overindulgent speed during driving, driving when intoxicated and therefore losing focus, and disregard for safety gear such as seat belts and helmets when operating a scooter.

That is why [4] demonstrated that innovative technologies of information and communications technology (ICT) have a crucial role in the operational planning of transportation systems by boosting the flow of observed data, enhancing the speed and caliber of information, and enabling real-time monitoring and coordination of operations. While emerging technologies like 5G, blockchain (BC), AI, and IoT [5] promise to revolutionize urban administration. These technologies have the power to change everything from energy grids and traffic systems to waste management, public safety, and citizen services. Even in 2021, according to [6], the Metaverse (Met) has grown in popularity. Additionally, it is the merging of the digital and real worlds into one virtual one. Hence, the technology behind it is augmented reality (AR) and virtual reality (VR), which allow for multimodal interactions with digital objects, virtual surroundings, and humans.

Eventually, [7] reported that uniform data standards for smart communities, smart buildings, and smart transportation may be adopted, combining to create a Metaverse of smart cities. Furthermore, Pradhan et al. [8] depicted that the concept of the Metaverse has been popularized in science fiction literature and media, and is now being actively developed and invested in by major tech companies. It has the potential to impact various sectors, such as e-commerce, gaming, entertainment, education, and marketing, and could reach a value of $5 trillion by 2030.Through [9], individuals can create and experience their own digital identities and environments through Met technology. It is a dynamic and evolving space that has the potential to revolutionize the way we interact with each other and with digital information. With the ability to provide real-time communication and experiences, Met has been compared to a next-level version of the internet. For instance, Seoul, South Korea, according to [10], has committed around $180 million to build a Metaverse ecosystem and has already launched the world's first urban Metaverse app. In the same vein [11], WayRay fosters an augmented reality (AR) navigation system that gives drivers real-time access to extremely accurate route and environmental data, enhancing road safety.

In confirmation of [7], scholars of [12] thought that the intervention of Met in transportation resulting in traffic issues would be fixed, that safety would improve, and that accidents would be prevented. Overall, Met leveraged in traffic into different perceptions where it can be used as a precautionary measure for implementing shared economies in traffic [13], as a driving instructor for novices [3], and additionally [14] employed Met as controlling drivers and public transportation vehicle training.

Herein, we are harnessing these perceptions of Met in traffic as alternatives to analyze and evaluate the role of Met. This evaluation is being conducted based on a set of obligations and subsidiary obligations. The relation between obligations and subsidiary obligations is elaborated and modeled into nodes of levels through leveraging tree soft sets (TrSSs), which were proposed by Smarandache [15], who is the founder of uncertainty theory "neutrosophic theory". Obligations and their subsidiaries, which are modeled into TrSSs, are analyzed and weighted by applying the Opinion Weight Criteria Method (OWCM), which was introduced by Ahmed [16] and utilized for the first time in evaluating blockchain Cybersecurity in [17]. The generated weights from OWCM are harnessed into the Root Assessment Method (RAM) that is suggested by Anvari in [18] to rank the determined alternatives of Met and recommend the optimal. Eventually, these techniques are included in Multi-Criteria Decision Making (MCDM) and work under the authority of neutrosophic theory to support MCDM techniques when there is incomplete data. Also, to support experts when there is ambiguity.

2. Around Related Literature

The objective of this section is to showcase general scholars' perspectives on Met technology and its role in traffic. For instance, [19] defined Met as a vast network of interconnected virtual worlds that augment and partially overlay the real world. In an immersive, scalable, synchronous, and permanent environment, users may engage and communicate with one another through avatar-based virtual worlds, as well as experience and consume user-generated content. There are incentives in an economic system for participating in the Met. While Todorovic et al. [20] revealed that autonomous vehicles are one alternate mode of transportation that might be included in the Metaverse. These vehicles are highly advanced and constantly advancing technologically. That is due to the large volumes of driver data that might be generated by the deployment of the vehicles in the virtual environment. This data could then be utilized to train autonomous vehicles for use in real-world situations. Because all avatars, vehicles, and services are linked to BC, [21] indicated that it is much simpler to keep an eye on how clients behave in the Metaverse. As a result, it is simpler for the sharing economy authority to provide the following clients with a better experience. Further details about AR or other technology integration in vehicles may be found in recent research on traffic safety [22]. Hence, [23] demonstrated that deploying these technologies is crucial in forecasting the driving conditions of vehicles, which enhances the precision of traffic safety detection.

Following that, [3] examined the possibilities of the Met and its alternatives to traffic safety. Logarithmic methodology of additive weights (LMAW) utilized under fuzzy for calculating criteria's weights, which are used in TOPSIS to rank candidates of alternatives. Three possibilities for evaluating freight fluidity are put forth in [24, 25]: using existing data to quantify fluidity through global control of freight operations, integrating freight activities into the Metaverse, and doing nothing. While thirteen criteria are used in the multi-criteria decision-making process. These criteria are grouped under four main aspects: technology, governance, efficiency, and environmental sustainability. These criteria are harnessed by LMAW, which is based on Dombi norms for obtaining the criteria's weights. Also, an extended evaluation based on the Distance from Average Solution (EDAS) approach is adopted for ranking alternatives. The findings indicated that the best course of action is to integrate freight activities into the Metaverse to measure fluidity; the least beneficial course of action is to take no action at all.

3. Problem Description and Wording

This study investigates how Met technology could enhance traffic safety and transit convenience. Whilst Met in traffic may play role as virtual driver training, keep an eye on and control traffic flow, and self-driving vehicle. These perceptions were treated in the study as alternatives. Moreover, these alternatives are evaluated based on set of obligations and subsidiary obligations. Herein, we are wording the problem which study discusses and try to solve. Firstly, alternatives of Met in traffic define as:

3.1 Interpretation of alternatives [3]

- $\mathcal{A}_1$: Simulation-Based Training for Drivers: Simulation-Based Training for Drivers: The Metaverse can provide immersive virtual reality simulations for driver training programs. This allows new drivers to practice various scenarios, including adverse weather conditions, heavy traffic, and emergency situations, in a safe environment before they hit the road.
- $\mathcal{A}_2$: Predictive Analytics for Accident Prevention: By analyzing traffic data and historical accident records within the metaverse, city authorities can identify high-risk areas and predict potential accident hotspots. This allows for targeted interventions, such as traffic calming measures, improved signage, and enhanced enforcement, to prevent accidents before they occur.
- $\mathcal{A}_3$: Virtual Traffic Calming Measures: City planners can use the Metaverse to test and simulate various traffic calming interventions, such as redesigned intersections, roundabouts, or traffic circles, before implementing them in the physical environment. This ensures that proposed changes are effective in improving safety without causing unintended consequences.

These alternatives will be ranked based on based on set of obligations and subsidiary obligations. Hence it is necessary to define these obligations and its subsidiary as:

3.2 Interpretation of Obligations and its Subsidiary [3, 14-25]

3.2.1 Safety feature C_1(beneficial):

- C_{12}: The necessity of a stable internet connection(non-beneficial):
  The 5G technology connection speed needs to be quick and reliable since system issues might arise from latency, loss of connection, or internet connection failure.
- C_{12}: Ensure data security (beneficial): Ensuring data security in the metaverse is a critical concern, especially since it operates directly through the internet and involves people's sensitive information. The cost of ensuring data security in the Metaverse for transportation in smart cities can vary depending on various factors such as the size of the Metaverse, the amount of data being processed, and the level of security measures required.
- C_{13}: Accuracy needs in data collection (non-beneficial): To avoid manipulation and inaccurate results, a survey or study's data gathering process plays a significant role. It also implies exactitude in application.
- C_{14}: Communication and payments (beneficial): are crucial for the success of the Metaverse in the context of transportation in a smart city. Communication is key to ensuring a smooth and efficient transportation experience for users, and any disruption in communication can lead to significant inconvenience and potential safety issues. Therefore, a high-capacity communication system is necessary to provide uninterrupted communication between vehicles, infrastructure, and users.

3.2.2 Traffic feature C_1(non-beneficial):

- C_{21}: Optimize traffic flow (beneficial): the Metaverse can significantly optimize traffic flow in smart city transportation beyond what has been achieved with Intelligent Transport Systems (ITS). By creating a virtual replica of the physical world, the Metaverse can provide a platform for testing and simulating traffic management strategies and systems in a controlled and safe environment. This can lead to the development of more effective traffic management plans, resulting in reduced congestion, improved traffic flow, and shorter travel times.
- C_{22}: Road accidents (non-beneficial): The Metaverse can significantly contribute to reducing road accidents in traffic safety by providing a virtual environment for training drivers and testing new transportation technologies. By creating a 3D environment, drivers can be trained to handle various traffic scenarios and improve their driving behavior, which can help achieve a zero road accident society. The Metaverse can also be used for testing and evaluating new traffic management technologies, such as autonomous vehicles and smart traffic signals, leading to improved traffic flow and reduced accidents. Additionally, the Metaverse can provide real-time monitoring and communication between transportation providers, enabling them to quickly respond to changing traffic conditions and optimize traffic flow, further reducing the risk of accidents.
- C_{23}: Improve road safety (beneficial): the integration of the Metaverse in transportation planning can significantly improve road safety. The Metaverse can provide a platform for real-time communication and coordination between transportation providers, enabling them to quickly respond to changing traffic conditions and optimize traffic flow. This can lead to improved traffic flow, reduced congestion, and improved road safety.

4. Methodology

Herein, we introduce a hybrid method, the OWCM-RAM method, using the structure of TrSSs to make it easier to divide criteria into levels and sublevels, get weights using the OWCM method, and then rank alternatives based on hierarchy using the RAM method. As shown in Figure 1.

Subsequently, this section divides into sub-sections. Each one has a responsibility for providing certain information.

4.1 Preliminaries

4.1.1 Tree Soft Set (TrSSs) [15]

The concept of TrSoT introduced by Smarandache [16] also, he is founder for Neutrosophic theory. Whilst Smarandache described and defined this concept as:

Let $\mathfrak{H}$ be a universe of discourse, and $\mathcal{H}$ a non-empty and subset of $\mathfrak{H}$, whilst the powerset of $\mathcal{H}$ denoted as P($\mathcal{H}$).

- Main nodes encompass main attributes/criteria/factors and symbolled as $\mathfrak{R}$. Accordingly, $\mathfrak{R}$ has set of $\mathfrak{R}_s$ with (one-digit indexes) = $\{\mathfrak{R}_1, \mathfrak{R}_2, \dots \mathfrak{R}_n\}$.
- Sub-nodes which have two-digit indexes and symbolled as:
  $\{\mathfrak{R}_{11}, .. \mathfrak{R}_{1n}\}$ are sub-nodes of $\mathfrak{R}_1$, $\{\mathfrak{R}_{21}, .. \mathfrak{R}_{2n}\}$ are sub-nodes of $\mathfrak{R}_2$, and $\{\mathfrak{R}_{31}, .. \mathfrak{R}_{3n}\}$ are sub-nodes of $\mathfrak{R}_3$.
- Generally, a graph-tree is formed, that we denote as Tree(ℵ), whose root is considered of level zero,
- Then nodes of level 1, level 2, up to level n.
- We call leaves of the graph-tree, all terminal nodes (nodes that have no descendants).
  Then TrSS is: F: P(Tree(ℵ)) → P($\mathcal{H}$).
- All node of TrSSs of level m are: Tree(ℵ) = {ℵi1 | i1= 1, 2, ... }.

4.2 Modelling Main Obligations/Criteria and its Subsidiary into TrSSs

- **A**ssign main obligations/ criteria into nodes which resident into level 1. Moreover, subsidiaries of obligations/ criteria are forming into sub-nodes of nodes of level 1. Thus, these sub-nodes are resident into level 2.
- Communicate with panel of experts who related to our field to rate obligations and its subsidiaries modelled into TrSSs

4.3 Weighting Obligations and Subsidiaries based on OWCM Method [16]

Opinion Weight Criteria Method, it's a type of combinative approach which combines subjective and objective methods. So, to extract weight for each obligation /criterion the following steps must be applied:

- Decision matrices are constructed based on number of DMs for evaluating alternatives based on main criteria through utilizing single value Neutrosophic scale (SVNS) as in [17].
- The constructed Neutrosophic matrices are convert to deneutrosophic matrices through Eq. (1).
  $$\mathrm{De_{ij}} = \frac{2+\mathrm{T}-\mathrm{I}-\mathrm{F}}{3} \quad (1)$$
  Where:
  T, $\mathcal{F}$, I refer to truth, false, and indeterminacy respectively.
- Deneutrosophic matrices are aggregated into single matrix called aggregated matrix by Eq. (2).
  $$\wp_{\mathrm{ij}} = \frac{\sum_{\mathrm{ij}}^{\mathrm{n}} \mathrm{De_{ij}}}{\mathbb{N}} \quad (2)$$
  Where:
  $\mathrm{De_{ij}}$ refers to value of criterion in deneutrosophic matrices, $\mathbb{N}$ refers to number of experts.
- Normalizing the decision matrix using Eq. (3).
  $$\boldsymbol{\mathcal{R}_{ij}} = \frac{\wp_{ij}}{\wp_j^{max}} \quad (3)$$
  Where $\boldsymbol{\mathcal{X}_j^{max}}$ is the max value for each obligation.
- Calculating the average score using Eq. (4).
  $$\boldsymbol{\mathcal{K}} = \frac{\mathbf{1}}{\mathbf{N}} \sum_{\mathbf{i=1}}^{\mathbf{m}} \boldsymbol{\mathcal{R}_{\mathbf{ij}}} \quad (4)$$

Where N numbers of alternatives.

- Calculating the degree of preference variation using Eq. (5).

$$\mathcal{Q}_j = \sum_{i=1}^{m}[\mathcal{R}_{ij} - \mathcal{K}]^2 \quad (5)$$

Determine the difference in preference level using Eq. (6).

$$\varphi_j = 1 - \mathcal{Q}_j \quad (6)$$

Final step to get weight for each criteria use Eq. (7).

$$\mathcal{W}_j = \frac{\varphi_j}{\sum_{j=1}^{n}\varphi_j} \quad (7)$$

4.4 Ranking the Alternatives based on RAM Method [19]

RAM method is used to rank the alternatives based on a radical expression which its radicand and index are the sums of benefit and cost criteria of each alternative.

The criteria must be divided into beneficial and non-beneficial

- Normalize the aggregated matrix in previous step using

$$r_{ij} = \frac{x_{ij}}{\sum_{i=1}^{m} x_{ij}} \quad (8)$$

- Compute the weighted normalized matrix

$$\mathcal{Y}_{ij} = r_{ij} \cdot \mathcal{W}_j \quad (9)$$

Where $\mathcal{W}_j$ the weighted values for each criteria calculated by OWCM method

- Calculate the summation for beneficial criteria and non-beneficial criteria using

$$\mathcal{S}_{+i} = \sum_{j=1}^{n}\mathcal{Y}_{+ij} \quad \text{for beneficial} \quad (10)$$

$$\mathcal{S}_{-i} = \sum_{j=1}^{n}\mathcal{Y}_{-ij} \quad \text{for non-beneficial} \quad (11)$$

- Calculate the overall score for each alternative by Eq. (12)

$$\mathcal{RJ}_i = \sqrt[2+\mathcal{S}_{-i}]{2 + \mathcal{S}_{+i}} \quad (12)$$

Finally, ranking alternatives based on the value of $\mathcal{RJ}_i$ as the bigst value of $\mathcal{RJ}_i$ the higher priority of its alternatives. It usually that small gab between the overall score of $\mathcal{RJ}_i$ value as results are very close to each other so they cannot be ranked. To Solve this problem we must equalize the $\mathcal{RJ}_i$ value to be in the range of [0, 1] and normalized it using min-max normalization method.

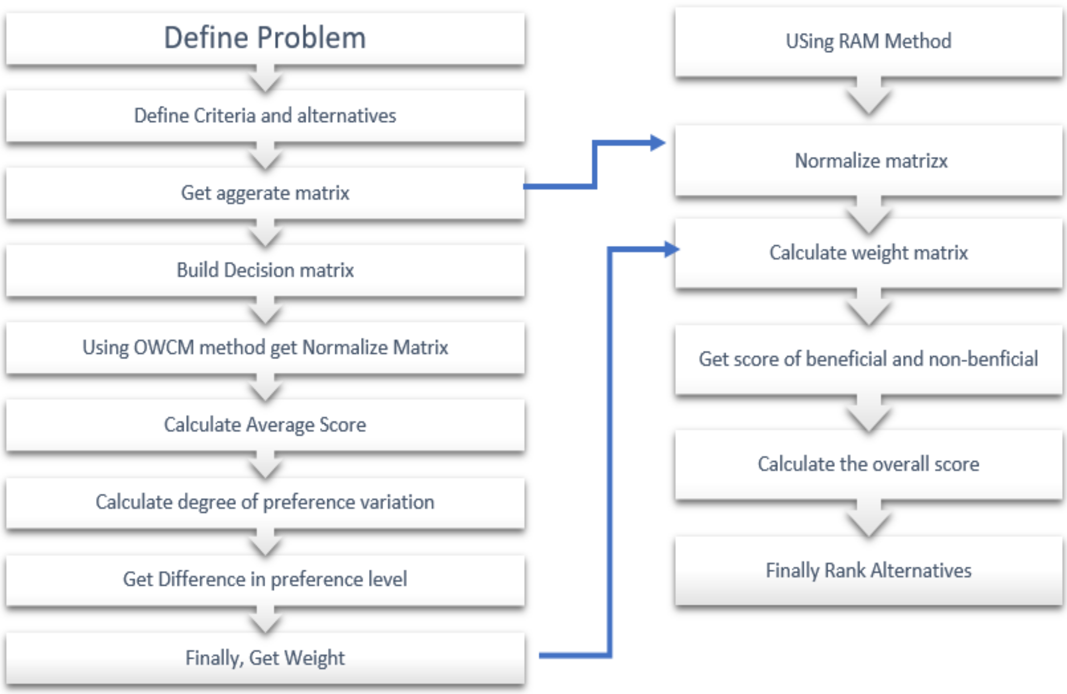

Figure 1. Evaluation methodology based on OWCM-RAM schema.

5. Case Study

The potential for the Metaverse to enhance traffic safety in smart cities is indeed significant. The ability to create a virtual replica of the physical world allows for extensive testing of traffic management systems, road designs, and vehicle technologies in a safe and controlled environment. This minimizes the risks associated with implementing new solutions directly in the real world and allows for thorough experimentation and optimization. Traffic simulations within the Metaverse can simulate various scenarios, including different weather conditions, road layouts, and traffic volumes. By running simulations, potential safety issues can be identified, and solutions can be developed and refined before implementation. This proactive approach can lead to the implementation of more effective traffic management systems and ultimately reduce accidents and congestion. The Metaverse provides an immersive platform for training drivers and traffic management personnel. Through realistic simulations and scenarios, individuals can develop their skills and understanding of traffic safety challenges, leading to improved decision-making and responses in real-world situations. Utilizing the Metaverse for real-time monitoring of traffic enables rapid responses to accidents, road closures, and other incidents. By analyzing traffic data and trends in real-time, traffic management personnel can make informed decisions to mitigate risks and improve safety on the roads. The Metaverse's data analysis capabilities allow for the identification of trends and patterns in traffic data. This information can inform the development of more effective traffic management strategies, leading to improved safety outcomes and enhanced efficiency in the transportation system. Integrating the Metaverse with traffic safety initiatives in smart cities has the potential to significantly improve road safety, reduce traffic congestion, and enhance the efficiency of the transportation system. By providing a platform for testing, training, monitoring, and analysis, the Metaverse can help create a safer and more sustainable transportation system for all users. Leveraging the Metaverse's capabilities for traffic safety in smart cities offers numerous benefits and opportunities for innovation. By harnessing its potential for simulation, training, real-time monitoring, and data analysis, cities can make significant strides towards achieving safer and more efficient transportation networks.

Hence, we are implementing the previous steps in the methodology section in real case study to verify the accuracy of this methodology toward ranking the alternative and selecting the optimal alternative.

5.1 Experimental of Proposed Methodology

First of all, Using OWCM method to get weights for each level of TrSSs as following:

1. Decision makers express their opinions and then transformed into crisp numbers then get the aggregate matrix as Table 1.
2. Using Eq. (3) for normalizing the decision matrix in Table 2.
3. Then, use Eq. (4) to get average score as Table 3.
4. Use Eq. (5) to calculate the degree of preference variation represented in Table 3.
5. After that determine the difference preference level using Eq. (6) in Table 3.
6. Finally, calculate weight using Eq. (7) as in Table 3.
7. Repeat the previous steps on sub criteria of level $1 \mathcal{C}_{11}, \mathcal{C}_{12}, \mathcal{C}_{13}, \mathcal{C}_{14}$ as shown in Table 4 and Table 5.
8. The last level, repeat the previous steps on sub criteria of level $1 \mathcal{C}_{21}, \mathcal{C}_{22}, \mathcal{C}_{23}$ as shown in Table 6 and Table 7.
9. Final weights for all levels of TrSSs are illustration in Figure 2.

Table 1. Decision matrix for level 1.

	$\mathcal{C}_1$	$\mathcal{C}_1$
$\mathcal{A}_1$	0.594444444	0.433333
$\mathcal{A}_2$	0.422222222	0.838889
$\mathcal{A}_3$	0.444444443	0.56

Table 2. Normalized decision matrix for level 1.

	$\mathcal{C}_1$	$\mathcal{C}_1$
$\mathcal{A}_1$	1	0.516556289
$\mathcal{A}_2$	0.710280374	1
$\mathcal{A}_3$	0.74766355	0.66754967

Table 3. Final weight for level 1.

	$\mathcal{C}_1$	$\mathcal{C}_1$
$\mathcal{K}$	0.819314641	0.72803532
$\mathcal{Q}_i$	0.049669549	0.122346682
φ_i	0.950330451	0.877653318
$\mathcal{W}_i$	0.519879042	0.480120958

Table 4. Decision matrix for sub-criteria of level 1 C1.

	$\mathcal{C}_{11}$	$\mathcal{C}_{12}$	$\mathcal{C}_{13}$	$\mathcal{C}_{14}$
$\mathcal{A}_1$	0.473333333	0.55	0.3777778	0.6233333
$\mathcal{A}_2$	0.391111113	0.4855556	0.6411111	0.6466666
$\mathcal{A}_3$	0.64333333	0.6488889	0.3855555	0.6388889

Table 5. Final weight for sub criteria of $\mathcal{C}_1$.

	$\mathcal{C}_{11}$	$\mathcal{C}_{12}$	$\mathcal{C}_{13}$	$\mathcal{C}_{14}$
$\mathcal{K}$	0.781232012	0.865296803	0.73021371	0.983963367
$\mathcal{Q}_j$	0.079956407	0.032149168	0.10925055	0.000675083
φ_j	0.920043593	0.967850832	0.89074945	0.999324917
$\mathcal{W}_j$	0.230786663	0.2074245	0.2646358	0.2971531

Table 6. Decision matrix for sub-criteria of level 1 C2.

	$\mathcal{C}_{31}$	$\mathcal{C}_{32}$	$\mathcal{C}_{33}$
$\mathcal{A}_1$	0.52999999	0.418889	0.445556
$\mathcal{A}_2$	0.58222221	0.501111	0.45
$\mathcal{A}_3$	0.732222233	0.487778	0.467778

Table 7. Final weight for sub-criteria of $\mathcal{C}_2$.

	$\mathcal{C}_{31}$	$\mathcal{C}_{32}$	$\mathcal{C}_{33}$
$\mathcal{K}$	0.839656027	0.936438	0.971496
$\mathcal{Q}_i$	0.041108568	0.01551	0.001264
φ_i	0.958891432	0.98449	0.998736
$\mathcal{W}_i$	0.325918751	0.33462	0.339462

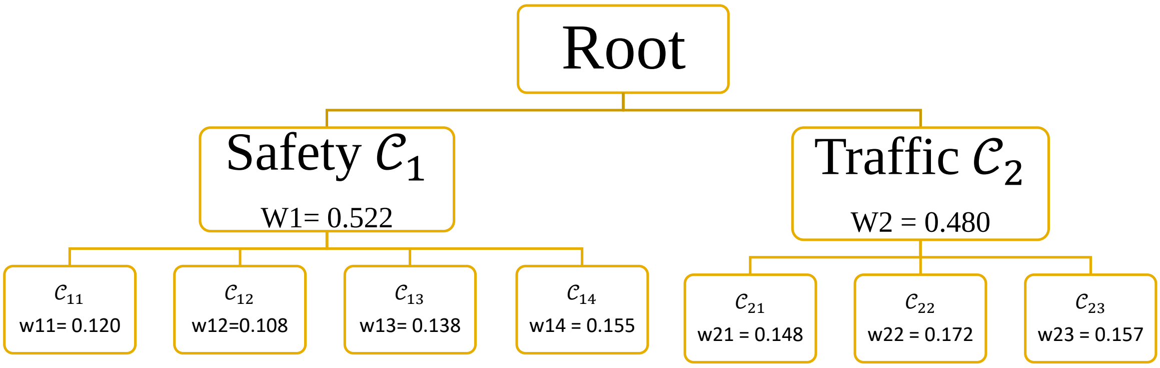

Figure 2. Final weights.

Second step, using RAM method to rank alternative for each level of tree as following:

1. Get normalized decision matrix for $\mathcal{C}_1$ *and* $\mathcal{C}_2$ and weights as Table 8 using Eq. (8).
2. Determine the weight normalized obtained from OWCM method using Eq. (9) as Table 9.
3. Then, calculate the sum of scores of beneficial and non-beneficial criteria (10, 11).
4. Calculate overall score of each alternative using Eq. (12).
5. Finally, rank alternatives based on value of dominance degree. As Table 10.
6. Repeat these steps for level 1 $\mathcal{C}_1$ to get result in Table 11 and Table 12.
7. Repeat these steps for level 1 $\mathcal{C}_2$ to get result in table 13 and Table 14.

Table 8. Normalized decision matrix of level 1.

r_{ij}	$\mathcal{C}_1+$	$\mathcal{C}_2 -$
Alt_1	0.288924559	0.327774583
Alt_2	0.302300696	0.453709028
Alt_3	0.408774746	0.218516389

Table 9. weight matrix.

y_{ij}	$\mathcal{C}_1+$	$\mathcal{C}_2 +$
Alt_1	0.151069497	0.156391639
Alt_2	0.158063456	0.216478953
Alt_3	0.213735363	0.104261093

Table 10. Final rank for level1.

	$\mathcal{S}_+$	$\mathcal{S}_-$	$\mathcal{RI}_i$	Normalized $\mathcal{RI}_i$	Rank
Alt_1	0.151069497	0.156391639	1.425	0.14634146	2
Alt_2	0.158063456	0.216478953	1.419	0	3
Alt_3	0.213735363	0.104261093	1.46	1	1

Table 11. Decision matrix of sub criteria $\mathcal{C}_1$.

	C11 -	C12 +	C13 -	C14 +
$\mathcal{A}_1$	0.370478413	0.4251701	0.252459	0.3091881
$\mathcal{A}_2$	0.151691949	0.127551	0.2754098	0.3091881
$\mathcal{A}_3$	0.477829638	0.4472789	0.4721311	0.3816237

Table 12. Decision matrix of sub criteria $\mathcal{C}_1$.

	$\mathcal{S}_+$	$\mathcal{S}_-$	$\mathcal{RI}_i$	Normalized $\mathcal{RI}_i$	Rank
Alt_1	0.0941513	0.0796387	1.425	0.6	2
Alt_2	0.0618728	0.0564132	1.422	0	3
Alt_3	0.1078035	0.1229888	1.427	1	1

Table 13. Decision matrix of sub criteria $\mathcal{C}_2$.

	C11 +	**C12 -**	**C13 +**
$\mathcal{A}_1$	0.423529	0.356997	0.305325
$\mathcal{A}_2$	0.174118	0.240041	0.210059
$\mathcal{A}_3$	0.402353	0.402962	0.484615

Table 14. Decision matrix of sub criteria $\mathcal{C}_2$.

	$\mathcal{S}_+$	$\mathcal{S}_-$	$\mathcal{RI}_i$	Normalized $\mathcal{RI}_i$	Rank
Alt_1	0.110702	0.061369	1.437	0.545455	2
Alt_2	0.058792	0.041264	1.425	0	3
Alt_3	0.135734	0.069271	1.447	1	1

6. Conclusions

This study has presented a MCDM framework to evaluate three alternative approaches to traffic safety in the Metaverse, considering criteria across two key aspects. For this purpose, a hybrid OWCM-RAM model has been presented based on the TreeSoft set. The findings show that the Metaverse A3 is the best choice for traffic safety alternatives in the Metaverse. To conclude, traffic safety systems in the Metaverse has strong potentials. In the Metaverse, traffic simulations can be run with different scenarios, including different weather conditions, road layouts, and traffic volumes, to identify potential safety issues and develop solutions. This can lead to the implementation of more effective traffic management systems, resulting in fewer accidents, reduced traffic congestion, and shorter travel times. The Metaverse can also be used to train drivers and traffic management personnel, providing them with realistic and immersive experiences that can help them better understand and respond to traffic safety challenges. This can lead to improved driving skills, better traffic management decisions, and a safer transportation system overall. In addition, the Metaverse can be used to monitor traffic in real-time, enabling traffic management personnel to quickly respond to accidents, road closures, and other incidents. By analyzing traffic data in the Metaverse, traffic management personnel can identify trends and patterns, enabling them to develop more effective traffic management strategies and improve traffic safety.

Acknowledgments
The author is grateful to the editorial and reviewers, as well as the correspondent author, who offered assistance in the form of advice, assessment, and checking during the study period.

Author Contributions
All authors contributed equally to this research.

Data availability

The datasets generated during and/or analyzed during the current study are not publicly available due to the privacy-preserving nature of the data but are available from the corresponding author upon reasonable request.

Funding
This research was not supported by any funding agency or institute.

Conflict of interest
The authors declare that there is no conflict of interest in the research.

References

1. Das, S., Kong, X., Lavrenz, S. M., Wu, L., & Jalayer, M. (2022). Fatal crashes at highway rail grade crossings: A US based study. International journal of transportation science and technology, 11(1), 107-117. https://doi.org/10.1016/j.ijtst.2021.03.002
2. Bachani, A., Peden, M., Gururaj, G., Norton, R., & Hyder, A. (2017). Road traffic injuries.
3. Deveci, M., Pamucar, D., Gokasar, I., Köppen, M., Gupta, B. B., & Daim, T. (2023). Evaluation of Metaverse traffic safety implementations using fuzzy Einstein based logarithmic methodology of additive weights and TOPSIS method. Technological Forecasting and Social Change, 194, 122681. https://doi.org/10.1016/j.techfore.2023.122681
4. Soussi, A., Tomasoni, A. M., Zero, E., & Sacile, R. (2023). An ICT-based decision support system (DSS) for the safety transport of dangerous goods along the Liguria and Tuscany Mediterranean Coast. In Intelligent Sustainable Systems: Selected Papers of WorldS4 2022, Volume 2 (pp. 629-638). Singapore: Springer Nature Singapore. https://doi.org/10.1007/978-981-19-7663-6_59
5. Razmjoo, A., Gandomi, A., Mahlooji, M., Astiaso Garcia, D., Mirjalili, S., Rezvani, A., ... & Memon, S. (2022). An investigation of the policies and crucial sectors of smart cities based on IoT application. Applied Sciences, 12(5), 2672. https://doi.org/10.3390/app12052672
6. Pamucar, D., Deveci, M., Gokasar, I., Tavana, M., & Köppen, M. (2022). A metaverse assessment model for sustainable transportation using ordinal priority approach and Aczel-Alsina norms. Technological Forecasting and Social Change, 182, 121778. https://doi.org/10.1016/j.techfore.2022.121778
7. Pu, Q. L., Pang, Y., Peng, B., Hu, C. J., & Zhang, A. Y. (2022). Metaverse report-Future is here. Global XR industry insight.
8. Onu, P., Pradhan, A., & Mbohwa, C. (2023). Potential to use metaverse for future teaching and learning. Education and Information Technologies, 1-32. https://doi.org/10.1007/s10639-023-12167-9
9. Dwivedi, Y. K., Hughes, L., Baabdullah, A. M., Ribeiro-Navarrete, S., Giannakis, M., Al-Debei, M. M., ... & Wamba, S. F. (2022). Metaverse beyond the hype: Multidisciplinary perspectives on emerging challenges, opportunities, and agenda for research, practice and policy. International Journal of Information Management, 66, 102542. https://doi.org/10.1016/j.ijinfomgt.2022.102542
10. Yaqoob, I., Salah, K., Jayaraman, R., & Omar, M. (2023). Metaverse applications in smart cities: Enabling technologies, opportunities, challenges, and future directions. Internet of Things, 100884. https://doi.org/10.1016/j.iot.2023.100884
11. Lee, L. H., Braud, T., Zhou, P., Wang, L., Xu, D., Lin, Z., ... & Hui, P. (2021). All one needs to know about metaverse: A complete survey on technological singularity, virtual ecosystem, and research agenda. arXiv preprint arXiv:2110.05352. https://doi.org/10.48550/arXiv.2110.05352
12. Huynh-The, T., Pham, Q. V., Pham, X. Q., Nguyen, T. T., Han, Z., & Kim, D. S. (2023). Artificial intelligence for the metaverse: A survey. Engineering Applications of Artificial Intelligence, 117, 105581. https://doi.org/10.1016/j.engappai.2022.105581
13. Shaheen, S., & Cohen, A. (2021). Shared micromobility: Policy and practices in the United States. A Modern Guide to the Urban Sharing Economy, 166-180. https://doi.org/10.4337/9781789909562.00020
14. Goldbach, C., Sickmann, J., Pitz, T., & Zimasa, T. (2022). Towards autonomous public transportation: Attitudes and intentions of the local population. Transportation research interdisciplinary perspectives, 13, 100504. https://doi.org/10.1016/j.trip.2021.100504

15. Smarandache, F. (2023). New Types of Soft Sets: HyperSoft Set, IndetermSoft Set, IndetermHyperSoft Set, and TreeSoft Set. Infinite Study.
16. Ahmed, A. D., Salih, M. M., & Muhsen, Y. R. (2024). Opinion Weight Criteria Method (OWCM): A New Method for Weighting Criteria with Zero Inconsistency. IEEE Access. https://doi.org/10.1109/ACCESS.2024.3349472
17. Smarandache, F. (2024). HyperSoft Set Methods in Engineering Evaluating Blockchain Cybersecurity Based on Tree Soft and Opinion Weight Criteria Method under Uncertainty Climate, 1, 1–10.
18. Sotoudeh-Anvari, A. (2023). Root Assessment Method (RAM): a novel multi-criteria decision making method and its applications in sustainability challenges. Journal of Cleaner Production, 423, 138695. https://doi.org/10.1016/j.jclepro.2023.138695
19. Weinberger, M. (2022). What is metaverse?—A definition based on qualitative meta-synthesis. Future Internet, 14(11), 310. https://doi.org/10.3390/fi14110310
20. Todorovic, M., Simic, M., & Kumar, A. (2017). Managing transition to electrical and autonomous vehicles. Procedia computer science, 112, 2335-2344. https://doi.org/10.1016/j.procs.2017.08.201
21. Nansubuga, B., & Kowalkowski, C. (2021). Carsharing: a systematic literature review and research agenda. Journal of Service Management, 32(6), 55-91. https://doi.org/10.1108/JOSM-10-2020-0344
22. Lv, Z., Chen, D., & Hossain, M. S. (2022, May). Traffic safety detection system by digital twins and virtual reality technology. In 2022 IEEE International Instrumentation and Measurement Technology Conference (I2MTC) (pp. 1-6). IEEE. http://doi.org/10.1109/I2MTC48687.2022.9806677
23. Skjermo, J., Roche-Cerasi, I., Moe, D., & Opland, R. (2022). Evaluation of road safety education program with virtual reality eye tracking. SN Computer Science, 3(2), 149. https://doi.org/10.1007/s42979-022-01036-w
24. Deveci, M., Gokasar, I., Castillo, O., & Daim, T. (2022). Evaluation of Metaverse integration of freight fluidity measurement alternatives using fuzzy Dombi EDAS model. Computers & Industrial Engineering, 174, 108773. https://doi.org/10.1016/j.cie.2022.108773
25. Ahmed, A. I. A., Ab Hamid, S. H., Gani, A., & Khan, M. K. (2019). Trust and reputation for Internet of Things: Fundamentals, taxonomy, and open research challenges. Journal of Network and Computer Applications, 145, 102409. https://doi.org/10.1016/j.jnca.2019.102409

Received: 29 Nov 2023, **Revised:** 04 Mar 2024,

Accepted: 30 Mar 2024, **Available online:** 02 Apr 2024.

NSWA Neutrosophic Systems with Applications, Vol. 16, 2024
https://doi.org/10.61356/j.nswa.2024.16205

Choosing Optimal Supply Radius of Transformer Substations (TSs) in Iraq's Cities Using Geometric Programming with Neutrosophic Coefficients

Ahmed K. Essa [1,2,*], Montifort Blessings Andrew Mitungwi [3], Tuweh Prince Gadama [4], and Ahmed A. Salama [5]

[1] Telafer University, Statistics Division, Telafer, Mosul, Iraq; ahmed.k.essa@uotelafer.edu.iq.
[2] Ph.D. Research Student, Texas Tech University and Cypress University, Malawi.
[3] Cypress International Institute University, Department of Electrical Engineering, Malawi; motorab@gmail.com.
[4] Vice Chancellor of Cypress International Institute University, Malawi; proftuwehprincegadamathegreat@gmail.com.
[5] Department of Mathematics and Computer Science, Faculty of Science, Port Said University, Egypt; drsalama44@gmail.com.

* Correspondence: ahmed.k.essa@uotelafer.edu.iq

Abstract: Numerous uncertainties exist in various electricity power system problems due to the size, complexity, geographical distribution, and influence of unforeseen events in these systems, making it difficult for traditional mathematics tools based on crisp set theory to have an impact on and solve many power system problems. As a new branch of mathematical uncertainty techniques, the neutrosophic expert systems approach has therefore emerged with the development of electric power systems and has proven successful when correctly linked. The expert typically uses ambiguous or neutrosophic language to describe their empirical knowledge, such as "very likely," "quite likely," "if x is large, then y is very likely to occur," "x should not be less than a," etc. To design an optimal radius of power supply in the electrical transformer substation, this article presents a new method for creating primal and dual neutrosophic geometric programming problems. It also provides a numerical example to evaluate the approximate optimal economic power supply radius.

Keywords: Optimal Supply Radius; Neutrosophic Geometric Programming; Neutrosophic Coefficients; Transformer Substations.

NOMENCLATURES	
TS	Transformer Substation
GPP	Geometric Programming Problem
SPP	Signomial Programming Problem
NGPP	Neutrosophic Geometric Programming Problem
H	An annual extraction coefficient is the annual running cost of the entire extracted investment.
a_1	Unconnected Part of TS's investment capacity $(unit, IQ)$
a_2	Investment in $(11kV)$ Line for Every Kilometre of Unconnected Wire $(unit, IQ/km)$
b_1	Coefficient of the Section Associated with the TS's Capacity in Investing $(unit, IQ/kV\ A)$
b_2	Coefficient of the Wire Section-Connected Part of the $(11\ kV)$ Line Investment $(unit, IQ/km \cdot mm^2)$
E	Coefficient of Terrain Correction

$\boldsymbol{\sigma}$	Average Load Density $(unit, kW/km^2)$
$\boldsymbol{K_c}$	Hold Ratio $(the\ 132k\ V - TS\ takes\ 2.2 \sim 2.5)$
$\boldsymbol{P_{av}}$	Mean Line Load Every Time $(unit, kW)$
$\boldsymbol{U_N}$	The Middle Voltage Distribution Network's Rated Voltage $(11k\ V)$
$\boldsymbol{j}$	Economical Current Density Wire $(unit, A/mm^2)$
$\boldsymbol{\rho}$	Wire in Resistivity $(unit,\ \Omega/km\ \cdot\ mm^2)$
$\boldsymbol{\tau}$	Annually Wasted Mean Maximum Load Hours
$\boldsymbol{C_0}$	Price of Each Wasted Watt-Hour $(unit, IQ/\ k\ W.h\ )$
$\boldsymbol{K_{Fe}}$	Coefficient of Transformer Iron Loss$(\approx\ 0.0085kW/(kV\ A)^{3/4})$
$\boldsymbol{\tau_b}$	Equivalent Hours of Transformer Copper Loss
$\boldsymbol{K_{cu}}$	Transformer Copper Loss Coefficient $(\approx\ 0.055kW/(kV\ A)^{3/4})$
$\boldsymbol{S_{NL}}$	Rated Load of Transformer $(unit, kV\ A)$
$\boldsymbol{S_N}$	Rated Capacity of Transformer $(unit, kV\ A)$
$\boldsymbol{Q}$	Voltage Range in Electrically-Distributed Cities $(unit, km^2)$.
$\boldsymbol{r}$	Mean Radius in the Supply Area, or it is the economic power supply radius
IQ	Iraqi Dinar

1. Introduction

The building of an optimal mathematical model for the annual cost function needs a geometric programming model because its variables have negative rational powers.

It is well known that any classical geometric programming problem neglects the uncertainty part of the sophisticated practical environment. So, the neutrosophic model will be more flexible having more information. In Iraq, the services of electricity supply are very poor in almost all cities for many reasons, such as the cascade wars, for example, the Arab Gulf War in 1990, where the Iraqi community suffered from many setbacks:

1. The economy block in the nineties of the last century,
2. Replace the system of the government with a parliamentary system of government,
3. In the twenty-one century the events of the sectarian and ethnic civil wars in Iraqi society.

All previous reasons and more, lead to infrastructural destruction.

This essay comes as an attempt to shed light on some important problems involving how can rebuild the Iraqi power electricity supply substations. The necessary point that this paper focused on is how to choose an optimal radius (r) of the electric power supply in the substations of Iraqi cities. The reader should pay attention that the monetary currency of the country is the Iraqi dinar (IQ).

2. Classical Geometric Programming Problem (CGPP)

To handle a class of non-linear optimization problems that are commonly seen in engineering design, an optimization technique known as geometric programming (GP) was developed. The GP technique was inspired by the work of Zener. Zener tried a novel approach in 1961 to solve a class of unconstrained non-linear optimization problems with polynomial terms in the objective function. To answer these problems, he used the well-known inequality between arithmetic and geometric means, which states that the arithmetic mean is greater than or equal to the geometric mean. Because the arithmetic-geometric mean inequality is applied, this method is referred to as the "GP technique". Only in cases when the objective function was unconstrained and the number of polynomial terms was one more than the number of variables did Zener employ this technique. Later in 1962, Duffin expanded the application of this method to resolve issues when the objective function's number of polynomial terms is arbitrary. In 1967, Peterson enhanced the application of this technique to issues that also incorporate inequality restrictions expressed as posynomials with the aid of Zener and Duffin [1]. Additionally, Passy and Wilde (1967) extended this method to tackle issues where some of the posynomial terms have negative coefficients [2].

For instance, Duffin demonstrated that a function "duality gap" could not develop in geometric programming by condensing the posynomial functions to monomial form (1970) and converting them to linear form using a logarithmic transformation. Posynomial programming with (posy) monomial objective and constraint functions is equivalent to linear programming. Duffin and Peterson (1972) demonstrate that each of these posynomial programs GPP can be reformulated so that every constraint function is a (posy) binomial in that it includes at most two posynomial terms. An effective and extremely flexible way of solution was desired since geometric programming has become a popular optimization methodology. Several factors became crucial as the complexity of the sample geometric programs to be solved grew: Canonically, the problem's level of difficulty and inactive constraints [3] reported an algorithm that might take these factors into account. Later, in 1976, Mcnamara suggested a method for solving geometric programming problems that involved formulating an augmented problem with a degree of complexity zero. As a result, many algorithms have been proposed for solving GP, the majority of which were made before (1980); these algorithms are somewhat more efficient and reliable when applied to the convex problem and also avoid problems with derivative singularities as variables raised to fractional powers approach zero because logs of such variables will approach$-\infty$, There should be significant negative lower bounds on those variables. A significant amount of interior point (IP) algorithms for general purpose (GP) were developed in the 1990s. An effective method for solving posynomial geometric programming was developed by Rajgopal and Bricker in 2002. Condensation was a concept that was employed in the method, which was integrated into an algorithm for the more broad (Signomial) GP issue. The reformulation's constraint structure sheds light on why this algorithm is effective in avoiding every computing issue usually connected to dual-based algorithms. A method for addressing (positive, zero, or negative) variables in SPP was put out by Li and Tsai in 2005. A linear or convex relaxation of the original problem is computed using the majority of current global optimization methods for SPP. These methods might occasionally offer an impractical answer, or they might constitute the genuine optimum to get around these restrictions. Shen, Ma, and Chen (2008) proposed a robust solution algorithm for the global algorithm optimization of SPP. This algorithm adequately ensures the achievement of a robust optimal solution that is both feasible and close to the actual optimal solution and is stable under small perturbations of the constraints [4].

Huda E. Khalid [5] suggested an innovative GPP algorithm for discovering the ranging analysis by examining the impact of perturbations in the coefficients without solving the issue, as this proposed procedure had been caught on two coefficients at once. Additionally, the reference [6] investigated an original GPP employing substitution effects in a sensitivity analysis for two coefficients at once based on a new extended theorem and adjusted new constants. Huda E. Khalid [7] proposed one of the incremental procedures required to appropriately compare the results obtained from the incremental analysis methodology and the sensitivity analysis approach. Additionally, there was an effort to develop a novel computational approach that could be used to examine the sensitivity analysis of the geometric programming problem (GPP) and the signomial geometric programming problem (SPP), both of which had a difficulty level larger than zero. The studies [8, 9] cast a bad light on multi-objective geometric programming's degree of challenges.

Definition 2.1: [10]: The vector x^* that makes the constraint inequalities $g_j(x) \leq 1,\ j = 1,2 \dots\dots, p \ and \ x > 0$ into exact equalities is the optimal solution to a GPP. We refer to the constraint set in such issues as being tight or active. As a result, we can assess any inactive constraints by assessing those for which $g_j(x) > 1$ or $g_j(x) < 1$.

Definition 2.2: [11] Let R_{++}^{m} stand for the set of real m-vectors with positive component values. Let there be m real positive vectors, $x_1, \dots, x_m$. A function with the definition $f : R_{++}^{m} \rightarrow R$ is called a monomial, and is defined as $f(x) = c\prod_{j=1}^{m} x_j^{a_j}$, $c > 0$ where $a_j \in R$. A polynomial is a sum of monomials or a function of the type $(x) = \sum_{i=1}^{n} c_k \prod_{j=1}^{m} x_j^{a_{ij}}$, with $c_k > 0$ and $a_{jk} \in R$.

3. Neutrosophic Geometric programming problems (NGPP) [4]

In 2016, Florentin Smarandache and Huda E. Khalid developed unconstrained neutrosophic geometric programming, where the models were constructed as posynomials. For this subject, the following definitions are thought to be fundamental:

3.1 **Definition:** Let $h(x)$ be any linear or non-linear neutrosophic function, where $x_i \in [0,1] \cup [0, nI]$ and $x = (x_1, x_2, \dots, x_m)^{T}$ an m-dimensional fuzzy neutrosophic variable vector.

We have the inequality

$$h(x) < ₦1 \quad (1)$$

where " $<₦$" denotes the neutrosophic version of " $\leq$ " with the linguistic interpretation being "less than (the original claimed), greater than (the anti-claim of the original less than), equal (neither the original claim nor the anti-claim)".

The inequality (1) can be redefined as follows:

$$\left.\begin{array}{r} h(x) < 1 \\ \text{anti}\ (h(x)) > 1 \\ \text{neut}(\ h(x)) = 1 \end{array}\right\} \quad (2)$$

3.2 **Definition:** Let

$$\left.\begin{array}{lll} \overset{N}{(P)} & \overset{N}{\min} & h(x) \\ & x_i \in FN_s & \end{array}\right\} \quad (3)$$

The neutrosophic unconstrained posynomial geometric programming, where $x = (x_1, x_2, \dots, x_m)^{T}$ is an m-dimensional fuzzy neutrosophic variable vector, "T" represents a transpose symbol and $h(x) = \sum_{k=1}^{J} c_k \prod_{l=1}^{m} x_l^{\gamma_{kl}}$ is a neutrosophic posynomial GP function of x, $c_k \geq 0$ a constant, γ_{kl} an arbitrary real number, $h(x) < ₦\, z \rightarrow \overset{N}{\min} g(x)$; the objective function $h(x)$ can be written as a minimizing goal to consider z as an upper bound; z is an expectation value of the objective function $h(x)$," $<₦$ " denotes the neutrosophic version of " $\leq$ " with the linguistic interpretation (see Definition 3.1), and $d_o > 0$ denotes a flexible index of $h(x)$.

Note that the above program is undefined and has no solution in the case of $\gamma_{kl} < 0$ with some x_l's taking indeterminacy value, for example,

$$\overset{N}{\min} \quad h(x) = 2x_1^{-.2} x_2^{.3} x_4^{1.5} + 7x_1^{3} x_2^{-.5} x_3, \quad (4)$$

where $x_i \in FN_s, i = 1,2,3,4$. This program is not defined at $x = (.2I, .3, .25, I)^{T}$, $h(x) = 2(.2I)^{-.2}(.3)^{.3} I^{1.5} + 7(.2I)^{3}(.3)^{-.5}(.25)$ is undefined at $x_1 = .2I$ with $\gamma_1 = -0.2$.

3.3 **Definition:** Let A_0 be the set of all neutrosophic non-liner functions $h(x)$ that are neutrosophically less than or equal to z, i.e.

$A_0 = \{x_i \in FN_m,\ h(x) < ₦\, z\}$.

The membership functions of $h(x)$ and $\text{anti}(h(x))$ are:

$$\mu_{A_o}(\ h(x)) = \begin{cases} 1 & 0 \leq h(x) \leq z \\ \left(e^{\frac{-1}{d_o}(g(x)-z)} + e^{\frac{-1}{d_o}(\text{anti}\ (g(x))-z)} - 1\right), & z < h(x) \leq z - d_o \ln 0.5 \end{cases} \quad (5)$$

$$\mu_{A_o}(\text{anti}(h(x))) = \begin{cases} 0 & 0 \leq h(x) \leq z \\ \left(1 - e^{\frac{-1}{d_o}(\text{anti}\ (h(x))-z)} - e^{\frac{-1}{d_o}(h(x)-z)}\right), & z - d_o \ln 0.5 \leq h(x) \leq z + d_o \end{cases} \quad (6)$$

Eq. (6) can be changed into

$$h(x) < ₦\, z, \quad x = (x_1, x_2, \dots, x_m), x_i \in FN_s \quad (7)$$

The above program can be redefined as follows:

$$\left.\begin{array}{l} h(x) < z \\ anti(h(x)) > z \\ neut(h(x)) = z \\ x = (x_1, x_2, \dots, x_m), x_i \in FN_s \end{array}\right\} \quad (8)$$

It is clear that $\mu_{A_o}(neut(h(x)))$ consists of the intersection of the following functions:

$$e^{\frac{-1}{d_o}(h(x)-z)} \quad \& \quad 1 - e^{\frac{-1}{d_o}(anti(h(x))-z)} \quad (9)$$

$$\mu_{A_o}(neut(h(x))) = \begin{cases} 1 - e^{\frac{-1}{d_o}(anti(h(x))-z)} & z \le h(x) \le z - d_o \ln 0.5 \\ e^{\frac{-1}{d_o}(h(x)-z)} & z - d_o \ln 0.5 < h(x) \le z + d_o \end{cases} \quad (10)$$

3.4 **Definition:** Let $\tilde{N}$ be a fuzzy neutrosophic set defined on $[0,1] \cup [0, nI], n \in [0,1]$; if there exists a fuzzy neutrosophic optimal point set A_o^* of $h(x)$ such that

$$\tilde{N}(x) = \begin{array}{c} \min\{\mu(neut\ h(x))\} \\ x = (x_1, x_2, \dots, x_m), x_i \in FN_s \end{array} \quad (11)$$

$$\tilde{N}(x) = e^{\frac{-1}{d_o}\left(\sum_{k=1}^{J} c_k \prod_{l=1}^{m} x_l^{\gamma_{kl}} - z\right)} \wedge 1 - e^{\frac{-1}{d_o}\left(anti\left(\sum_{k=1}^{J} c_k \prod_{l=1}^{m} x_l^{\gamma_{kl}}\right) - z\right)}, \quad (12)$$

Then $\max \tilde{N}(x)$ is said to be a neutrosophic geometric programming (the unconstrained case) concerning $\tilde{N}(x)$ of $h(x)$.

3.5 Definition: Let x^* be an optimal solution to $\tilde{N}(x)$, i.e. $\tilde{N}(x^*) = \max \tilde{N}(x)$, $x = (x_1, x_2, \dots, x_m), x_i \in FN_s$, and the fuzzy neutrosophic set $\tilde{N}$ satisfying Eq. (11) is a fuzzy neutrosophic decision in Eq. (8).

4. Designing an Optimal Radius of Power Supply in Transformers Substation Using Classical Geometric Programming Problems GPP [12]

The annual-cost way had been built with consideration to the following assumptions:

1. 132 KV-TS power supply to its consumers in a city by the direct-step-down method of 11 KV.
2. The load density is even over the whole electrified wire netting cover. Therefore, a static model is built using an annual cost as follows:

$$F = \frac{Z}{N} + \mu \quad (13)$$

Where Z denotes the cost of total investment, μ is the annual cost of investment operational under a certain load level, $N(8 - 10\ years)$ is an investment-recovery deadline, i.e., the total investment is returned within $(8 - 10)$ redeemable years.

The annual cost function in a unit capacity is denoted by

$$F_o = \frac{F}{S} = \frac{\frac{(Z_b + Z_l)}{N} + \mu_1 + \mu_2 + \mu_3}{S} \quad (14)$$

Where,

$$Z_b = a_1 + b_1 S \quad (IQ) \quad (15)$$

Is the investment in the construction of 132 KV-TS [14].

$$Z_l = L(Ma_2 + b_2 S_l) \quad (IQ) \quad (16)$$

Denotes the construction investment in the main-supply lines of the (11 KV) middle voltage distribution network, where $M = S\cos\phi / P_{av}$ is a circle line of $(11KV)$ middle voltage distribution network, $L = Er\ (km)$ is each circle-line length of it, and $S_l = \frac{S}{\sqrt{3}U_{Nj}}\ (mm^2)$ denotes the wire total selection in the main-supply lines of all $(11\ KV)$ middle voltage distribution net-work in $(132\ KV) - TS$; S is the capacity in the $TS\ (unit, KVA)$.

$$\mu_1 = H(Z_b + Z_l) \quad (17)$$

Behaves as a direct proportion function of the unchangeable part in operations cost (large repair, small repair, and depreciation charge) and in the total investment of $(132\,KV - TS)$ and $(11\,KV)$ middle voltage distribution net line.

$$\mu_2 = \Delta P_\tau C_o = 7.26 \frac{E_{\rho j\tau} C_o}{U_N cos^2\phi} \frac{1}{\sqrt{\sigma}} S^{3/2}\, 10^{-5} \quad (18)$$

Stands for the depreciation charge of $(11\,KV)$ line in a year, while by [15], the depreciation charge to transformers of

$(132\,K\,V - TS)$ is $\mu_3 = (C_0 K_{Fe} 8760 + C_0 \tau_b K_{cu}) \times \gamma S^{3/4}\, NL$ (19)

Where γ denotes the number of transformers. When the rated capacity as S_N hours for a chosen transformer is 11 kV-TS, γ is taken to denote an average number of transformers S/S_N in the$11k\,V - TS$.

Substitute (15)-(19) for (14), then

$$K_0 = \left(\frac{1}{N} + H\right)\left(\frac{a_1}{S} + b_1\right) + E\left[\left(\frac{1}{N} + H\right)\sqrt{\frac{1}{\pi\sigma K_c}}\left(\frac{a_2 \cos\emptyset}{P_{av}} + \frac{b_2}{\sqrt{3}\,U_{Nj}}\right) + 7.26\,\frac{p_j \tau C_0}{U_N \cos^2\emptyset}\,\frac{10^{-5}}{\sqrt{\sigma}}\right] S^{\frac{1}{2}} + (8760 C_0 K_{Fe} + C_0 \tau_b K_{cu}) \frac{S^{3/4}\, NL}{S_N} \quad (20)$$

The determination of the objective function of a static (classical) model aims at making unit capacity annual cost minimum, i.e., $in\,K_0$, with the limits to constraint $S > 0$, such that we have the following model:

$$\begin{aligned} &\min K_0 \\ &s.t. \quad S > 0 \end{aligned} \quad (21)$$

Where K_0 is illustrated in Eqs. (20), and (21) are called classical geometric programming models, concerned with the model I.

5. Geometric Programming with Neutrosophic Coefficients

In this section, the objective function K_0 will be reformulated from classical annual coast in unit capacity into minimum neutrosophic function. We expect that there are many vague or incomplete factors in load, investment process, and electricity prices, where they hold many neutrosophic phenomena.

It is well known that the transformer substations' capacity is non-negative (i.e. $S > 0$), also K_0 is an exponential polynomial function having neutrosophic coefficients with respect to S, therefore the classical model can be changed into finding an answer to a neutrosophic minimum of annual cost under the capacity $S > 0$ in constraint, such that the geometric programming with neutrosophic coefficients can be written as a forthcoming model (22).

5.1 Building a Neutrosophic GPP Model in an Iraqi's Transformer Substation Depending Upon Neutrosophic Truth Membership Function Related to the Coefficient C_2

Solve the following problem

$$\begin{aligned} &min \quad K_0 \\ &s.t. \quad S > 0 \end{aligned} \quad (22)$$

Where,

$$K_0 = 91800 S^{-1} + 0.77\sigma^{-0.5} S^{0.5} \quad (23)$$

Having the first coefficient $c_1 = 91800$ as an ordinary real number, while the second coefficient $c_2 = 0.77\sigma^{-0.5}$ is a neutrosophic number varying in a certain interval. Suppose the truth membership function μ_A, indeterminacy membership function σ_A, and falsity of membership function v_A for the coefficient c_2 are defined as follows:

Let $A = [0.008, 0.03]$ be a certain neutrosophic interval in which $c_2 \in A$,

$$\mu_A(c_2) = \begin{cases} 0 & c_2 \le 0.008 \\ \left(\frac{c_2 - 0.008}{0.022}\right)^2 & 0.008 < c_2 < 0.03 \\ 1 & c_2 > 0.03 \end{cases} \quad (24)$$

$$\sigma_A(c_2) = \begin{cases} (\frac{c_2-0.008}{0.011})^2 & 0.008 < c_2 < 0.011 \\ \frac{1}{2} - (\frac{c_2-0.011}{0.03})^2 & 0.011 \le c_2 \le 0.03 \\ 0 & 0.008 \ge c_2 \ge 0.03 \end{cases} \quad (25)$$

$$v_A(c_2) = \begin{cases} 1 & c_2 \le 0.008 \\ 1 - (\frac{c_2-0.008}{0.022})^2 & 0.008 < c_2 < 0.03 \\ 0 & c_2 > 0.03 \end{cases} \quad (26)$$

It is easy to draw the above truth, indeterminacy, and falsity membership functions.

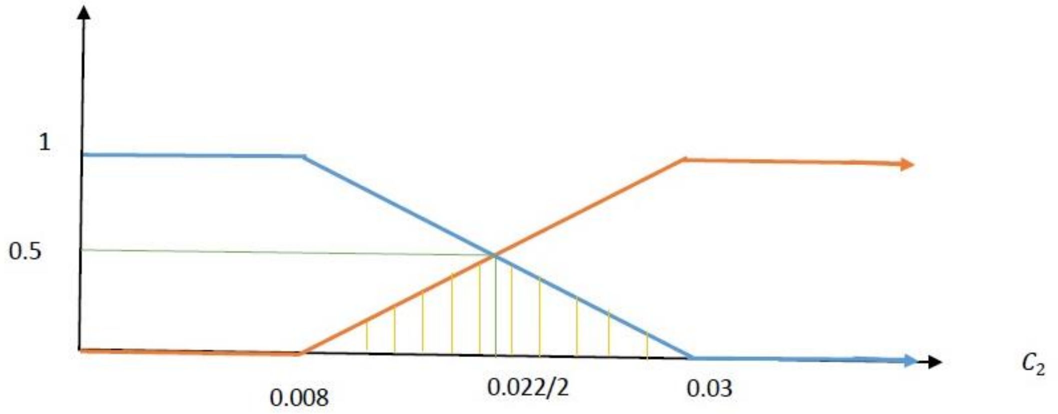

Figure 1: The blue linear function represents the region covered by $\mu_A(c_2)$, while the orange function represents the region covered by $v_A(c_2)$, and finally, the intersection region (yellow-shaded color) is the intersection region between $\mu_A(c_2)$ and $v_A(c_2)$ represents the region covered by $\sigma_A(c_2)$.

On the other hand, and depending upon [16], we have

$$(\frac{c_2-0.008}{0.022})^2 = 1 - \alpha \Rightarrow c_2 = 0.008 + 0.022\sqrt{1-\alpha} \quad (27)$$

Here, α denotes the $\alpha - cut$ related to the truth membership functions $\mu_A(c_2)$.

Consequently, the program (22) is turned into

$$\min K_0 = \{91800S^{-1} + (0.008 + 0.022\sqrt{1-\alpha})S^{0.5}\}$$
$$s.t. \; S > 0 \quad (28)$$

Program (28) is called neutrosophic polynomial geometric programming problems (NPGPP), we should not forget that the degree of the dual program for eq. (28) is equal to zero, so it is immediate to find the solution by means of the dual program. To solve this problem more easily way, we try to rewrite this program (i.e. eq. 28) in its dual form as follows:

$$\max \quad D = (\frac{91800}{\omega_0})^{\omega_0} (\frac{0.008+0.022\sqrt{1-\alpha}}{\omega_1})^{\omega_1}$$
$$s.t. \quad \omega_0 + \omega_1 = 1$$
$$-\omega_0 + 0.5\omega_1 = 0 \quad (29)$$
$$\omega_0, \omega_1 > 0, \;\; \alpha \in [0,1]$$

By solving the above (normality and orthogonality conditions), the values $\omega_0 = \frac{1}{3}, \omega_1 = \frac{2}{3}$ are obtained.

The well-known relationship between the primal of the GPP and its dual program is concluded by the below theorem:

Theorem [13]: If (P) is canonical and there exists a $\bar{x}$ such that $g_k(\bar{x}) < 1$ for $= 1,2,\dots,p$, then the following mathematical phrases are true:

i. The dual program (D) has a maximizing point δ^*,

ii. The maximum value $v(\delta^*)$ of problem(D) equals to the minimum value $g_\circ(x^*)$ of (P), {i.e. the primal and the dual problems are related through the fact that, for the optimal solution, $\min g_\circ(x) = \max v(\delta)$}.

iii. Each minimizing point x for (P) for the optimal solution $\min g_0(x) = \max v(\delta)$ satisfies

$$u_i(x) = \begin{cases} \delta_i^* v(\delta^*) & \text{for} \quad i = 0 \\ \dfrac{\delta_i^*}{\lambda_k(\delta^*)} & \forall\, i = 1,2,\dots k \text{ and } \lambda_k(\delta^*) \neq 0 \end{cases}$$

However, there is a good opportunity to study the various values of the dual objective function D depending on the values of α. The following formulas are:

- r is the mean radius in the supply area, or it is the economic power supply radius,

$$r = \sqrt{\frac{S_{av}}{\pi\sigma K_c}} \tag{30}$$

Suppose that the mean load density of Telafer township / Nineveh province/ Iraq country will raised to $\sigma = 5195\ kW/km^2$ by the year 2025, suppose the economic capacity of the specific transformer substation as S_{av}.

Average item N_b (which denotes the amount of 132 kV-TS that needs to be built up in Telafer district to meet the growing demand for electricity) given by the following formulas

$$N_b = \frac{\sigma Q K_c}{S} = \frac{\sigma Q K_c}{r_i^2 \pi \sigma K_c} = \frac{Q}{\pi {r_i}^2} \tag{31}$$

Keep in mind, the fact that, the area of the electrical supply on Telafer township station cover $Q = 1743.69\ km^2$.

- The numbers n_b in a unit area in the specific transformers substation TS,

$$n_b = \frac{N_b}{Q} = \frac{\sigma Q K_c}{S} = \frac{1}{\pi r_i^2} \tag{32}$$

- Note that $c_2 = 0.008 + 0.022\sqrt{1-\alpha}$, $\alpha \in [0,1]$, at $\alpha = 0 \Rightarrow c_2 = 0.03$, while at $\alpha = 1 \Rightarrow c_2 = 0.008$, as $0 < \alpha < 1 \Rightarrow 0.008 < c_2 < 0.03$.

The following Table 1 illustrates the $\max D$ are the approximate optimal solutions and optimal values for (29),

Table 1. The range values of D.

Index i	$\alpha_i \in [0,1]$	$\max D = (\frac{91800}{\omega_0})^{\omega_0}(\frac{0.008+0.022\sqrt{1-\alpha_i}}{\omega_1})^{\omega_1}$	$r_i = \sqrt{\frac{S_{av_i}}{\pi\sigma K_c}}$ $K_c = 2.2\ kV$; $\sigma = 5915\ kW/km^2$
1	0	$d_1 = 8.23119687$	0.641439553 km
2	0.1	$d_2 = 8.02337386$	0.649671351 km
3	0.3	$d_3 = 7.56001993$	0.66923184 km
4	0.5	$d_4 = 7.00574202$	0.695134289 km
5	0.7	$d_5 = 6.29202210$	0.733404644 km
6	0.8	$d_6 = 5.82046397$	0.762466041 km
7	0.9	$d_7 = 5.17541713$	0.808481231 km
8	1	$d_8 = 3.41016566$	0.995585028 km

Note that, the values of α's were selected depending on the author's decision. To evaluate the values of r_i. Now we need to determine the average values S_{av_i}, by the previous theorem. we have the following relationship between the terms of the primal program and its corresponding terms of dual program:

$91800\,S^{-1} = \frac{1}{3}\,d_i \quad \forall\, i = 1,2,\ldots,8$ (33)

$\left(0.008 + 0.022\sqrt{1-\alpha_i}\right)S^{0.5} = \frac{2}{3}d_i \quad \forall\, i = 1,2,\ldots,8$ (34)

Suppose that all evaluated S through Eq. (33) are symbolized by S_1, and all computed S through eq. (34) symbolized by S_2. The following Table 2 illustrates all values of S_1 and S_2, this is for each $i = 1,2,\ldots 8$:

Table 2. The Average Values of S_1 and S_2 Denoted by S_{av} .

index i	$S_1 = \frac{91800}{1/_3\, d_i} = \frac{275400}{d_i}$	$S_2 = \left(\frac{\frac{2}{3}d_i}{0.008 + 0.022\sqrt{1-\alpha_i}}\right)^2$	$S_{av_i} = \frac{S_1 + S_2}{2}$
1	33458.0747	182.915482	16820.4951
2	34324.7124	185.269297	17254.9909
3	36428.4754	190.862453	18309.669
4	39310.6111	198.269037	19754.4401
5	43769.7128	209.212124	21989.4625
6	47315.8156	217.52199	23766.6688
7	53213.1021	230.679653	26721.8909
8	80758.54	284.180472	40521.3603

Substituting all amounts of S_{av_i}, in the Table 1 to enumerate the values of r_i. Now, the last duty is to determine the optimal value of S_{av_i} that gives the optimal solution for problem (28), tracking the concluded values of the below Table 3:

Table 3. The approximate values of the primal program.

index i	$S_{av_i} = \frac{S_1 + S_2}{2}$	$\min K_0 = \left\{91800(S_{avi})^{-1} + \left(0.008 + 0.022\sqrt{1-\alpha}\,\right)(S_{avi})^{0.5}\right\}$
1	16820.4951	9.34844324
2	17254.9909	9.11264828
3	18309.669	8.58689587
4	19754.4401	7.95791296
5	21989.4625	7.14789479
6	23766.6688	6.61264497
7	26721.8909	5.88038304
8	40521.3603	3.87586527

From Tables 2 and 3, and in terms of Eqs. (33) and (34), the approximate optimal value of $K_0 \cong 3.8758627$ which holds at the optimal economic capacity $S_{av8} = 40521.3603$ of 132 kV- TS. Moreover, by the results of Table 1, we can see that the value of the approximate optimal economic power supply radius is $r_8 = 0.995585028\ km$, as well as the optimal value of $N_b \cong 559.96332$ occurs at r_8 (i.e., about (560) 132 $kV - TS$ needs to build up in Telafer township).

5.2 Building a Neutrosophic Model Depending Upon Either Falsity or Indeterminacy Membership Functions Related to the Coefficient C_2

The fact that many researchers in the field of neutrosophic optimization may ignore or may have been unaware of it, is that the indeterminacy membership function exactly represents the intersection region of the truth membership function and the falsity membership function as we sighted it by the representing diagram (1). Hence, for this manuscript, we took the vagueness for the second coefficientc_2, so the following mathematical intersection is completely true:

$$\sigma_A(c_2) = \mu_A(c_2) \cap \nu_A(c_2) \tag{35}$$

For solving the program (22) with respect to its falsity membership function and depending upon the thoughts presented in [ ], we can suppose:

$$1 - \left(\frac{c_2 - 0.008}{0.022}\right)^2 = \beta \Rightarrow \left(\frac{c_2 - 0.008}{0.022}\right)^2 = 1 - \beta = \alpha \tag{36}$$

Here, β is the β- cut related to the falsity membership function $\nu_A(c_2)$, eq. (29) is exactly given the same solution as Eq. (27), which means Eq. (36) is somehow considered a dual form to Eq. (27). Also, there is another unfathomable program that gives the solution of neutrosophic polynomial geometric programming (22) by using the indeterminacy membership function $\sigma_A(c_2)$:

$$\frac{1}{2} - \left(\frac{c_2 - 0.008}{0.022}\right)^2 = \gamma \tag{37}$$

Where $\gamma \in [0,1]$ is the γ- cut corresponding to $\sigma_A(.)$, Eq. (30) implies that :$\left(\frac{c_2 - 0.008}{0.022}\right)^2 = \frac{1}{2} - \gamma \Rightarrow c_2 - 0.011 = 0.0009\sqrt{0.5 - \gamma} \Rightarrow$

$c_2 = 0.011 + 0.0009\sqrt{0.5 - \gamma}$.

Consequently, the program (15) can be reformulated as:

$$\begin{aligned} \min K_0 &= \left\{91800S^{-1} + (0.011 + 0.0009\sqrt{0.5 - \gamma})S^{0.5}\right\} \\ & s.t.\ S > 0 \end{aligned} \tag{38}$$

Program (38) is defined as a neutrosophic posynomial geometric programming problem, and the main difference between program (28) and program (38): is that program (28) is NPGP related to the truth-membership function of the coefficientc_2, while the program (38) is NPGP related to the indeterminacy membership function of the same coefficientc_2. Also, the same previous analysis tables (1, 2, 3) that were for $\alpha, \max D$, r_i can be re-written and re-analysis for $\gamma, \max D, r_i$.

6. Conclusions

This manuscript discussed an innovative trying to analyze the annual cost of investment in the power supply systems with respect to the validity of some uncertainty by assuming the neutrosophic coefficient c_2, to be able to calculate the mean of the economic capacity and economic supply radius of 132 kV- transformer substation in Telafer township, all these issues held by building mathematical non-linear programming named Neutrosophic Geometric Programming Problems (NGPP) this was for the first time, also there more analyzing techniques can be made for the same geometric programming problems with the neutrosophic point of view, either by a truth membership function, or by a falsity membership function, or by an indeterminacy membership function, to their corresponding α, β, γ- cuts.

Acknowledgments
This research is supported by the Neutrosophic Science International Association (NSIA) in both of its headquarters at New Mexico University and its Iraqi branch at Telafer University, for more details about (NSIA) see the URL http://neutrosophicassociation.org/.

Author Contributions
All authors contributed equally to this research.

Data availability
The datasets generated during and/or analyzed during the current study are not publicly available due to the privacy-preserving nature of the data but are available from the corresponding author upon reasonable request.

Funding
This research received all its funding from the Neutrosophic Science International Association (NSIA)/ Iraqi Branch.

Conflict of interest
The authors declare that there is no conflict of interest in the research.

References

1. Peterson, E. L., (1976) "Geometric Programming" SIAM Review Society for Industrial and Applied Mathematics (18), 1-51.
2. Passy, U., & Wilde, D. J. (1967). Generalized polynomial optimization. SIAM Journal on Applied Mathematics, 15(5), 1344-1356. https://doi.org/10.1137/0115117
3. Dinkel, J. J., & Kochenberger, G. A. (1974). Note—A Note on "Substitution Effects in Geometric Programming". Management Science, 20(7), 1141-1143. https://doi.org/10.1287/mnsc.20.7.1141
4. Al-Bayati, A. Y. and Khalid H. E. (2009). "An Original GPP Algorithm to Solve Two Coefficients Sensitivity Analysis " American J. of Engineering and Applied Sciences 2(2):pp.481-487.
5. Al-Bayati, A. Y., & Khalid, H. E. (2009). An Alternative Geometric Programming Algorithm to solve two Coefficients Sensitivity Analysis Problems. Australian Journal of Basic and Applied Sciences, 3(3), 2838-2846.
6. Al-Bayati, A. Y. and Khalid H. E. (2013) "Generalized Increment Analysis in Geometric Programming Problems'' The Second International Scientific Conference, University of Mosul, College of Basic Education, 518-534.
7. Y Al-Bayati, A., & E Khalid, H. (2011). Multi-Objective GPP with General Negative Degree of Difficulty: New Insights. IRAQI JOURNAL OF STATISTICAL SCIENCES, 11(2), 35-51.
8. Al-Bayati, A. Y., & Khalid, H. E. (2012). On multi-objective geometric programming problems with a negative degree of difficulty. Iraqi Journal of Statistical Science, 21, 1-14.
9. Ecker, J. G. (1980). Geometric programming: methods, computations and applications. SIAM review, 22(3), 338-362. https://doi.org/10.1137/1022058
10. Hsiung, K. L., Kim, S. J., & Boyd, S. (2008). Tractable approximate robust geometric programming. Optimization and Engineering, 9, 95-118. https://doi.org/10.1007/s11081-007-9025-z
11. Y. Y. Yu, X.Z. Wang, Y.W. Yang (1991). Optirnizational selection for substation feel econornic radius. 1 of Changsha Normal University of Water Resources and Electric Power, 6(1): 118-124.
12. H. E. Khalid, A. Y. Al-Bayati, (2010). Investigation in the Sensitivity Analysis of Generalized Geometric Programming Problems, PhD Thesis, The Council of the College of Computers Sciences and Mathematics University of Mosul.
13. Q.Y.Yang, Z.L.Zhang, M.Z.Yang, (1987). Transformer substation capacity dynarnic optirnizing in city power network planning. Proc. of Colleges and Univ. Speciality of Power System and Its Automation. The Third a Academic Annual Conference, Xian: Xian Jiao Tong Univ. Press, 7-11.

14. Mikic, O. M. (1986). Mathematical dynamic model for long-term distribution system planning. IEEE transactions on power systems, 1(1), 34-40.
15. Khalid, H. E., & Essa, A. K. (2021). The Duality Approach of the Neutrosophic Linear Programming. Neutrosophic Sets and Systems, 46, 9-23.

Received: 03 Nov 2023, **Revised:** 28 Feb 2024,

Accepted: 28 Mar 2024, **Available online:** 04 Apr 2024.

Neutrosophic Systems with Applications, Vol. 16, 2024
https://doi.org/10.61356/j.nswa.2024.16214

B_{V2}TrS Appraiser Model: Enforcing BHARAT Version2 in Tree Soft Modelling for Appraising E-Mobility Hurdles

Mona Mohamed [1,*], Florentin Smarandache [2], and Michael Voskoglou [3]

[1] Higher Technological Institute, 10th of Ramadan City 44629, Egypt; mona.fouad@hti.edu.eg.
[2] University of New Mexico, 705 Gurley Ave., Gallup, NM 87301, USA; smarand@unm.edu.
[3] School of Engineering, University of Peloponnese (ex-Graduate TEI of Western Greece), 26334 Patras, Greece; mvoskoglou@gmail.com.

* Correspondence: mona.fouad@hti.edu.eg

Abstract: Electric vehicles (EVs) are being introduced to lessen greenhouse gas (GHG) emissions, air pollution, and reliance on fossil fuels. As a result of the government's aggressive promotion of EVs and rising environmental consciousness, EVs are quickly rising to the top of the low-carbon transportation market. Several viewpoints suggested that shifting to electric vehicles has been seen as a potential way to achieve sustainable mobility. Nevertheless, many studies discussed the obstacles and hurdles that obstruct the embracing of various electric-mobility (E-mobility) as EVs and electric-scooters (E-scooters) as eco-friendly means. Herein, we discussed these hurdles and determined them through surveys for prior studies. Therefore, appraising these hurdles is the objective of our study. Best Holistic Adaptable Ranking of Attributes Technique – version 2 (BHARAT -v2) as a novel Multi-Criteria Decision Making (MCDM) technique is leveraged as an appraiser technique for these hurdles. Tree Soft (TrS) methodology is utilized for modeling these hurdles. Hence, we hybridized and integrated two methodologies for constructing BHARAT v2 Tree Soft (Bv2TrS) as an appraiser model. Subsequently, we discussed the findings of the Bv2TrS appraiser model.

Keywords: Electric Vehicles (EVs); Electric-Mobility (E-mobility); Tree Soft; Multi-Criteria Decision Making (MCDM); Best Holistic Adaptable Ranking of Attributes Technique - version2 (BHARAT-v2).

1. Introduction

A global effort is underway to employ renewable energy sources to cut greenhouse gas emissions ;hence achieving a green environment. There are several motivations why nations embrace the concept of a green environment. Whilst [1] highlighted two well-known important environmental issues that are facing the world now are climate change and global warming. Also, the scholars demonstrated that the transport sector is considered the main contributor to these issues. This has been confirmed by [2] where more than 20% of the world's CO_2 emissions come from the transportation sector. [3] stated that fossil fuels like petroleum and diesel, whose burning produces carbon dioxide and other greenhouse gases, are largely used in transportation. As well [4] indicated that India's swift industrialization and commercialization will increase the country's need for transportation, which would increase the demand for vehicles. One growing concern among these forecasts of affluence in the future is global warming. Thereby [5] fossil fuel-powered vehicles are starting to be banned by several territories. An impending shift in the transportation system [6] toward a low-carbon, ecologically sustainable regime is necessary to combat the danger posed by greenhouse gas (GHG) emissions, air pollution, and reliance on finite fossil fuels.

Given a variety of technologies, approaches, and innovations in [7] to help decarbonization, the market for electric vehicles (EVs) is expanding quickly. Moreover, EVs were introduced by Kumar et al. [8] as one of the best ways to address the current climate crisis. This alteration provides safe, emission-free transportation, improves health, lowers energy prices and consumption, preserves land, and creates jobs [9]. According to [10] As environmentally beneficial and sustainable substitutes for traditional internal combustion engine (ICE)-based automobiles, EVs have drawn a lot of interest.

Even while EVs are better for the environment, there are still significant barriers to their widespread adoption. prior perspectives as [11] categorized the obstacles and hurdles to market penetration from the viewpoints of investors, manufacturers, and governmental organizations. Others as [12] highlighted three categories have been identified as the elements influencing consumers' inclinations to embrace electric vehicles: A user's psychological factors include driving experience, attitudes, emotions, perceived behavioral control, societal influence, and symbolic value. (i) Situational factors include technical specifications, price, environmental factors, and subsidy policy. (ii) Individual variables include gender, age, occupation, income, and education. (iii) Household variables include vehicle ownership, accessibility to plug-in vehicles at home, and household size.

Accordingly, various scholars as [13] Prior research have attempted to determine the hurdles to EV adoption from the viewpoints of experts or users. A pilot study of the clients and expert opinion have been utilized to direct the research to narrow down the identified hurdles. Thereby [14] emphasized the existence of interrelatedness between the examined EV hurdles using factor analysis and recommended, simplifying the problem, concentrating on the reduced set of barriers according to the degree of linkage between those.

Herein, we are analyzing electric mobility in other words e-mobility's hurdles in the form of categories and sub-categories. Hence, we are structuring this problem into a hierarchical shape by using a novel methodology of tree soft sets (TSSs) introduced by Smarandache [15]. Also, this methodology has proven its efficiency and implemented in other studies and applications as evaluating Cloud Services [16] also, in bioinformatics problems [17]. Nevertheless, analyzing mobility's hurdles is based on experts who are related to this field. The appraising process is conducted through leveraging the ability of Multi-Criteria Decision Making (MCDM) techniques which are able to treat conflicting criteria[18–22]. Accordingly, this study contributed to harnessing a novel technique of MDM is Best Holistic Adaptable Ranking of Attributes Technique (BHARAT). this technique is proposed by Rao [23] which harnessed BHARAT version-1 for the first time in selecting optimal electronic commerce (E-commerce) websites in [24].

Generally speaking, the study's objectives are illustrated in a set of points:

1. Conducting surveys related to our scope based on prior studies.
2. Highlighting the importance of e-mobility and EVs toward bolstering the green environment as a result of the previous point. Also, e-mobility's hurdles impede the embracing and implementation of e-mobility and EVs.
3. Determining the hurdles of e-mobility and classifying it into a set of levels through leveraging TSSs.
4. Appraising the determined hierarchical hurdles through BHARAT -v2 of MCDM techniques based on a soft scale used by an expert for appraising. Resulting in, constructing a BHARAT-v2 tree soft model ($B_{v\text{-}2}$TrS) to appraise e-mobility's hurdles.
5. The most and least influential hurdle is the result of the $B_{v\text{-}2}$TrS model.

2. Survey of the Scientific Studies and Methodologies

The intent of conducting this section is to survey and examine the related studies that serve and cover the study's objectives which are stated in previous points.

2.1 Obstacles to Embracing Electric Mobility

For analyzing the e-mobility's hurdles, the crucial step is determining contraindications that retard the implementation of e-mobility for achieving a green environment. The result of conducted surveys of [4, 25] is aggregated in Figure 1.

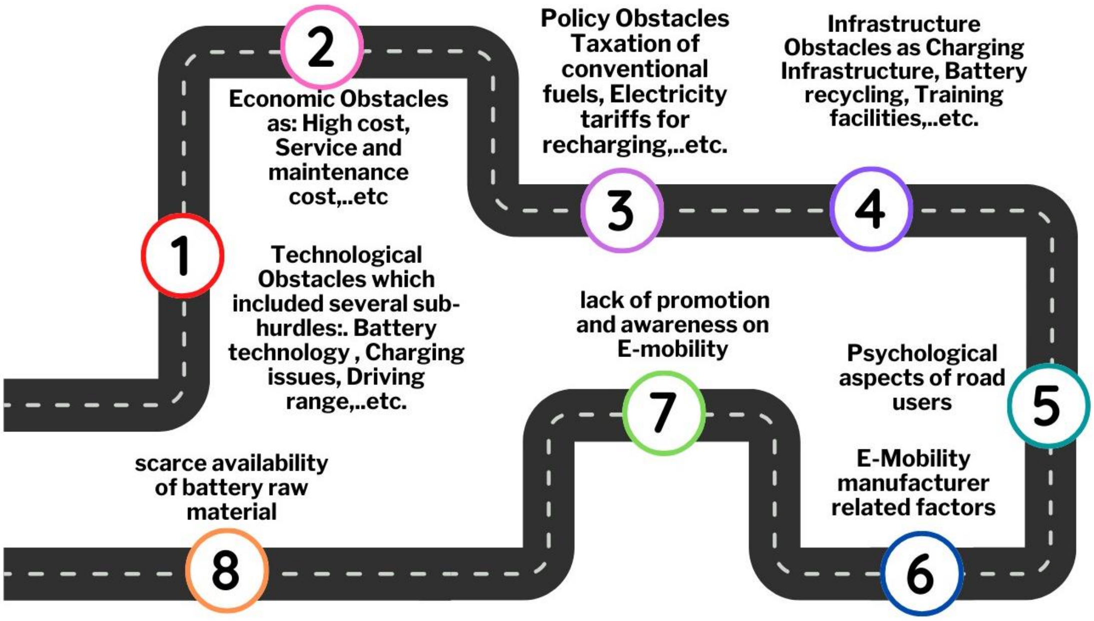

Figure 1. Electric-mobility hurdles.

2.2 *Methodologies for Evaluation E-Mobility*

Herein, we highlight the utilized methodologies that volunteered for appraising e-mobility with various purposes.

The appraising process for e-mobility is conducted by constructing pair-wise matrices based on the Analytical Hierarchical Process (AHP) in [26]. the best and worst criterion that contributes to appraising e-mobility is determined through [27] by employing the best-worst method (BWM). Others rank a set of alternatives of e-mobility and select the optimal one amongst the determined alternatives with support of the Technique for Order of Preference by Similarity to the Ideal Solution (TOPSIS) [28]. Another ranker of MCDM is exploited for ranking alternatives which is represented in VIsekriterijumska optimizacija KOmpromisno Resenje (VIKOR) [29] with support from objective MCDM method of entropy for obtaining criteria's weights. Ecer et al. [30] Used weight-multiplied comparable and weight-similar sequences for performance analysis, the COmbined COmpromise Solution (CoCoSo) technique generates a ranking list. MCDM techniques and the Delphi study are used in [31] to identify and assess the drivers for addressing LIB recycling and explore its key drivers.

2.3 *Core Concepts: New Methodologies in Decision-Making*

This sub-section intends to illustrate the utilized key conceptions in this study and their role in the appraising process.

2.3.1 **Tree Soft Methodology: Structuring Appraising Problem into Hierarchical Form**

We are using a novel expansion of the soft set involved in TSSs in this investigation, which was first introduced by Smarandache and emphasized in [15]. After that scholars of [16] embraced this new expansion and described it as:

Let $\aleph$ be a universe of discourse that includes τ a non-empty as a subset of $\aleph$, thus the powerset of τ expressed as p (τ).

Assume that our tree soft set encompasses a set of levels, each one has a multitude of nodes:

Level 1: consists of a multitude of nodes where each node represents the main criteria or hurdles, then expressed as Hu = {Hu_1, Hu_2,..Hu_n} for integer n ≥ 1.

Level 2: includes several sub-nodes of {Hu_1, Hu_2, ..Hu_n} and stated as { $Hu_{1-1,}$ …Hu_{1-n} } branched of Hu_1 , { $Hu_{2-1,}$ …Hu_{2-n} } branched of Hu_2 , finally { $Hu_{n-m,}$ …Hu_{n-m} } branched of Hu_n .

We call the leaves of the graph-tree, all terminal nodes (nodes that have no descendants).

Then, Tree Soft Set: F: P (Tree (Hu)) → p (τ).

Tree (Hu) is the set of all nodes and leaves (from level 1 to level n) of the graph tree, and P (Tree(δ)) is the powerset of the Tree (Ind). All node sets of TSSs of level n as Tree (Hu) = {Hu_{nm} | nm= 1, 2, ...}.

2.3.2 **Novel BHARAT: Analyzing Hurdles and Sub-hurdles in Constructed Tree Soft**

Generally, BHARAT is considered a novel MCDM technique proposed by Rao [23]. Moreover, it is illustrated and applied in [24]. Herein, we applied BHARAT -v2 in our appraising problem through pair-wise matrices for hurdles and sub-hurdles in tree soft as follows:

1. For generating nodes' weights in level 1:
   1.1 Constructing pairwise matrices for main hurdles based on a number of decision-makers (DMs) who contribute to ranking hurdles. MS utilized soft scales in [32] for ranking main hurdles with each other.
   1.2 Aggregate the constructed matrices into a single decision matrix. Then, computational operations are conducted to obtain the main hurdles' weights based on Eqs. (1) and (2).

$$\wp = \sum_{i=1}^{i} \frac{1}{x_j} \tag{1}$$

$$w_i = \frac{1/\wp}{\sum_{i=1}^{m} 1/\wp} \tag{2}$$

   where x_j indicates to rank of the criterion
2. For generating sub-node weights in level 2:
   2.1 Constructing pairwise matrices for each sub-hurdle by soft scale used by DMs.
   2.2 Aggregate the constructed matrices into a single decision matrix for each sub-hurdle. After that, local weights are generated based on Eqs (1) and (2), and global weights are obtained by multiplying the main hurdles' weights by local sub-hurdles' weights.
3. Ranking main hurdles and sub-hurdles based on weight values.
   - Rank 1: largest main and sub-hurdle weight.
   - least rank: smallest main and sub-hurdle weight.

3. Description of BHARAT-v2 Tree Soft Model: Bv_2TrS

The methodologies in the previous two sub-sections are leveraged in appraising the problem of this study. The following steps illustrate procedures for implementing these novel methodologies in solving our problem of appraising.

3.1 Gathering Information and Prioritizes

- Determining the influenced hurdles and sub-hurdles.
- Forming a panel of experts or DMs who related to our appraising problem. These DMs are contributing to appraising and ranking main and sub-hurdles.
- Soft scale in [32] we utilized a 7-point scale for non-beneficial attributes, where hurdles and sub-hurdles were considered non-beneficial attributes.

3.2 Modeling Influenced Hurdles and Sub-Hurdles into Tree Soft Structure

- Forming the influenced main and sub hurdles into a multitude of levels.
- At level 1: Main hurdles resident in tree soft as nodes in this level.
- At level 2: Sub-hurdles resident in tree soft as nodes which inherent from nodes in level 1.

3.3 Implementing BHARAT v2 in Tree Soft to Obtain Main and Sub-Hurdles' Weights

BHARAT v2 works in nodes of TreeSoft to solve the problem of appraising.

3.3.1 **N of Pairwise Matrices are Constructed Based on N of DMs**

- Forming the influenced main and sub hurdles into a multitude of levels.
- At level 1: for each node or main hurdle, N of pairwise matrices is constructed.
- For each node, Eq. (3) is implemented for generating an aggregated matrix.
- $\text{Average or Aggregated of DMs'rating} = \frac{DM_{1+}\ DM_{2+\cdots\ldots\ldots+}DM_n}{n}$ (3)

  Where n is the number of DMs.
- In the aggregated matrix for each node, the average for each hurdle per column is calculated. Hence vector of values is generated.
- The generated vector is utilized to produce a new matrix. Calculating the average for each hurdle per raw ($\mathcal{g}$) and calculating the sum of the average column ($\hbar$).
- Weights of main hurdles are computing as in Eq. (4).

  $w_{i=} \frac{\mathcal{g}}{\hbar}$ (4)
- At level 2: for each Sub-node or sub-hurdle, N of pairwise matrices is constructed.
- The aggregated matrix for each sub-hurdle is computing. The average for each sub-hurdle per column is calculated. Hence vector of values is generated.
- Eq. (4) is utilized for obtaining local weight for each sub-hurdle ($\mho_i$).
- Finally, the global weight for each sub-hurdle $\mathfrak{R}_i$ based on Eq. (5).

  $\mathfrak{R}_{i=} w_i * \mho_i$ (5)
- Ranking sub-hurdles based on values of $\mathfrak{R}_i$.

4. An Empirical Case Study: Validating B$_{v2}$TrS

The purpose of this section is to verify the authenticity of our constructed B$_{v2}$TrS. Thus, we applied this B$_{v2}$TrS model in a case study. Accordingly, the previous procedures of B$_{v2}$TrS are implemented in this case study as the following.

4.1 We are communicating with a group of DMs to form a DMs panel. Thereby, three DMs are contributing to appraising e-mobility's hurdles

4.2 The appraising is conducted for three main hurdles and ten sub-hurdles as mentioned in Figure 2

4.3 Tree soft illustrates three main hurdles and ten sub-hurdles in a hierarchical structure.

4.4 BHARAT-v2 is leveraging in constructed tree soft to appraise the main hurdles of e-mobility and obtaining weights for hurdles

4.4.1 4BHARAT-v2 starts with level one to obtain weights for three nodes by appraising these nodes according to three DMs (see Appendix A, Table A1).

4.4.2 An aggregated matrix is generated by calculating the mean of three pair-wise matrices through applying Eq. (3) as listed in Table 1.

4.4.3 Vector for mean for main hurdles (H_n) through calculating the average for each main hurdle per column. Hence, {1.65666667, 1.342211, 0.59256667} are mean for H_1, H_2, H_3.

4.4.4 This vector is utilized in Table 2 to obtain hurdles weights.

4.4.5 Through applying Eq. (4), the hurdles' weights.

Table 1. Aggregated matrix

Aggregated	H_1	H_2	H_3
H_1	0.5	0.666633	0.7222
H_2	2.73	0.5	0.5555
H_3	1.74	2.86	0.5

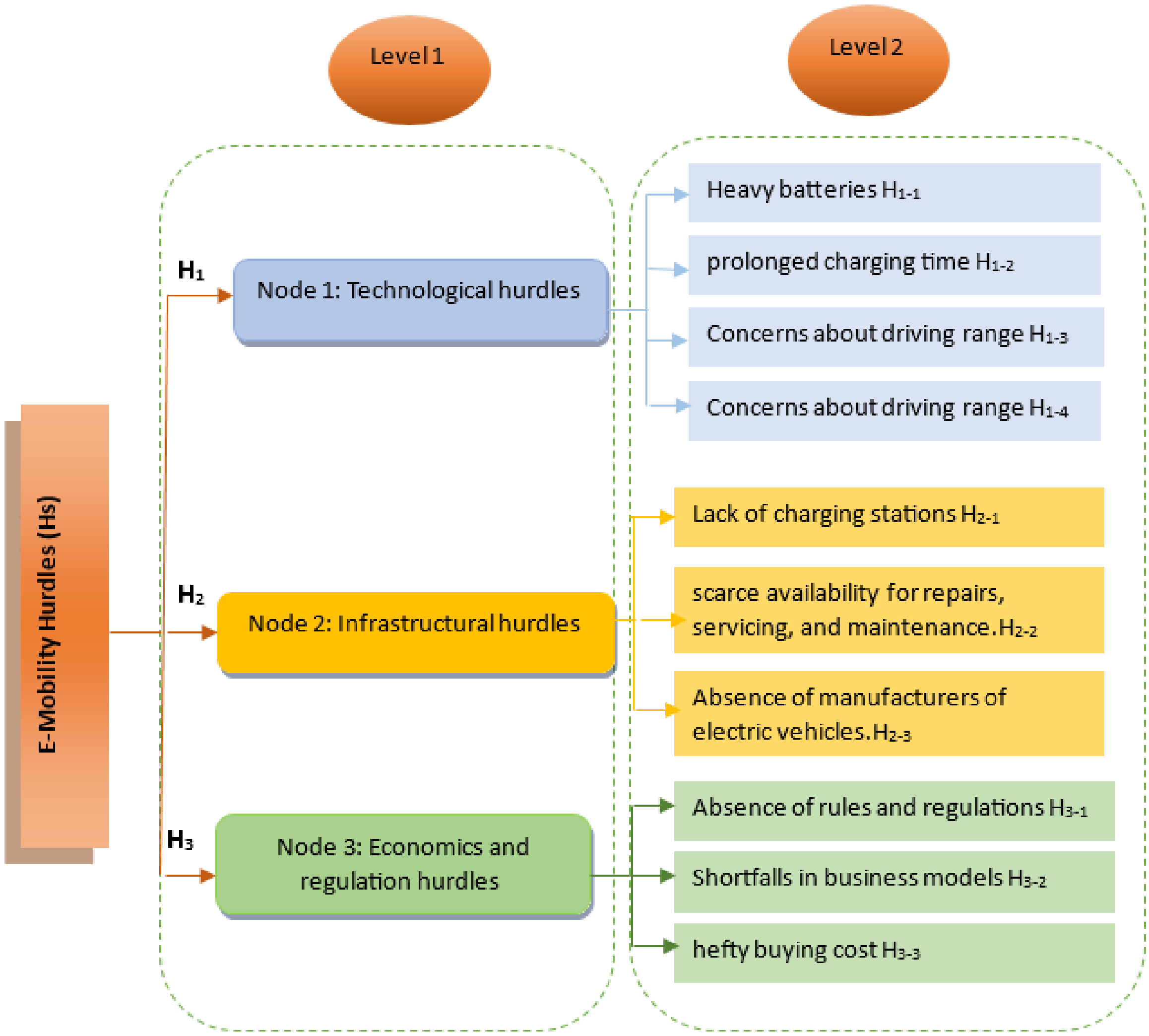

Figure 2. Tree soft model for main and sub-hurdles for e-mobility.

4.5 BHARAT-v2 is leveraging in level 2 of Tree Soft to appraise sub-hurdles of Technology and obtain weights for it

4.5.1 For each sub-hurdle, three DMs are generating pair-wise matrices (see Appendix A, in Tables A2).

4.5.2 The Aggregated matrix for each sub-hurdle is generated as listed in Table 3.

4.5.3 Vector for mean for sub-hurdles ($H_{1\text{-}n}$) through calculating the average for each sub-hurdle per column. Hence, {2.900333, 1.493688889, 0.555533} are mean for $H_{1\text{-}1}$, $H_{1\text{-}2}$, $H_{1\text{-}3}$.

4.5.4 Eq. (4) is utilized for obtaining local weights for sub-hurdles of Technology as in Table 4 and global weight is computed through using Eq. (5) and listed in Table 4.

4.6 BHARAT-v2 is leveraging in level 2 of Tree soft to appraise sub-hurdles of Infrastructure and obtain weights for it

4.6.1 For each sub-hurdle, three DMs are generating pair-wise matrices (see Appendix A, in Tables A3).

4.6.2 The Aggregated matrix for each sub-hurdle is generated as listed in Table 5.

4.6.3 Vector for mean for sub-hurdles ($H_{2\text{-}n}$) through calculating the average for each sub-hurdle per column. Hence, {2.203333, 0.972211111, 0.555533} are mean for $H_{2\text{-}1}$, $H_{2\text{-}2}$, $H_{2\text{-}3}$.

4.6.4 Eq. (4) is utilized for obtaining local weights for sub-hurdles of Technology as in Table 6 and global weight is computed through using Eq. (5) and listed in Table 6.

4.7 BHARAT-v2 is leveraging in level 2 of Tree Soft to appraise sub-hurdles of Economics and regulation and obtain weights for it

4.7.1 For each sub-hurdle, three DMs are generating pair-wise matrices (see Appendix A, in Tables A4).

4.7.2 The aggregated matrix for each sub-hurdle is generated as listed in Table 7.

4.7.3 Vector for mean for sub-hurdles ($H_{3\text{-}n}$) through calculating the average for each sub-hurdle per column. Hence, {0.78, 0.798877778, 0.648022} are mean for $H_{3\text{-}1}$, $H_{3\text{-}2}$, $H_{2\text{-}3}$.

4.7.4 Eq. (4) is utilized for obtaining local weights for sub-hurdles of Technology as in Table 6 and global weight is computed through using Eq. (5) and listed in Table 8.

4.8 Ranking sub-hurdles based on global weight values in Tables 4, 6, 8

Table 2. The main hurdles weigh in level 1.

	H_1	H_2	H_3	Average	weights
H_1	1.65666667/1.65666667	1.34/1.65666667	0.59256667/1.65666667	0.721	0.721/3.461=0.208321
H_2	1.65666667/1.34	1.34/1.34	0.59256667/1.34	0.89	0.89/3.461=0.257151
H_3	1.65666667/59256667	1.34/.59256667	59256667/59256667	1.85	1.85/3.461=0.534528
Total Sum				3.461	1

Table 3. Aggregated matrix for sub-hurdles of technology.

Aggregated	$H_{1\text{-}1}$	$H_{1\text{-}2}$	$H_{1\text{-}3}$
$H_{1\text{-}1}$	0.5	0.611066667	0.7222
$H_{1\text{-}2}$	2.851	0.5	0.4444
$H_{1\text{-}3}$	5.35	3.37	0.5

Table 4. Global weights of sub-hurdles of technology in level 2.

	$H_{1\text{-}1}$	$H_{1\text{-}2}$	$H_{1\text{-}3}$	Average	Local weight	Global weight
$H_{1\text{-}1}$	2.900333/2.900333	1.493688889/2.900333	0.555533/2.900333	0.57	0.57/4.63=0.12311	0.025646
$H_{1\text{-}2}$	2.900333/1.493688889	1.493688889/1.493688889	0.555533/1.493688889	1.11	1.11/4.63=0.239741	0.049943
$H_{1\text{-}3}$	2.900333/0.555533	1.493688889/0.555533	0.555533/0.555533	2.95	2.95/4.63=0.637149	0.132732
Total Sum				4.63	1	0.208321

Table 5. Aggregated matrix for sub-hurdles of infrastructure.

Aggregated	$H_{2\text{-}1}$	$H_{2\text{-}2}$	$H_{2\text{-}3}$
$H_{2\text{-}1}$	0.5	0.666633333	0.4444
$H_{2\text{-}2}$	1.81	0.5	0.7222
$H_{2\text{-}3}$	4.3	1.75	0.5

Table 6. Global weights of sub-hurdles of infrastructure in level 2.

	$H_{2\text{-}1}$	$H_{2\text{-}2}$	$H_{2\text{-}3}$	Average	Local weight	Global weight
$H_{2\text{-}1}$	2.203333/2.203333	0.9722111/2.203333	0.555533/2.203333	0.57	0.57/4.07=0.14004914	0.036014
$H_{2\text{-}2}$	2.203333/.97	0.9722111/0.9722111	0.555533/.0.9722111	1.28	1.28/4.07=0.314496314	0.080873
$H_{2\text{-}3}$	2.203333/.56	0.9722111/.0.555533	0.555533/0.555533	2.22	2.22/4.07=0.545454545	0.140264
Total Sum				4.07	1	0.257151

Table 7. Aggregated matrix for sub-hurdles of economics and regulation.

Aggregated	H_{3-1}	H_{3-2}	H_{3-3}
H_{3-1}	0.5	0.666633333	0.610867
H_{3-2}	1.84	0.5	0.8332
H_{3-3}	4.2.84	1.23	0.5

Table 8. Global weights of sub-hurdles of economics and regulations in level 2.

	H_{3-1}	H_{3-2}	H_{3-3}	Average	Local weight	Global weight
H_{3-1}	0.78/0.78	.799/.78	0.65/.78	0.953	0.953/3.033=0.314210353	0.167954104
H_{3-2}	.78/.799	.799/.799	.65/.799	0.94	0.94/3.033=0.309924167	0.165663019
H_{3-3}	.78/.65	.799/.65	.65//.65	1.14	1.14/3.033=0.37586548	0.20091047
Total Sum				3.033	1	0.534527593

5. Discussion

To validate the authenticity of the $B_{v2}TrS$ model, we applied it to a case study. Also, determining technological, infrastructure, and economics and regulations as the main hurdles for e-mobility. Accordingly, its sub-hurdles are determined.

In this study tree soft is utilized for modeling these influenced hurdles into a multitude of nodes in various levels as shown in Figure 2. After that BHARAT-v2 was implemented in tree soft modeling to obtain weights for each node contained in each level. Subsequently, the influenced hurdles of e-mobility are ranked according to global weights for each sub-hurdle. Figure 3 represents the ranking of each sub-hurdle for every main hurdle. For instance, H_{1-3} is the most influential hurdle in technology, otherwise H_{1-1} is the least. Also, H_{2-3} is the most influenced hurdle in infrastructure, otherwise H_{2-1} is the least. Finally, H_{3-3} is the most influenced hurdle in infrastructure, otherwise H_{3-2} is the least influenced.

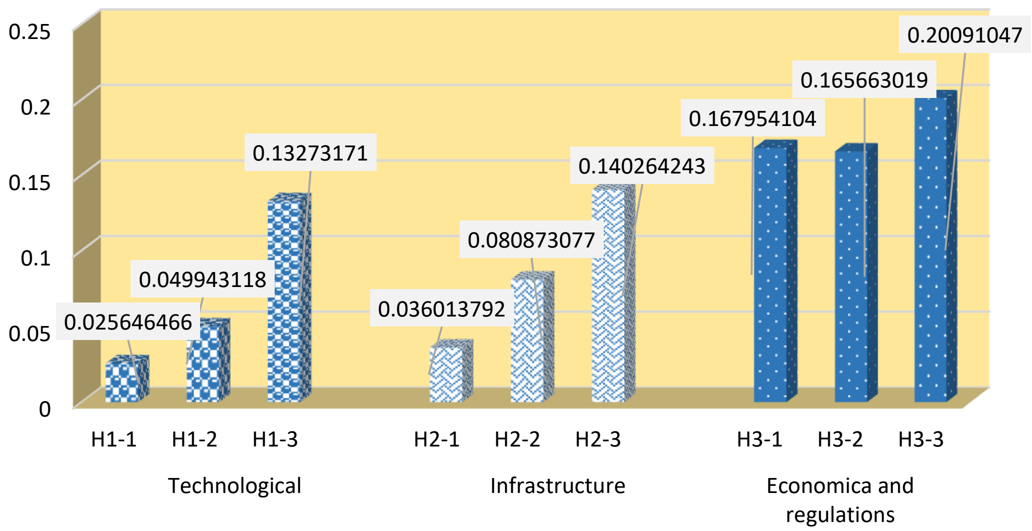

Figure 3. Ranking of sub-hurdles of e-mobility based on global weights.

6. Conclusions

E-mobility as EVs and e-scooters is an effective inducement to adopt the notion of a green environment. Consequently, the market for EVs is quickly expanding thanks to a variety of decarbonization-supporting technologies, methods, and inventions. This is due to a multitude of factors. For instance, Per the International Energy Agency's (IEA) transportation CO_2 emission report for 2022, automobiles and vans accounted for 48% of the total CO_2 emissions. All over the globe economies are moving toward the adoption of alternate fuel technologies because of the rising worldwide concern about climate change brought on by greenhouse gas emissions from vehicles and the depletion of natural resources. Hence, Electric vehicles (EVs) are positioned as a clean, green alternative technology that may make it possible to preserve natural resources and move to a low-carbon transportation system with efficiency. Although the importance of embracing EVs in our daily lives, it suffers from a set of hurdles.

Herein, the objective of this study is to analyze these hurdles and prioritize them. Therefore, to achieve this objective, we are modeling the determined hurdles through tree soft methodology. For appraising these hurdles which are modeled in tree soft, BHARAT -v2 is applied as a novel MCDM technique to appraise the influence of hurdles on e-mobility. Hence, we constructed $B_{v2}TrS$ as an appraiser model for ranking these hurdles.

The findings of this model and according to Figure 3 indicated that H_{1-3} is the highest-influenced hurdle in technology with a global weight is 0.13, otherwise, H_{1-1} is the least with a global weight is 0.025. In the same vein, H_{2-3} is the most influenced hurdle in infrastructure with a global weight is 0.14 and H_{2-1} is the least with a global weight is 0.036. Finally, H_{3-3} is the most influenced hurdle in infrastructure where its global weight is 0.20, Unlike H_{3-2} is the least influenced.

Acknowledgments

The author is grateful to the editorial and reviewers, as well as the correspondent author, who offered assistance in the form of advice, assessment, and checking during the study period.

Author Contributions

All authors contributed equally to this research.

Data availability

The datasets generated during and/or analyzed during the current study are not publicly available due to the privacy-preserving nature of the data but are available from the corresponding author upon reasonable request.

Funding

This research was not supported by any funding agency or institute.

Conflict of interest

The authors declare that there is no conflict of interest in the research.

References

1. Murugan, M., & Marisamynathan, S. (2022). Analysis of barriers to adopt electric vehicles in India using fuzzy DEMATEL and Relative importance Index approaches. Case studies on transport policy, 10(2), 795–810.
2. Murugan, M., Marisamynathan, S., & Nair, P. (2022). Investigating the Barriers for Electric Vehicle Adoption Using Analytical Hierarchy Process Approach. In Recent advances in transportation systems engineering and management: select proceedings of ctsem 2021 (pp. 837–850). Springer.
3. Golui, S., Mahapatra, B. S., & Mahapatra, G. S. (2024). A new correlation-based measure on Fermatean fuzzy applied on multi-criteria decision making for electric vehicle selection. Expert systems with applications, 237, 121605.

4. James, A. T., Kumar, G., Pundhir, A., Tiwari, S., Sharma, R., & James, J. (2022). Identification and evaluation of barriers in implementation of electric mobility in India. Research in transportation business & management, 43, 100757.
5. Hamurcu, M., & Eren, T. (2023). Multicriteria decision making and goal programming for determination of electric automobile aimed at sustainable green environment: a case study. Environment systems and decisions, 43(2), 211–231. DOI:10.1007/s10669-022-09878-8
6. Biresselioglu, M. E., Kaplan, M. D., & Yilmaz, B. K. (2018). Electric mobility in Europe: A comprehensive review of motivators and barriers in decision making processes. Transportation research part a: policy and practice, 109, 1–13.
7. Manirathinam, T., Narayanamoorthy, S., Geetha, S., Ahmadian, A., Ferrara, M., & Kang, D. (2024). Assessing performance and satisfaction of micro-mobility in smart cities for sustainable clean energy transportation using novel APPRESAL method. Journal of cleaner production, 436, 140372.
8. Kumar, R., Lamba, K., & Raman, A. (2021). Role of zero emission vehicles in sustainable transformation of the Indian automobile industry. Research in transportation economics, 90, 101064.
9. Wei, F., Walls, W. D., Zheng, X., & Li, G. (2023). Evaluating environmental benefits from driving electric vehicles: The case of Shanghai, China. Transportation research part d: transport and environment, 119, 103749.
10. Ashok, B., Kannan, C., Usman, K. M., Vignesh, R., Deepak, C., Ramesh, R., … Kavitha, C. (2022). Transition to Electric Mobility in India: Barriers Exploration and Pathways to Powertrain Shift through MCDM Approach. Journal of the institution of engineers (india): series c, 103(5), 1251–1277. DOI:10.1007/s40032-022-00852-6
11. Goel, P., Sharma, N., Mathiyazhagan, K., & Vimal, K. E. K. (2021). Government is trying but consumers are not buying: A barrier analysis for electric vehicle sales in India. Sustainable production and consumption, 28, 71–90.
12. Chu, W., Im, M., Song, M. R., & Park, J. (2019). Psychological and behavioral factors affecting electric vehicle adoption and satisfaction: A comparative study of early adopters in China and Korea. Transportation research part d: transport and environment, 76, 1–18.
13. Tarei, P. K., Chand, P., & Gupta, H. (2021). Barriers to the adoption of electric vehicles: Evidence from India. Journal of cleaner production, 291, 125847.
14. Berkeley, N., Jarvis, D., & Jones, A. (2018). Analysing the take up of battery electric vehicles: An investigation of barriers amongst drivers in the UK. Transportation research part d: transport and environment, 63, 466–481.
15. Smarandache, F. (2023). New Types of Soft Sets: HyperSoft Set, IndetermSoft Set, IndetermHyperSoft Set, and TreeSoft Set.
16. Gharib, M., Smarandache, F., & Mohamed, M. (2024). CSsEv: Modelling QoS Metrics in Tree Soft Toward Cloud Services Evaluator based on Uncertainty Environment. Infinite Study.
17. Gharib, M., Rajab, F., & Mohamed, M. (2023). Harnessing Tree Soft Set and Soft Computing Techniques' Capabilities in Bioinformatics: Analysis, Improvements, and Applications. Neutrosophic sets and systems, 61(1), 30.
18. Mohamed, R., & Ismail, M. M. (2024). Harness Ambition of Soft Computing in Multi-Factors of Decision-Making Toward Sustainable Supply Chain in the Realm of Unpredictability. Multicriteria algorithms with applications, 2, 29–42, DOI: https://doi.org/10.61356/j.mawa.2024.26561.
19. Abdelhafeez, A., Mahmoud, H., & Aziz, A. S. (2023). Identify the most Productive Crop to Encourage Sustainable Farming Methods in Smart Farming using Neutrosophic Environment. Neutrosophic systems with applications, 6, 17–24, DOI: https://doi.org/10.61356/j.nswa.2023.34.
20. El-Douh, A., Lu, S., Abdelhafeez, A., & Aziz, A. (2023). A Neutrosophic Multi-Criteria Model for Evaluating Sustainable Soil Enhancement Methods and their Cost 2 Implications in Construction. SMIJ, 5(2), 11, DOI:https://doi.org/10.61185/SMIJ.
21. Sallam, K. M., & Mohamed, A. W. (2023). Single Valued Neutrosophic Sets for Assessment Quality of Suppliers under Uncertainty Environment. Multicriteria algorithms with applications, 1(1), 1–10, DOI: https://doi.org/10.61356/j.mawa.2023.15861.

22. Abdel-aziem, A. H., Mohamed, H. K., & Abdelhafeez, A. (2023). Neutrosophic Decision Making Model for Investment Portfolios Selection and Optimizing based on Wide Variety of Investment Opportunities and Many Criteria in Market. Neutrosophic systems with applications, 6, 32–38, DOI: https://doi.org/10.61356/j.nswa.2023.36.
23. Rao, R. (2024). BHARAT: A simple and effective multi-criteria decision-making method that does not need fuzzy logic, Part-1: Multi-attribute decision-making applications in the industrial environment. International journal of industrial engineering computations, 15(1), 13–40.
24. Mohamed, M. (2024). BHARAT Decision Making Model: Harness an Innovative MCDM Methodology for Recommending Beneficial E-Commerce Website. Multicriteria algorithms with applications, 2, 53–64, DOI: https://doi.org/10.61356/j.mawa.2024.26761.
25. Schmalfuß, F., Mühl, K., & Krems, J. F. (2017). Direct experience with battery electric vehicles (BEVs) matters when evaluating vehicle attributes, attitude and purchase intention. Transportation research part f: traffic psychology and behaviour, 46, 47–69.
26. Bakioglu, G., & Atahan, A. O. (2021). AHP integrated TOPSIS and VIKOR methods with Pythagorean fuzzy sets to prioritize risks in self-driving vehicles. Applied soft computing, 99, 106948.
27. Gao, X., Simeone, A., & Zhang, J. (2023). Smart decision-making for design adaptation of electric vehicles using big sales data. Procedia cirp, 119, 710–715.
28. Mateusz, P., Danuta, M., Małgorzata, Ł., Mariusz, B., & Kesra, N. (2018). TOPSIS and VIKOR methods in study of sustainable development in the EU countries. Procedia computer science, 126, 1683–1692.
29. Lam, W. S., Lam, W. H., Jaaman, S. H., & Liew, K. F. (2021). Performance evaluation of construction companies using integrated entropy–fuzzy VIKOR model. Entropy, 23(3), 320.
30. Ecer, F., Küçükönder, H., Kaya, S. K., & Görçün, Ö. F. (2023). Sustainability performance analysis of micro-mobility solutions in urban transportation with a novel IVFNN-Delphi-LOPCOW-CoCoSo framework. Transportation research part a: policy and practice, 172, 103667.
31. Tripathy, A., Bhuyan, A., Padhy, R. K., Mangla, S. K., & Roopak, R. (2023). Drivers of lithium-ion batteries recycling industry toward circular economy in industry 4.0. Computers & industrial engineering, 179, 109157.
32. Rao, R. V. (2024). BHARAT: A simple and effective multi-criteria decision-making method that does not need fuzzy logic, Part-1: Multi-attribute decision-making applications in the industrial environment. International journal of industrial engineering computations, 15(1), 13–40. DOI:10.5267/j.ijiec.2023.12.003

Appendix A

Table A1. Pair-wise prioritize matrices for main hurdles in level 1.

DM_1	H_1	H_2	H_3	DM_2	H_1	H_2	H_3	DM_3	H_1	H_2	H_3
H_1	0.5	0.8333	0.3333	H_1	0.5	0.1666	1	H_1	0.5	1	0.8333
H_2	1/0.8333	0.5	0.6666	H_2	1/0.1666	0.5	0.8333	H_2	1	0.5	0.1666
H_3	1/0.3333	1/0.6666	0.5	H_3	1.0000	1/0.8333	0.5	H_3	1/0.8333	1/0.1666	0.5

Table A2. Pair-wise prioritize matrices for sub-hurdles of technological in level 2.

DM_1	H_{1-1}	H_{1-2}	H_{1-3}	DM_2	H_{1-1}	H_{1-2}	H_{1-3}	DM_3	H_{1-1}	H_{1-2}	H_{1-3}
H_{1-1}	0.5	0.1666	0.8333	H_{1-1}	0.5	1	0.3333	H_{1-1}	0.5	0.6666	1
H_{1-2}	1/0.1666	0.5	0.3333	H_{1-2}	1	0.5	0.1666	H_{1-2}	1/0.6666	0.5	0.8333
H_{1-3}	1/0.8333	1/0.3333	0.5	H_{1-3}	1/0.3333	1/0.1666	0.5	H_{1-3}	1	1/0.8333	0.5

Table A3. Pair-wise prioritize matrices for sub-hurdles of infrastructural in level 2.

DM_1	**H_{2-1}**	**H_{2-2}**	**H_{2-3}**	**DM_2**	**H_{2-1}**	**H_{2-2}**	**H_{2-3}**	**DM_3**	**H_{2-1}**	**H_{2-2}**	**H_{2-3}**
H_{2-1}	0.5	0.3333	0.1666	H_{2-1}	0.5	0.8333	0.1666	H_{2-1}	0.5	0.8333	1
H_{2-2}	1/0.3333	0.5	0.8333	H_{2-2}	1/0.8333	0.5	1	H_{2-2}	1/0.8333	0.5	0.3333
H_{2-3}	1/0.1666	1/0.8333	0.5	H_{2-3}	1/0.1666	1	0.5	H_{2-3}	1	1/0.3333	0.5

Table A4. Pair-wise prioritize matrices for sub-hurdles of economics and regulation in level 2.

DM_1	H_{3-1}	H_{3-2}	H_{3-3}	DM_2	H_{3-1}	H_{3-2}	H_{3-3}	DM_3	H_{3-1}	H_{3-2}	H_{3-3}
H_{3-1}	0.5	0.3333	0.1666	H_{3-1}	0.5	0.8333	0.1666	H_{3-1}	0.5	0.8333	1
H_{3-2}	1/0.3333	0.5	0.8333	H_{3-2}	1/0.8333	0.5	1	H_{3-2}	1/0.8333	0.5	0.3333
H_{3-3}	1/0.1666	1/0.8333	0.5	H_{3-3}	1/0.1666	1	0.5	H_{3-3}	1	1/0.3333	0.5

Received: 06 Nov 2023, **Revised:** 05 Mar 2024,
Accepted: 01 Apr 2024, **Available online:** 06 Apr 2024.

Neutrosophic Systems with Applications, Vol. 16, 2024
https://doi.org/10.61356/j.nswa.2024.16215

A Novel Approach on Energy of λ_J-dominating Single-Valued Neutrosophic Graph Structure

S.N. Suber Bathusha [1,*], and S. Angelin Kavitha Raj [2]

[1] Department of Mathematics, Sadakathullah Appa College, Tirunelveli, Tamil Nadu, India.
Emails: mohamed.suber.96@gmail.com; mohamed.suber.96@sadakath.ac.in.
[2] Department of Mathematics, Sadakathullah Appa College, Tirunelveli, Tamil Nadu, India.
Emails: angelinkavitha.s@gmail.com; angelinkavitha.s@sadakath.ac.in.

* Correspondence: mohamed.suber.96@sadakath.ac.in.

Abstract: The concept of dominance is one of the most important ideas in graph theory for handling random events, and it has drawn the interest from many scholars. Research related to graph energy has garnered a lot focus recently. The application of single-valued neutrosophic graphs (SVNGs) for energy, Laplacian energy, and dominating energy has been recommended by previous studies. In this research, we apply the concepts of single-valued neutrosophic sets (SVNS) to graph structures (GSs) and investigate some intriguing features of single-valued neutrosophic graph structures (SVNGS). Moreover, the notions of λ_J-dominating energy GS in an SVNGS environment is analyzed in this study. More specifically, illustrative examples are used to develop the adjacency matrix of a λ_J-dominating SVNGS, as well as the spectrum of the adjacency matrix and their related theory. Further, the SVNGS λ_J-dominating energy is determined. We go over various characteristics and constraints for the energy of SVNGS with λ_J-dominating. Further, we introduce the idea of isomorphic and identical λ_J-dominating SVNGS energy, which has been studied using relevant examples, and some of its established properties are presented.

Keywords: SVNGS; λ_J-dominating; Energy; Isomorphic; Identical.

1. Introduction

The graph spectrum finds application in mathematical issues related to combinatorial optimization as well as statistical physics. The graph's spectrum can be more practically applied in a variety of real-world situations, including operations management, networking systems, science and technology, and medical science data held in databases. The adjacency matrix of the graph's eigenvalues is defined as the sum of their absolute values. The graph's energy is used in quantum theory and many other energy-related applications by connecting the graph's edge to a particular type of molecule's electron energy. Motivated by chemical applications, Gutman [1] first proposed this idea in 1978. The Laplacian energy of a graph was later defined by Gutman and Zhou [2] as the sum of the absolute values of the differences between the average vertex degree of G and the Laplacian eigenvalues of G. [3-6] contains information on the characteristics of Laplacian energy and graph energy.

Real-world problems with uncertainty and ambiguity are not always flexible to the common methods of classical mathematics. In 1965, Zadeh [7] developed the notion of a fuzzy set (FS) as an extension of the conventional concept of sets. Since then, other researchers have investigated the idea of fuzzy sets and fuzzy logic to solve a variety of real-world issues involving ambiguous and uncertain situations, as represented by a membership function with a value in the real unit interval [0, 1]. Because it is a single-valued function, the membership function, however, cannot always be used to collect both support and opposition evidence. Atanassov [8] developed the intuitionistic fuzzy set (IFS) as a generalization of Zadeh's fuzzy set. It is possible to create IFS, which has both a membership and a non-membership function, by deriving a new component, degree of membership and non-membership, from the characteristics of the fuzzy set. One of the most useful techniques for controlling ambiguity and unpredictability is the IFS. The magnitudes of satisfaction and discontent are included in an intuitionistic fuzzy set, which is a collection of fuzzy values. Yager [9] invented the ordered weighted average operators' concept for IFS. Weighted averaging operators were created for the first time by Xu [10] in the IFS theory. The neutrosophic set, which the author Smarandache [11-14] devised to handle the ambiguous and inconsistent data, has been extensively investigated and is used in a variety of domains. The indeterminacy value is explicitly quantified and truth membership, indeterminacy membership, and false membership are defined completely independently if the sum of all of these values in the neutrosophic set is between 0 and 3. Neutrosophy: Neutral Logic, Neutral Probability, and Neutral Set Explain in greater detail the terms neutrosophy, neutrosophic probability, set, and logic. The neutrosophic set has quickly caught the interest of many researchers due to the wide range of description situations it covers. Xindong Peng and Jingguo Dai [15] reference is also given a thorough analysis. The neutrosophic collection has undergone a bibliometric analysis from 1998 to 2017 that is presented.

Fuzzy graph theory was created by Rosenfeld [16] in 1975 and analyzed the fuzzy graphs (FGs) for which Kauffmann developed the essential idea in 1973. He researched numerous fundamental concepts in graph theory and established some of their characteristics. When there is uncertainty or ambiguity regarding the existence of an actual object or the relationship between two objects, FGs are a useful tool for representing object relationship structures. Some of the FG applications can be found in [18-20]. The idea of computing the constrained shortest path in a network with mixed fuzzy arc weights applied in wireless sensor networks was recently presented by Peng, Z., Abbaszadeh Sori, A., et al. [28]. For more information, it is recommended to read the research papers Applications of graph's total degree with bipolar fuzzy information and Estimation of most affected cycles and busiest network route based on complexity function of the graph in a fuzzy environment in 2022 by Soumitra Poulik and Ganesh Ghorai [29-31]. Further, introduced the Connectivity Concepts in Bipolar Fuzzy Incidence Graphs.

The concept of domination in graphs can be applied to a wide range of problems, such as transportation systems, combining theory, coding theory, social network analysis, communication networks, security systems, and congestion. Somasundaram and Somasundaram [21] first presented the novel ideas of domination in FGs in 1998. After that, Somasundaram [22] presented various operations on FGs and investigated domination in products of FGs. To find out more, it is suggested to study at the research papers. The following studies [23-25] provide some helpful information about these kinds of structures. In 2022, Bera, S., and Pal, M. [26] presented a new idea regarding domination in m-polar interval-valued FG. The idea of edge-vertex domination on interval graphs in 2024 was recently introduced by Shambayati, H., Shafiei Nikabadi, M., Saberi, S., et al. [27]. In the FS environment, the energy of a graph was first proposed by Anjali and Mathew [32]. Sharbaf and Fayazi [33] introduced the idea of LE of FGs and extended some results on LE bounds to FGs. The concept of energy of Pythagorean FGs with applications was recently introduced by Muhammad Akram and Sumera Naz [34]. Moreover, they presented the concept of Bipolar FG Energy and Energy of double dominating bipolar FGs [35, 36]. Many scholars have integrated the study of energy graphs, dominating sets, and NSs since the development of the NS. The dominating energy in a single-valued NG was recently proposed by Mullai and Broumi [37]. Novel Concept of Energy in Bipolar Single-Valued NGs with Applications was proposed by Mohamad, S.N.F., Hasni, R., Smarandache, et al. [38].

By generalizing an undirected graph, a Graph Structure (GS) may be produced. Signed graphs and other types of graphs can then be studied using this structure. The concept of GSs was initially introduced in Sampath Kumar's [40] work in 2006. The idea of an FGS was first put forth by T. Dinesh and T. V. Ramakrishnan [41] in their 2011 investigation. The ideas of Operations on Intuitionistic FGS and Single-Valued NGSs were recently introduced by Muhammad Akram [42, 43]. In an additional development, Bathusha, S. N. S., et al. [44, 45] presented the energy of interval-valued Complex NGS as well as the idea of interval-valued Complex Pythagorean FGS with application. A few LE-bound findings were expanded to include interval-valued Complex NGS and applications. In 2024, new works were unveiled.

Specifically, the objective of this work is to present λ_J-dominating SVNGS that were first described. After that, the energy principles for λ_J-dominant SVNGS are explained. Furthermore, we discuss several properties and restrictions for the energy of λ_J-dominating SVNGS. We also introduce the concept of identical and isomorphic λ_J-dominating SVNGS.

1.1 Motivation

Many graph theory problems consider pairwise relations of objects, and certain properties of the objects can be connected in such a way that they produce irreflexive, symmetric, and mutually disjoint relations. By graphically representing a GS, this type of information loss can be prevented. The study of SVNS as applied to the GS and their applications is motivated by the need to handle difficult decision-making situations when faced with imprecise information. Although there is some flexibility available with existing fuzzy models, SVNGSs offer a more flexible tool for controlling uncertainty. In SVNS, values for true membership, indeterminate membership, and false membership are included in consideration. The focus of our study is specifically drawn to the features and limitations of energy of λ_J-dominating SVGCS.

Once again expressed abstractly, this concept can be used in the energy of λ_J-dominating SVGCS. Figure 1 and the following describe the organizational structure of this work: Section preliminaries present the fundamental ideas of the neutrosophic set. Next, the ideas of SVNGSs and λ_J-dominating energy SVNGSs are defined. Moreover, we discussed the energy of λ_J-dominating SVNGS including its properties and bounds. In the conclusion section, we have provided an explanation of the study's future directions as well as the importance of the findings.

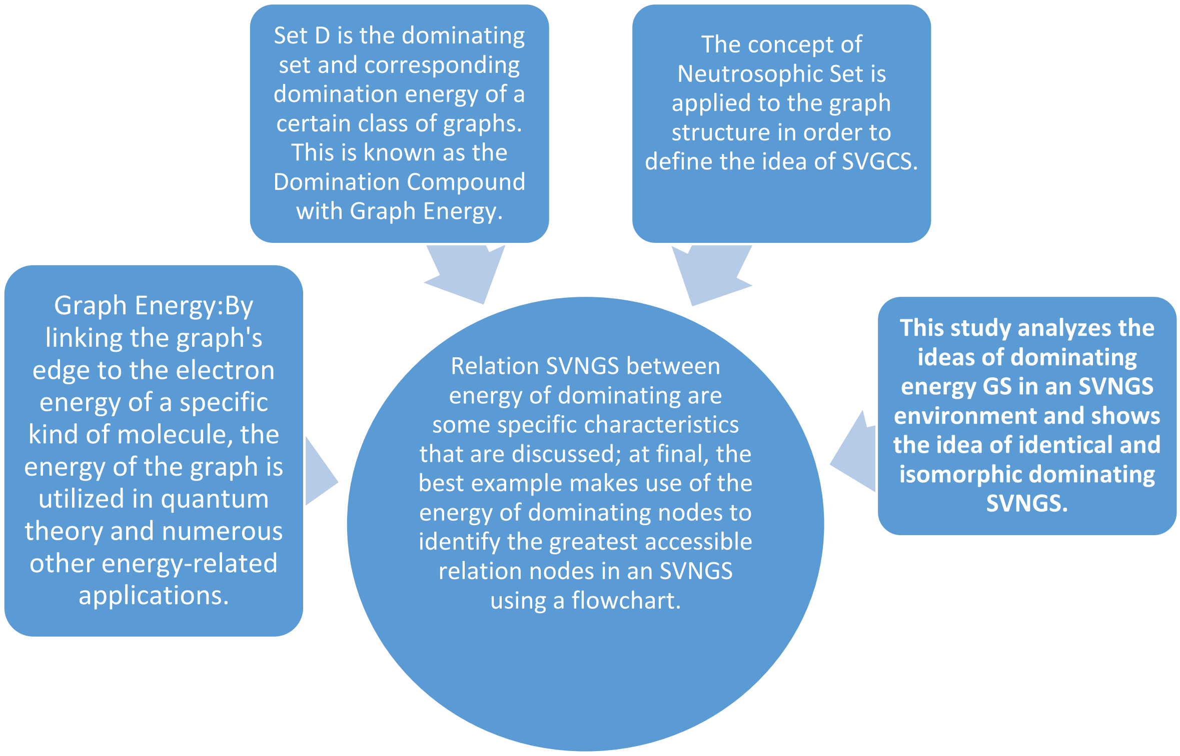

Figure 1

2. Preliminaries

The basic definitions of domination and the single-valued neutrosophic graph (SVNG) that are relevant to this study are presented in this section.

Definition 2.1. [41] Let $\zeta^* = (Q, R_1, R_2, \ldots, R_k)$ be a graph structure in which Q is a non-empty set and $R_1, R_2, \ldots, R_k$ are mutually disjoint, irreflexive, and symmetric relations on Q.

Definition 2.2. [11] Let Y be a universal set. The NS μ in Y defined membership functions $\mu_1(a), \mu_2(a),$ *and* $\mu_3(a)$ represent the true, indeterminate, and false values found in the $\mu = \{a, \mu_1(a), \mu_2(a), \mu_3(a) | a \in Y\}, where$ non-standard subset of $]0^-, 1^+[$ and the real standard, respectively, such that:
$\mu = \{a, \mu_1(a), \mu_2(a), \mu_3(a) | a \in Y\}, where \mu_1, \mu_2, \mu_3 : Y \rightarrow]0^-, 1^+[$ and $0^- \leq \mu_1(a), \mu_2(a), \mu_3(a) \leq 3^+$.

Definition 2.3. [39] Let Y be a universal set. The SVNS μ in Y is an object form $\mu_1, \mu_2, \mu_3 : Y \rightarrow [0,1]$ and $0 \leq \mu_1(a), \mu_2(a), \mu_3(a) \leq 3$.

Definition 2.4 [38] A SVNG $\zeta = (\mu, \lambda)$ is a pair, where $\mu: Q \rightarrow [0,1]$ is a SVNS on Q and $R: Q \times Q \rightarrow [0,1]$ is a SVN relation on Q such that

$$\lambda_1(a,b) \leq \min\{\mu_1(a), \mu_1(b)\},$$
$$\lambda_2(a,b) \leq \max\{\mu_2(a), \mu_2(b)\},$$
$$\lambda_3(a,b) \leq \max\{\mu_3(a), \mu_3(b)\},$$

For all $a, b \in Q$. μ *and* λ are referred to be SVN vertex set of ζ and the SVN edge set of ζ , respectively.
Definition 2.5. [37] An SVNG $\zeta = (\mu, \lambda)$ be a SVNG and $a, b \in Q$ *in* ζ, there we say that a dominates b if

$$\lambda_{1R}(a,b) \leq \mu_{1Q}(a) \wedge \mu_{1Q}(b),$$
$$\lambda_{2R}(a,b) \leq \mu_{2Q}(a), \vee \mu_{2Q}(b),$$
$$\lambda_{3R}(a,b) \leq \mu_{3Q}(a) \vee \mu_{3Q}(b).$$

3. Energy of λ_J-dominating Single-Valued Neutrosophic Graph Structure

The basic definitions of domination and the single-valued neutrosophic graph (SVNG) that are relevant to this study are presented in this section.

The energy of $\boldsymbol{\lambda_J}$-dominating GS is defined, and its properties are discussed in this section using the frameworks of SVNG theory.

Definition 3.1. Let $\zeta = (\mu, \lambda_1, \lambda_2, \ldots, \lambda_k)$ is referred to as an SVNGS of GS $\zeta^* = (Q, R_1, R_2, \ldots, R_k)$ if $\mu = \{r, \mu_1(r), \mu_2(r), \mu_3(r)\}$ is an SVN set on Q and $\lambda_J = \{rs, \lambda_{1J}(rs), \lambda_{2J}(rs), \lambda_{3J}(rs)\}$ are SVCN sets on Q and R_J such that

$$\lambda_{1J}(r,s) \leq \min\{\mu_1(r), \mu_1(s)\},$$
$$\lambda_{2J}(r,s) \leq \max\{\mu_2(r), \mu_2(s)\},$$
$$\lambda_{3J}(r,s) \leq \max\{\mu_3(r), \mu_3(s)\}$$

such that $0 \leq \lambda_{1J}(r,s) + \lambda_{2J}(r,s) + \lambda_{3J}(r,s) \leq 3$ for all $(r,s) \in R_J, J = 1,2,\ldots,k$.

Definition 3.2. The adjacency matrix $A\zeta = \{A\lambda_1, A\lambda_2, \ldots, A\lambda_k\}$ of a SVNGS $\zeta = \{\mu, \lambda_1, \lambda_2, \ldots, \lambda_k\}$, where $A\lambda_J, (J = 1,2,\ldots,k)$ is a square matrix as $[u_{jk}]$ in which

$$u_{jk} = (\lambda_{1J}(u_j u_k), \lambda_{2J}(u_j u_k), \lambda_{3J}(u_j u_k)),$$
$$\forall u_j u_k \in R_J \text{ and } J = 1,2,\ldots,k.$$

The adjacency matrix $A\zeta = \{A\lambda_1, A\lambda_2, \ldots, A\lambda_k\}$ of a SVNGS $\zeta = (\mu, \lambda_1, \lambda_2, \ldots, \lambda_k)$. Then the λ_J degree of vertex u in $A(\zeta)$ is defined as

$$Ad_{\lambda_J}(u) = (Ad_{\lambda_{1J}}(u), Ad_{\lambda_{2J}}(u), Ad_{\lambda_{3J}}(u))$$

$$Ad_{\lambda_{1J}}(u) = (\sum_{z=1}^{k} \lambda_{1J}(u_{jz})),$$

$$Ad_{\lambda_{2J}}(u) = (\sum_{z=1}^{k} \lambda_{2J}(u_{jz})),$$

$$Ad_{\lambda_{3J}}(u) = \left(\sum_{z=1}^{k} \lambda_{2J}(u_{jz})\right), \forall J = 1,2, \ldots, k.$$

Definition 3.3. A graph structure of the form $\zeta = (\mu, \lambda_1, \lambda_2, \ldots, \lambda_k)$ is referred to as an λ_J-dominating SVNGS, where $\lambda_{1J}: Q \to [0,1]$ denoted degree of truth membership, $\lambda_{2J}: Q \to [0,1]$ denoted the degree of indeterminacy membership and $\lambda_{3J}: Q \to [0,1]$ denoted degree of false membership defined such as:

$$\lambda_{1J}(r) = \min_{(r,s)\in R_J} \left(\lambda_{1J}(r,s)\right),$$

$$\lambda_{2J}(r) = \min_{(r,s)\in R_J} \left(\lambda_{2J}(r,s)\right),$$

$$\lambda_{3J}(r) = \min_{(r,s)\in R_J} \left(\lambda_{3J}(r,s)\right), \forall J = 1,2, \ldots, k.$$

Definition 3.4. Let $\zeta = (\mu, \lambda_1, \lambda_2, \ldots, \lambda_k)$ be a λ_J-dominating SVNGS. Let $r, s \in Q$, we state that r dominates s in ζ if there exists a strong arc from r to s for all $(r, s) \in R_J$ and $J = 1,2, \ldots, k$. A subset $D_J \subseteq Q$ is referred to as a λ_J-dominant set in ζ^* if for each $s \in Q - D_J$, there exists one vertex $r \in D_J$ such that r dominates s for all $(r, s) \in R_J$ and $J = 1,2, \ldots, k$.

Definition 3.5. Let $\zeta = (\mu, \lambda_1, \lambda_2, \ldots, \lambda_k)$ be a λ_J-dominating SVNGS. The adjacency matrix of a λ_J-dominating SVNGS ζ is defined as $A_{D_J}(\zeta) = [d_{rs}]$, where

$$d_{rs} = \begin{cases} (\lambda_{1J})_{rs}, (\lambda_{2J})_{rs}, (\lambda_{3J})_{rs} & \text{if } (r, s) \in R_J \\ (1,1,1) & \text{if } r = s \text{ and } r \in D_J \\ (0,0,0) & otherwise \end{cases}$$

This adjacency matrix of a λ_J -dominating SVNGS $A_{D_J}(\zeta)$ can be written as $A_{D_J}(\zeta) = (\lambda_{1J}(\zeta), \lambda_{2J}(\zeta), \lambda_{3J}(\zeta))$ where

$$\lambda_{1J}(\zeta) = \begin{cases} (\lambda_{1J})_{rs} & \text{if } (r, s) \in R_J \\ 1 & \text{if } r = s \text{ and } r \in D_J \\ 0 & otherwise \end{cases}$$

$$\lambda_{2J}(\zeta) = \begin{cases} (\lambda_{2J})_{rs} & \text{if } (r, s) \in R_J \\ 1 & \text{if } r = s \text{ and } r \in D_J \\ 0 & otherwise \end{cases}$$

$$\lambda_{3J}(\zeta) = \begin{cases} (\lambda_{3J})_{rs} & \text{if } (r,s) \in R_J \\ 1 & \text{if } r = s \text{ and } r \in D_J \\ 0 & otherwise \end{cases}$$

Definition 3.6. The spectrum of an adjacency matrix of a λ_J-dominating SVNGS is defined as $\left\langle P_D^{\lambda_{1J}}, P_D^{\lambda_{2J}}, P_D^{\lambda_{3J}} \right\rangle$, where $P_D^{\lambda_{1J}}, P_D^{\lambda_{2J}}, P_D^{\lambda_{3J}}$ are the sets of eigenvalues of $\lambda_{1J}(\zeta), \lambda_{2J}(\zeta), \lambda_{3J}(\zeta)$, respectively.

Definition 3.7. The energy of a λ_J-dominating SVNGS $\zeta = (\mu, \lambda_1, \lambda_2, \ldots, \lambda_k)$ is defined as

$$\begin{aligned} E_D^{\lambda_J}(\zeta) &= (E(P_D^{\lambda_{1J}}), E(P_D^{\lambda_{2J}}), E(P_D^{\lambda_{3J}})) \\ &= \left\langle \sum_{i=1}^{n} |(\alpha_i)_{\lambda_J}|, \sum_{i=1}^{n} |(\beta_i)_{\lambda_J}|, \sum_{i=1}^{n} |(\gamma_i)_{\lambda_J}| \right\rangle, \end{aligned}$$

where $P_D^{\lambda_{1J}} = \{(\alpha_i)_{\lambda_J}\}_{i=1}^n$, $P_D^{\lambda_{2J}} = \{(\beta_i)_{\lambda_J}\}_{i=1}^n$ and $P_D^{\lambda_{3J}} = \{(\gamma_i)_{\lambda_J}\}_{i=1}^n$, for all $J = 1,2,\ldots,k$.

Example 3.8. An λ_J-dominating SVCNGS $\zeta = (\mu, \lambda_1, \lambda_2)$ of a GS $\zeta^* = (Q, R_1, R_2)$ given Figure 2 is a λ_J -dominating SVCNGS $\zeta = (\mu, \lambda_1, \lambda_2)$ such that $\mu = \{u_1(0.6,0.4,0.3), u_2(0.5,0.4,0.6), u_3(0.6,0.4,0.5), u_4(0.3,0.5,0.4)\}$.

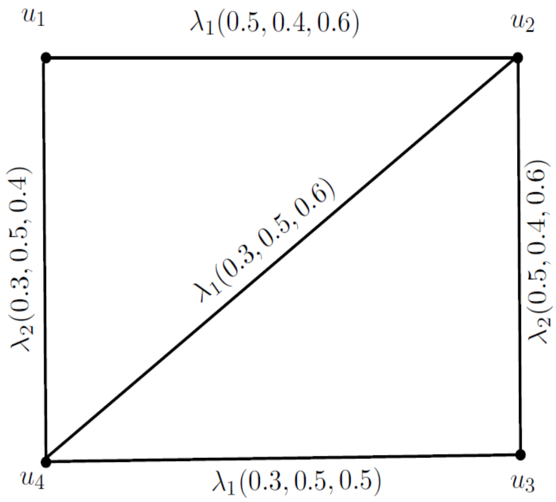

Figure 1

And λ_{1J}, $\lambda_{2J}, \lambda_{3J}$ are defined by $\lambda_{1J}: Q \to [0,1]$, $\lambda_{2J}: Q \to [0,1]$, $\lambda_{3J}: Q \to [0,1]$, as shown in Figure 2, where

$$\lambda_{11}(u_1) = \min_{(u_1,u_2)\in R_1} (\lambda_{11}(u_1, u_2)) = 0.5$$

Similarly, $\lambda_{11}(u_2) = 0.3$, $\lambda_{11}(u_3) = 0.3$, $\lambda_{11}(u_4) = 0.3$,

$$\lambda_{12}(u_1) = \min_{(u_1,u_4)\in R_2} (\lambda_{12}(u_1, u_4)) = 0.3$$

Similarly, $\lambda_{12}(u_2) = 0.5$, $\lambda_{12}(u_3) = 0.5$, $\lambda_{12}(u_4) = 0.3$.

The λ_1-dominating SVNGS

$$\lambda_1(u_1) = (0.5,0.4,0.6),\ \lambda_1(u_2) = (0.3,0.5,0.6),\ \lambda_1(u_3) = (0.3,0.5,0.5),$$

$$\lambda_1(u_4) = (0.3,0.5,0.6).$$

The λ_2-dominating SVNGS

$$\lambda_2(u_1) = (0.3,0.5,0.4),\ \lambda_2(u_2) = (0.5,0.4,0.6),\ \lambda_2(u_3) = (0.5,0.4,0.6),$$

$$\lambda_1(u_4) = (0.3,0.5,0.4).$$

Here, $u_1\lambda_1$-dominates u_2 and $u_3\lambda_1$-dominates u_4 because

$$\lambda_{11}(u_1,u_2) \leq \min\{\lambda_{11}(u_1), \lambda_{11}(u_2)\},\ \lambda_{21}(u_1,u_2) \leq \min\{\lambda_{21}(u_1), \lambda_{21}(u_2)\},$$
$$\lambda_{31}(u_1,u_2) \leq \min\{\lambda_{31}(u_1), \lambda_{31}(u_2)\},\ \lambda_{11}(u_3,u_4) \leq \min\{\lambda_{11}(u_3), \lambda_{11}(u_4)\},$$
$$\lambda_{21}(u_3,u_4) \leq \min\{\lambda_{21}(u_3), \lambda_{21}(u_4)\},\ \lambda_{31}(u_3,u_4) \leq \min\{\lambda_{31}(u_3),\ \lambda_{31}(u_4)\}$$

$u_1\ \lambda_2$-dominates u_4 and $u_3\lambda_2$-dominates u_2 because

$$\lambda_{12}(u_1,u_4) \leq \min\{\lambda_{12}(u_1), \lambda_{12}(u_4)\},\ \lambda_{22}(u_1,u_4) \leq \min\{\lambda_{22}(u_1), \lambda_{22}(u_4)\},$$
$$\lambda_{32}(u_1,u_2) \leq \min\{\lambda_{32}(u_1), \lambda_{32}(u_2)\}\ \lambda_{12}(u_2,u_3) \leq \min\{\lambda_{12}(u_2), \lambda_{12}(u_3)\},$$
$$\lambda_{22}(u_2,u_3) \leq \min\{\lambda_{22}(u_2), \lambda_{22}(u_3)\},\ \lambda_{32}(u_2,u_3) \leq \min\{\lambda_{32}(u_2),\ \lambda_{32}(u_3)\}$$

Thus $D_J = \{u_1, u_3\}$ is a λ_J-dominating set because every vertex in $Q - D_J$, is λ_J-dominated by atleast one vertex in D_J for all $J = 1,2$.

The adjacency matrix of λ_1-dominating SVNGS given in Figure 2 is

$$A\lambda_1 = \begin{bmatrix} (1,1,1) & (0.5,0.4,0.6) & (0,0,0) & (0,0,0) \\ (0.5,0.4,0.6) & (0,0,0) & (0,0,0) & (0.3,0.5,0.6) \\ (0,0,0) & (0,0,0) & (1,1,1) & (0.3,0.5,0.5) \\ (0,0,0) & (0.3,0.5,0.6) & (0.3,0.5,0.5) & (0,0,0) \end{bmatrix}$$

The adjacency matrix of λ_2-dominating SVNGS given in Figure 2 is

$$A\lambda_2 = \begin{bmatrix} (1,1,1) & (0,0,0) & (0,0,0) & (0.3,0.5,0.4) \\ (0,0,0) & (0,0,0) & (0.5,0.4,0.6) & (0,0,0) \\ (0,0,0) & (0.5,0.4,0.6) & (1,1,1) & (0,0,0) \\ (0.3,0.5,0.4) & (0,0,0) & (0,0,0) & (0,0,0) \end{bmatrix}$$

The adjacency matrix of λ_2-dominating SVNGS given in Figure 2 is

$$A\lambda_2 = \begin{bmatrix} (1,1,1) & (0,0,0) & (0,0,0) & (0.3,0.5,0.4) \\ (0,0,0) & (0,0,0) & (0.5,0.4,0.6) & (0,0,0) \\ (0,0,0) & (0.5,0.4,0.6) & (1,1,1) & (0,0,0) \\ (0.3,0.5,0.4) & (0,0,0) & (0,0,0) & (0,0,0) \end{bmatrix}$$

This can be written in six different matrices as:

$$A\lambda_{11} = \begin{bmatrix} 1 & 0.5 & 0 & 0 \\ 0.5 & 0 & 0 & 0.3 \\ 0 & 0 & 1 & 0.3 \\ 0 & 0.3 & 0.3 & 0 \end{bmatrix}, A\lambda_{21} = \begin{bmatrix} 1 & 0.4 & 0 & 0 \\ 0.4 & 0 & 0 & 0.5 \\ 0 & 0 & 1 & 0.5 \\ 0 & 0.5 & 0.5 & 0 \end{bmatrix},$$

$$A\lambda_{31} = \begin{bmatrix} 1 & 0.6 & 0 & 0 \\ 0.6 & 0 & 0 & 0.6 \\ 0 & 0 & 1 & 0.5 \\ 0 & 0.6 & 0.5 & 0 \end{bmatrix}, A\lambda_{12} = \begin{bmatrix} 1 & 0 & 0 & 0.3 \\ 0 & 0 & 0.5 & 0 \\ 0 & 0.5 & 1 & 0 \\ 0.3 & 0 & 0 & 0 \end{bmatrix},$$

$$A\lambda_2 = \begin{bmatrix} 1 & 0 & 0 & 0.5 \\ 0 & 0 & 0.4 & 0 \\ 0 & 0.4 & 1 & 0 \\ 0.5 & 0 & 0 & 0 \end{bmatrix}, A\lambda_2 = \begin{bmatrix} 1 & 0 & 0 & 0.4 \\ 0 & 0 & 0.6 & 0 \\ 0 & 0.6 & 1 & 0 \\ 0.4 & 0 & 0 & 0 \end{bmatrix}.$$

Since,

$$\begin{aligned}
spec(AP_D^{\lambda_{11}}(\zeta)) &= (-0.4245,0.1202,1.0801,1.2242),\\
spec(AP_D^{\lambda_{21}}(\zeta)) &= (-0.6268,0.2354,1.1173,1.2741),\\
spec(AP_D^{\lambda_{31}}(\zeta)) &= (-0.7728,0.2154,1.1647,1.3927),\\
spec(AP_D^{\lambda_{12}}(\zeta)) &= (-0.2071,-0.0831,1.0831,1.2071),\\
spec(AP_D^{\lambda_{22}}(\zeta)) &= (-0.2071,-0.1403,1.1403,1.2071),\\
spec(AP_D^{\lambda_{32}}(\zeta)) &= (-0.2810,-0.1403,1.1403,1.2810).
\end{aligned}$$

Therefore,

$$spec\left(A_{P_D^{\lambda_1}}(\zeta)\right) = \{(-0.4245,-0.6268,-0.7728),(0.1202,0.2354,0.2154),$$

$$(1.0801,1.1173,1.1647),(1.2242,1.2741,1.3927)\},$$

$$spec\left(A_{P_D^{\lambda_2}}(\zeta)\right) = \{(-0.2071,-0.2071,-0.2810),(-0.0831,-0.1403,-0.1403),$$

$$(1.0831,1.1403,1.1403),(1.2071,1.2071,1.2810)\}.$$

The energy of λ_1-dominating SVNGS ζ is

$$E_D^{\lambda_1}(\zeta) = \left(E(P_D^{\lambda_{11}}),E(P_D^{\lambda_{21}}),E(P_D^{\lambda_{31}})\right)$$

$$= \left\langle \sum_{i=1}^{n} |(\alpha_i)_{\lambda_1}|, \sum_{i=1}^{n} |(\beta_i)_{\lambda_1}|, \sum_{i=1}^{n} |(\gamma_i)_{\lambda_1}| \right\rangle = (2.6086,2.7829,3.1150)$$

The energy of λ_2-dominating SVNGS ζ is

$$E_D^{\lambda_2}(\zeta) = \left(E(P_D^{\lambda_{12}}),E(P_D^{\lambda_{22}}),E(P_D^{\lambda_{32}})\right)$$

$$= \left\langle \sum_{i=1}^{n} |(\alpha_i)_{\lambda_2}|, \sum_{i=1}^{n} |(\beta_i)_{\lambda_2}|, \sum_{i=1}^{n} |(\gamma_i)_{\lambda_2}| \right\rangle = (2.5804,2.6948,2.8427)$$

Theorem 3.9. Let $\zeta = (\mu,\lambda_1,\lambda_2,\ldots,\lambda_k)$ be a λ_J-dominating SVNGS with n vertices and m R_J-edges. Let $D_J = \{a_1,a_2,a,\ldots,a_w\}$ be a λ_J-dominating set. If

$(\alpha_1)_{\lambda_J}, (\alpha_2)_{\lambda_J}, \ldots, (\alpha_n)_{\lambda_J}, (\beta_1)_{\lambda_J}, (\beta_2)_{\lambda_J}, \ldots, (\beta_n)_{\lambda_J}$ and $(\gamma_1)_{\lambda_J}, (\gamma_2)_{\lambda_J}, \ldots, (\gamma_n)_{\lambda_J}$ are the eigenvalues of the adjacency matrix $P_D^{\lambda_J}(\zeta)$, then

1. $\sum_{i=1}^{n}(\alpha_i)_{\lambda_{1J}} = \eta_{1J}$, $\sum_{i=1}^{n}(\beta_i)_{\lambda_{2J}} = \eta_{2J}$, $\sum_{i=1}^{n}(\gamma_i)_{\lambda_{3J}} = \eta_{3J}$.

2. $\sum_{i=1}^{n}(\alpha_i)_{\lambda_{1J}}^2 = \sum_{i=1}^{n}(P_{ii}^{\lambda_{1J}})^2 + 2\sum_{1\le i<j\le n} P_{ij}^{\lambda_{1J}} P_{ji}^{\lambda_{1J}}$,

$$\sum_{i=1}^{n}(\beta_i)_{\lambda_{2J}}^2 = \sum_{i=1}^{n}(P_{ii}^{\lambda_{2J}})^2 + 2\sum_{1\le i<j\le n} P_{ij}^{\lambda_{2J}} P_{ji}^{\lambda_{2J}},$$

$$\sum_{i=1}^{n}(\gamma_i)_{\lambda_{3J}}^2 = \sum_{i=1}^{n}(P_{ii}^{\lambda_{3J}})^2 + 2\sum_{1\le i<j\le n} P_{ij}^{\lambda_{3J}} P_{ji}^{\lambda_{3J}}, \text{where } \eta_{1J} = |D_J|,\ \forall J = 1,2,\ldots,k.$$

Proof 1. The result of the matrices' trace property, we have $\sum_{i=1}^{n}(\alpha_i)_{\lambda_{1J}} = P_{ii}^{\lambda_{1J}} = \eta_{1J}$

Analogously, we can show that

$$\sum_{i=1}^{n}(\beta_i)_{\lambda_{2J}} = P_{ii}^{\lambda_{1J}} = \eta_{2J}, \sum_{i=1}^{n}(\gamma_i)_{\lambda_{3J}} = P_{ii}^{\lambda_{3J}} = \eta_{3J}$$

2. Equivalently, the sum of the square of eigenvalues of $(P_D^{\lambda_J}(\zeta))^2$

$$\sum_{i=1}^{n}(\alpha_i)_{\lambda_{1J}}^2 = \text{ trace of } (P_D^{\lambda_J}(\zeta))^2$$

$$= P_{11}^{\lambda_{1J}}P_{11}^{\lambda_{1J}} + P_{12}^{\lambda_{1J}}P_{21}^{\lambda_{1J}} + \cdots + P_{1n}^{\lambda_{1J}}P_{n1}^{\lambda_{1J}} + P_{21}^{\lambda_{1J}}P_{12}^{\lambda_{1J}} + P_{22}^{\lambda_{1J}}P_{22}^{\lambda_{1J}} + \cdots + P_{2n}^{\lambda_{1J}}P_{n2}^{\lambda_{1J}}$$
$$+ \cdots + P_{n1}^{\lambda_{1J}}P_{1n}^{\lambda_{1J}} + P_{n2}^{\lambda_{1J}}P_{2n}^{\lambda_{1J}} + \cdots + P_{nn}^{\lambda_{1J}}P_{nn}^{\lambda_{1J}}$$

$$= \sum_{i=1}^{n}(P_{ii}^{\lambda_{1J}})^2 + 2\sum_{1\le i<j\le n} P_{ij}^{\lambda_{1J}} P_{ji}^{\lambda_{1J}}$$

Analogously, we can show that

$$\sum_{i=1}^{n}(\beta_i)_{\lambda_{2J}}^2 = \sum_{i=1}^{n}(P_{ii}^{\lambda_{2J}})^2 + 2\sum_{1\le i<j\le n} P_{ij}^{\lambda_{2J}} P_{ji}^{\lambda_{2J}},$$
$$\sum_{i=1}^{n}(\gamma_i)_{\lambda_{3J}}^2 = \sum_{i=1}^{n}(P_{ii}^{\lambda_{3J}})^2 + 2\sum_{1\le i<j\le n} P_{ij}^{\lambda_{3J}} P_{ji}^{\lambda_{3J}}.$$

Theorem 3.10. Let $\zeta = (\mu, \lambda_1, \lambda_2, \ldots, \lambda_k)$ be a λ_J-dominating SVNGS with n vertices and m R_J-edges. Let D_J is the λ_J-dominating set, then

1. $\sqrt{\sum_{i=1}^{n}(P_{ii}^{\lambda_{1J}})^2 + 2\sum_{1\le i<j\le n} P_{ij}^{\lambda_{1J}} P_{ji}^{\lambda_{1J}} + n(n-1)(\delta_{1J})^{\frac{2}{n}}} \le$

$$E(P_D^{\lambda_{1J}} \le \sqrt{n\left(\sum_{i=1}^{n}(P_{ii}^{\lambda_{1J}})^2 + 2\sum_{1\le i<j\le n} P_{ij}^{\lambda_{1J}} P_{ji}^{\lambda_{1J}}\right)},$$

2. $\sqrt{\sum_{i=1}^{n}(P_{ii}^{\lambda_{2J}})^2 + 2\sum_{1\le i<j\le n} P_{ij}^{\lambda_{2J}} P_{ji}^{\lambda_{2J}} + n(n-1)(\delta_{2J})^{\frac{2}{n}}} \le$

$$E(P_D^{\lambda_{2J}} \le \sqrt{n\left(\sum_{i=1}^{n}(P_{ii}^{\lambda_{2J}})^2 + 2\sum_{1\le i<j\le n} P_{ij}^{\lambda_{2J}} P_{ji}^{\lambda_{2J}}\right)},$$

3. $\sqrt{\sum_{i=1}^{n}(P_{ii}^{\lambda_{3J}})^2 + 2\sum_{1\le i<j\le n} P_{ij}^{\lambda_{3J}} P_{ji}^{\lambda_{3J}} + n(n-1)(\delta_{3J})^{\frac{2}{n}}} \le$

$$E(P_D^{\lambda_{3J}} \le \sqrt{n\left(\sum_{i=1}^{n}(P_{ii}^{\lambda_{3J}})^2 + 2\sum_{1\le i<j\le n} P_{ij}^{\lambda_{3J}} P_{ji}^{\lambda_{3J}}\right)}$$

Where $\chi_{xJ} = det(P_D^{\lambda_J}(\zeta))$ and $\delta_{xJ} = |\chi_{xJ}|$, $x = 1,2,3$ and $J = 1,2,\ldots,k$.

Proof. According to Cauchy Schwarz inequality, $(\sum_{(u_i,v_i)\in R_J} u_i\,, v_i)^2 \le (\sum_{(u_i,v_i)\in R_J} u_i^2)(\sum_{(u_i,v_i)\in R_J} v_i^2)$

Upper bound

If $u_i = 1$ and $v_i = |(\alpha_i)_{\lambda_{1J}}|$, then $(\sum_{(u_i,v_i)\in R_J} |\,(\alpha_i)_{\lambda_{1J}}|)^2 \le (\sum_{(u_i,v_i)\in R_J} 1)(\sum_{(u_i,v_i)\in R_J} \alpha_i)_{\lambda_{1J}}^2)$

$$(E_D^{\lambda_{1J}}(\zeta))^2 \le n\left(\sum_{i=1}^{n}(P_{ii}^{\lambda_{1J}})^2 + 2\sum_{1\le i<j\le n} P_{ij}^{\lambda_{1J}} P_{ji}^{\lambda_{1J}}\right)$$

$$(E_D^{\lambda_{1J}}(\zeta)) \le \sqrt{n\left(\sum_{i=1}^{n}(P_{ii}^{\lambda_{1J}})^2 + 2\sum_{1\le i<j\le n} P_{ij}^{\lambda_{1J}} P_{ji}^{\lambda_{1J}}\right)}$$

Lower bound

$$(E_D^{\lambda_{1J}}(\zeta))^2 = (\sum_{(u_i,v_i)\in R_J} |\,(\alpha_i)_{\lambda_{1J}}|)^2 = \left(\sum_{i=1}^{n}|P_{ii}^{\lambda_{1J}}|^2 + 2\sum_{1\le i<j\le n} |P_{ij}^{\lambda_{1J}}||P_{ji}^{\lambda_{1J}}|\right)$$

$$= \left(\sum_{i=1}^{n}(P_{ii}^{\lambda_{1J}})^2 + 2\sum_{1\le i<j\le n} P_{ij}^{\lambda_{1J}} P_{ji}^{\lambda_{1J}}\right) + 2\frac{n(n-1)}{2} AM_{1\le i<j\le n}\left\{|(\alpha_i)_{\lambda_{1J}}||(\alpha_j)_{\lambda_{1J}}|\right\}.$$

But,

$$AM_{1\le i<j\le n}\left\{|(\alpha_i)_{\lambda_{1J}}||(\alpha_j)_{\lambda_{1J}}|\right\} \ge GM_{1\le i<j\le n}\left\{|(\alpha_i)_{\lambda_{1J}}||(\alpha_j)_{\lambda_{1J}}|\right\}.$$

Therefore,

$$(E_D^{\lambda_1 J}(\zeta)) \geq \sqrt{\sum_{i=1}^{n}(P_{ii}^{\lambda_1 J})^2 + 2\sum_{1\le i<j\le n} P_{ij}^{\lambda_1 J} P_{ji}^{\lambda_1 J} + n(n-1)GM_{1\le i<j\le n}\left\{|(\alpha_i)_{\lambda_1 J}||(\alpha_j)_{\lambda_1 J}|\right\}}$$

$$GM_{1\le i<j\le n}\left\{|(\alpha_i)_{\lambda_1 J}||(\alpha_j)_{\lambda_1 J}|\right\} = \left(\prod_{1\le i<j\le n}|(\alpha_i)_{\lambda_1 J}||(\alpha_j)_{\lambda_1 J}|\right)^{\frac{2}{n(n-1)}}$$

$$= \left(\prod_{1\le i<j\le n}|(\alpha_i)_{\lambda_1 J}|^{n-1}\right)^{\frac{2}{n(n-1)}} = \left(\prod_{1\le i<j\le n}|(\alpha_i)_{\lambda_1 J}|\right)^{\frac{2}{n}} = \delta_{1J}^{\frac{2}{n}}$$

$$\left(E_D^{\lambda_1 J}(\zeta)\right) = \sqrt{\sum_{i=1}^{n}(P_{ii}^{\lambda_1 J})^2 + 2\sum_{1\le i<j\le n} P_{ij}^{\lambda_1 J} P_{ji}^{\lambda_1 J} + n(n-1)(\delta_{1J})^{\frac{2}{n}}}$$

Combining these bounds, we have

$$1.\ \sqrt{\sum_{i=1}^{n}(P_{ii}^{\lambda_1 J})^2 + 2\sum_{1\le i<j\le n} P_{ij}^{\lambda_1 J} P_{ji}^{\lambda_1 J} + n(n-1)(\delta_{1J})^{\frac{2}{n}}}$$

$$\leq \quad E(P_D^{\lambda_1 J}(\zeta) \leq \sqrt{n\left(\sum_{i=1}^{n}(P_{ii}^{\lambda_1 J})^2 + 2\sum_{1\le i<j\le n} P_{ij}^{\lambda_1 J} P_{ji}^{\lambda_1 J}\right)}$$

Analogously, we can show that

$$2.\ \sqrt{\sum_{i=1}^{n}(P_{ii}^{\lambda_2 J})^2 + 2\sum_{1\le i<j\le n} P_{ij}^{\lambda_2 J} P_{ji}^{\lambda_2 J} + n(n-1)(\delta_{2J})^{\frac{2}{n}}}$$

$$\leq \quad E(P_D^{\lambda_2 J}(\zeta) \leq \sqrt{n\left(\sum_{i=1}^{n}(P_{ii}^{\lambda_2 J})^2 + 2\sum_{1\le i<j\le n} P_{ij}^{\lambda_2 J} P_{ji}^{\lambda_2 J}\right)}$$

$$3.\ \sqrt{\sum_{i=1}^{n}(P_{ii}^{\lambda_3 J})^2 + 2\sum_{1\le i<j\le n} P_{ij}^{\lambda_3 J} P_{ji}^{\lambda_3 J} + n(n-1)(\delta_{3J})^{\frac{2}{n}}}$$

$$\leq \quad E(P_D^{\lambda_3 J}(\zeta) \leq \sqrt{n\left(\sum_{i=1}^{n}(P_{ii}^{\lambda_3 J})^2 + 2\sum_{1\le i<j\le n} P_{ij}^{\lambda_3 J} P_{ji}^{\lambda_3 J}\right)}$$

Theorem 3.11. Let $A\zeta = (A\lambda_1, A\lambda_2, \ldots, A\lambda_k)$ be the adjacency matrix of ζ. Let $\zeta = (\mu, \lambda_1, \lambda_2, \ldots, \lambda_k)$ be a λ_J-dominating SVNGS and $A_{D_J}(\zeta)$ be a λ_J-dominating SVNGS adjacency matrix of ζ. Then

1. $(E_D^{\lambda_1 J}(\zeta))^2 \leq n\left(\sum_{i=1}^{n}(P_{ii}^{\lambda_1 J})^2 + (E(P_D^{\lambda_1 J})(\zeta))^2\right)$,

2. $\left(E_D^{\lambda_{2J}}(\zeta)\right) \leq \left(\sum_{i=1}^{n}(P_{ii}^{\lambda_{2J}})^2 + (E(P_D^{\lambda_{2J}})(\zeta))^2\right)$,

3. $(E_D^{\lambda_{2J}}(\zeta)) \leq n\left(\sum_{i=1}^{n}(P_{ii}^{\lambda_{2J}})^2 + (E(P_D^{\lambda_{2J}})(\zeta))^2\right)$, $\forall\, J = 1,2,\ldots,k$.

Proof. 1. $(E\left(P_D^{\lambda_{1J}}\right)(\zeta))^2 \geq 2\sum_{1\leq i<j\leq n} P_{ij}^{\lambda_{1J}}\, P_{ji}^{\lambda_{1J}} + n(n-1)(\delta_{1J})^{\frac{2}{n}}$

$$\geq 2\sum_{1\leq i<j\leq n} P_{ij}^{\lambda_{1J}}\, P_{ji}^{\lambda_{1J}}$$

$i.e\ 2\sum_{1\leq i<j\leq n} P_{ij}^{\lambda_{1J}}\, P_{ji}^{\lambda_{1J}} \leq (E(P_D^{\lambda_{1J}})(\zeta))^2$ (1)

Now,

$$(E_D^{\lambda_{1J}}(\zeta))^2 \leq n\left(\sum_{i=1}^{n}(P_{ii}^{\lambda_{1J}})^2 + 2\sum_{1\leq i<j\leq n} P_{ij}^{\lambda_{1J}}\, P_{ji}^{\lambda_{1J}}\right)$$

$$(E_D^{\lambda_{1J}}(\zeta))^2 \leq n\left(\sum_{i=1}^{n}(P_{ii}^{\lambda_{1J}})^2 + (E(P_D^{\lambda_{1J}})(\zeta))^2\right) \text{ by eq-(1)}$$

Analogously, we can show that

$$(E_D^{\lambda_{2J}}(\zeta)) \leq n\left(\sum_{i=1}^{n}(P_{ii}^{\lambda_{2J}})^2 + (E(P_D^{\lambda_{2J}})(\zeta))^2\right)$$

$$(E_D^{\lambda_{3J}}(\zeta)) \leq n\left(\sum_{i=1}^{n}(P_{ii}^{\lambda_{3J}})^2 + (E(P_D^{\lambda_{3J}})(\zeta))^2\right),\ \forall\, J = 1,2,\ldots,k.$$

Definition 3.12. Let $\zeta = \{\mu, \lambda_1, \lambda_2, \ldots, \lambda_k\}$ be a λ_J-dominating SVNGS of GS $\zeta^* = (Q, R_1, R_2, \ldots, R_k)$ is isomorphic to λ_J-dominating SVNGS $\zeta_S = \{\mu', \lambda_1', \lambda_2', \ldots, \lambda_k'\}$ of GS $\zeta_S^* = \{Q', R_1', R_2', \ldots, R_k'\}$ if we have (f, Ψ) where $f: Q \to Q'$ is bijection and Ψ is a permutation on set $\{1,2,\ldots,k\}$ and following relation are satisfied
$\mu_1(u) = \mu_1'(f(u))$, $\mu_2(u) = \mu_2'(f(u))$ and $\mu_3(u) = \mu_3'(f(u))$ for all $u \in N$ and $\lambda_{1J}(uv) = \lambda_{1\Psi(J)}'(f(u)f(v)), \lambda_{2J}(uv) = \lambda_{2\Psi(J)}'(f(u)f(v))$ and $\lambda_{3J}(uv) = \lambda_{3\Psi(J)}'(f(u)f(v))$ for all $(u,v) \in R_J$, $J = 1,2,\ldots,k$.

Remark 3.13.] If two adjacency matrices of λ_J-dominating SVNGS are $A(\zeta_1) = \{A\lambda_1, A\lambda_2, \ldots, A\lambda_k\}$ and $A(\zeta_2) = \{A\lambda_1', A\lambda_2', \ldots, A\lambda_k'\}$, they are isomorphic if

1. $\sum_{i=1}^{n} Ad_{\lambda_{1J}}(u_i) = \sum_{i=1}^{n} Ad_{\lambda_{1J}'}(f(u_i))$, $\sum_{i=1}^{n} Ad_{\lambda_{2J}}(u_i) = \sum_{i=1}^{n} Ad_{\lambda_{2J}'}(f(u_i))$

$$\sum_{i=1}^{n} Ad_{\lambda_{3J}}(u_i) = \sum_{i=1}^{n} Ad_{\lambda'_{3J}}(f(u_i)), \forall J = 1,2,\ldots,k.$$

2. The energy of SVNGS $\zeta_1 = \{\mu, \lambda_1, \lambda_2, \ldots, \lambda_k\}$ is equal to the energy of SVNGS $\zeta_1 = \{\mu', \lambda'_1, \lambda'_2, \ldots, \lambda'_k\}$.

$$i.e \quad \epsilon(\zeta_1) = \epsilon(\zeta_2)$$

$$< \epsilon(\lambda_1), \epsilon(\lambda_2), \ldots, \epsilon(\lambda_k) >=< \epsilon(\lambda'_1), \epsilon(\lambda'_2), \ldots, \epsilon(\lambda'_k) >$$

Example 3.14. The adjacency matrix $A(\zeta) = \{A\lambda_1, A\lambda_2\}$ of λ_J-dominating SVNGS $\zeta = \{\mu, \lambda_1, \lambda_2\}$ is isomorphic to the adjacency matrix $A(\zeta_2) = \{A\lambda'_1, A\lambda'_2\}$ of λ_J-dominating SVNGS $\zeta_2 = \{\mu', \lambda'_1, \lambda'_2\}$ as shown in Figure 2 and Figure 3 under (f, Ψ) where $f: Q \to Q'$ is a bijection and Ψ is a permutation on set $\{1,2\}$ defined as $\Psi(1) = 2, \Psi(2) = 1$ and following relations are satisfied, by above Definition-[d8], Remark-[r1]. Such that $\mu = \{u_4(0.3,0.5,0.4), u_3(0.6,0.4,0.5), u_2(0.5,0.4,0.6), u_1(0.6,0.4,0.3)\}$ As shown in Figure 3, we can easy to verify

$$\sum_{i=1}^{4} Ad_{\lambda_{1J}}(u_i) = \sum_{i=1}^{4} Ad_{\lambda'_{1J}}(f(u_i)), \sum_{i=1}^{4} Ad_{\lambda_{2J}}(u_i) = \sum_{i=1}^{4} Ad_{\lambda'_{2J}}(f(u_i)),$$

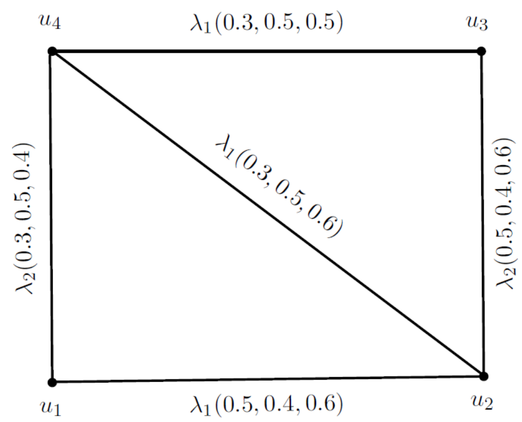

Figure 2

$$\sum_{i=1}^{4} Ad_{\lambda_{3J}}(u_i) = \sum_{i=1}^{4} Ad_{\lambda'_{3J}}(f(u_i)), \forall J = 1,2.$$

The $D_J = \{u_1, u_3\}$ is a λ_J-dominating SVNGS ζ is equal to the $D'_J = \{u_1, u_3\}$ is a λ_J-dominating SVNGS ζ_2 for all $J = 1,2$. The energy of λ_J-dominating SVNGS ζ is equal to the energy of λ_J-dominating SVNGS ζ_2 for all $J = 1,2$.

$$\epsilon(\zeta) = \epsilon(\zeta_2)$$

$$< \epsilon(\lambda_1), \epsilon(\lambda_2) >=< \epsilon(\lambda'_1), \epsilon(\lambda'_2) >$$

Definition 3.15. Let $\zeta = \{\mu, \lambda_1, \lambda_2, \ldots, \lambda_k\}$ be a λ_J-dominating SVNGS of GS $\zeta^* = \{Q, R_1, R_2, \ldots, R_k\}$ is identical to SVNGS $\zeta_S = \{\mu', \lambda'_1, \lambda'_2, \ldots, \lambda'_k\}$ of GS $\zeta_S^* = \{Q', R'_1, R'_2, \ldots, R'_k\}$ is a bijection and the following relations are satisfied.

$\mu_1(u) = \mu'_1(f(u))$, $\mu_2(u) = \mu'_2(f(u))$ and $\mu_3(u) = \mu'_3(f(u))\ \forall u \in Q$ and $\lambda_{1J}(uv) = \lambda'_{1J}(f(u)f(v))$, $\lambda_{2J}(uv) = \lambda'_{2J}(f(u)f(v))$, $\lambda_{3J}(uv) = \lambda'_{3J}(f(u)f(v))\ \forall\ (uv) \in R_J$, $J = 1,2, \ldots, k$.

Example 3.16. Let $\zeta = \{\mu, \lambda_1, \lambda_2\}$ and $\zeta_S = \{\mu', \lambda'_1, \lambda'_2\}$ be a two λ_J-dominating SVNGS of GS $\zeta^* = \{Q, R_1, R_2\}$ and $\zeta_S^* = \{Q', R'_1, R'_2\}$ respectively, as shown in Figure 4. SVNGS of GS ζ^* is identical to ζ_S^* under $f: Q \to Q'$ define as

$f(u_1) = v_3$, $f(u_2) = v_4$, $f(u_3) = v_1$, $f(u_4) = v_2$ and $\mu_1(u_i) = \mu'_1(f(u_i)), \forall\ u_i \in Q$ and $\lambda_{1J}(u_i v_j) = \lambda'_{1J}(f(u_i)f(v_j)), \lambda_{2J}(u_i v_j) = \lambda'_{3J}(f(u_i)f(v_j))$ and $\lambda_{3J}(u_i v_j) = \lambda'_{3J}(f(u_i)f(v_j))$, for all $(u_i v_j) \in R_J$ and $J = 1,2$.

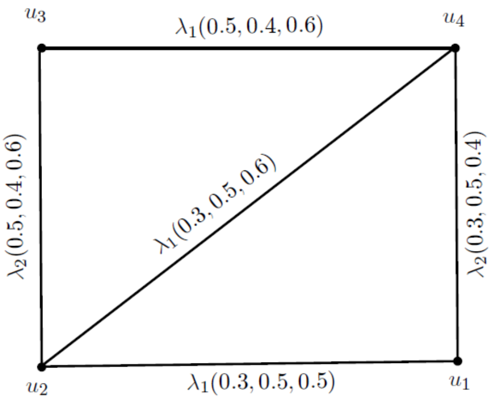

Figure 3

Hence, ζ^* is identical to ζ_S^*

Remark 3.17. If two adjacency matrices of λ_J- dominating SVNGS are $A(\zeta_1) = \{A\lambda_1, A\lambda_2, \ldots, A\lambda_k\}$ and $A(\zeta_S) = \{A\lambda'_1, A\lambda'_2, \ldots, A\lambda'_k\}$. then ζ^* is identical to ζ_S^* which is satisfied 1 to 3 condition in remark-3.13.

Theorem 3.18 Let $\zeta = \{\mu, \lambda_1, \lambda_2, \ldots, \lambda_k\}$ and $\zeta_S = \{\mu', \lambda'_1, \lambda'_2, \ldots, \lambda'_k\}$ be two σ_J-dominating SVNGS of GS $\zeta^* = \{Q, R_1, R_2, \ldots, R_k\}$ and $\zeta_S^* = \{Q', R'_1, R'_2, \ldots, R'_k\}$. Then ζ is identical to ζ_S under $f: Q \to Q'$.

Proof. Let $\zeta = \{\mu, \lambda_1, \lambda_2, \ldots, \lambda_k\}$ and $\zeta_S = \{\mu', \lambda'_1, \lambda'_2, \ldots, \lambda'_k\}$ be two σ_J-dominating SVNGS of GS $\zeta^* = \{Q, R_1, R_2, \ldots, R_k\}$ and $\zeta_S^* = \{Q', R'_1, R'_2, \ldots, R'_k\}$.

$$\lambda_{1J}(u_i v_j) = \min\{\mu_1(u_i), \mu_1(u_j)\} = \min\left\{\mu'_1\left(f(u_j)\right), \mu'_1(f(u_i))\right\} = \mu'_1(f(u_j)f(u_i))$$

Therefore, $\lambda_{1J}(u_i v_j) = \mu'_1(f(u_j)f(u_i))$

Similarly, we derive the equation $\lambda_{2J}(u_i v_j) = \mu'_2\left(f(u_j)f(u_i)\right), \lambda_{3J}(u_i v_j) = \mu'_3(f(u_j)f(u_i))$, $\forall J = 1,2, \ldots, k$.

Hence, ζ is identical to ζ_S under $f: Q \to Q'$.

3.1 Flow chart for Computing the Energy of λ_J-dominating SVNGS

The proposed flowchart in Figure 5, for calculating the energy of λ_J-dominating SVNGS are presented in this section. Using the energy of λ_J-dominating nodes, a flowchart is used to identify the greatest accessible λ_J-relation nodes in an SVNGS.

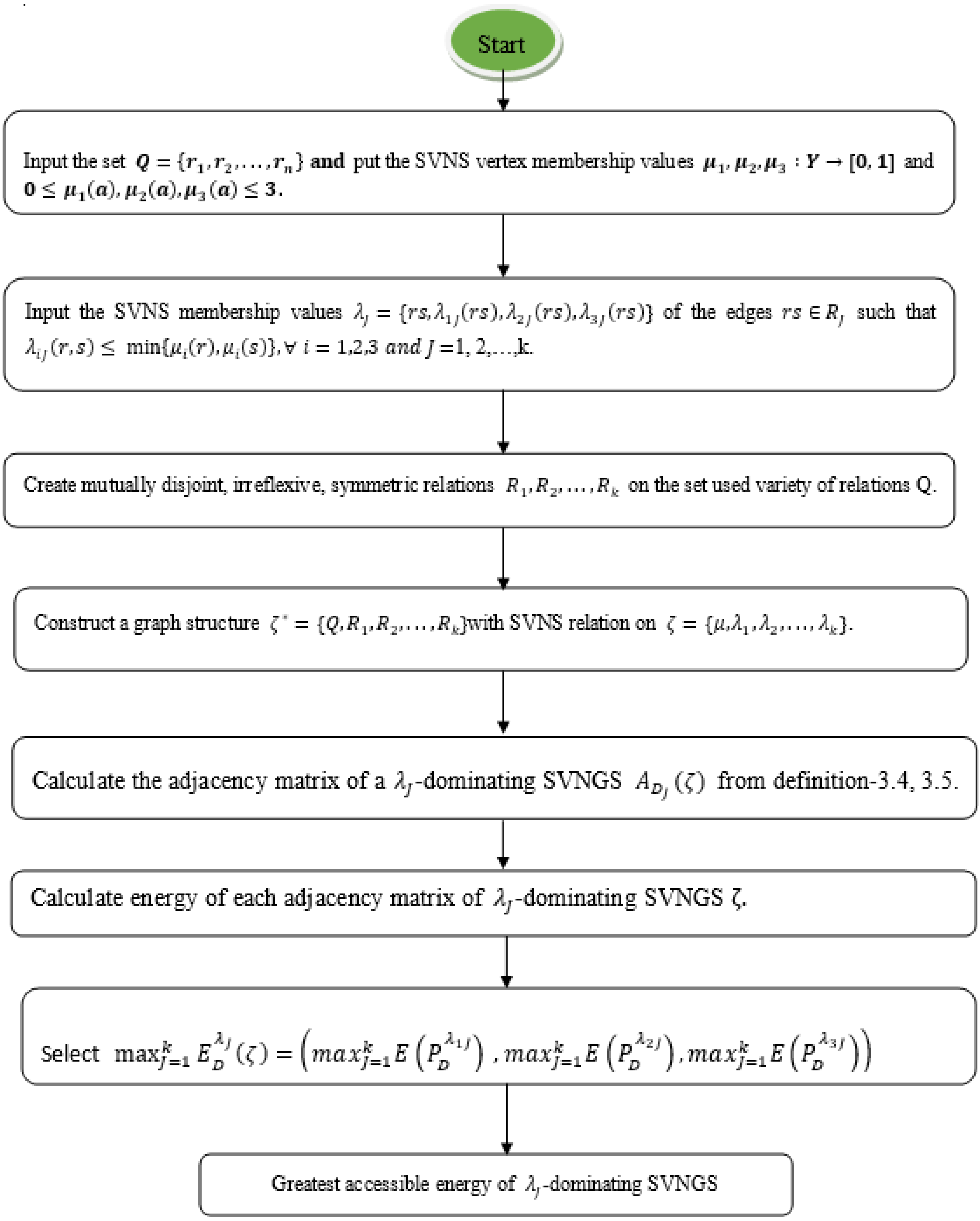

Figure 5. Flow chart for computing the energy of λ_J-dominating SVNGS.

4. Discussion

The concept of Generalized GSs was first proposed by E. Sampathkumar [40], and Generalized FGSs were then proposed by T. Dinesh et al. [41]. Recently, Akram [43] developed the SVNGS concept. S. Mathew [32] introduced the idea of an FG's energy, and Mullai, M., and Broumi, S. (2020) introduced the idea of Dominating Energy in NGs. But, when a SVNGS comes in a real-life situation, it is very necessary to know about the SVNGS with its energy of λ_J-dominating. The results of this research may reveal its applications in many ways, especially in finding optimal functions. Its manifestations can be found in our flowchart section. The studies presented so far have only addressed fuzzy with graph energy and graph dominating energy; we now find results for SVN with graph structures energy of λ_J-dominating, isomorphic, and identical as an improvement, which makes their expression even more flexible in many applications.

5. Advantages and Limitations

The main advantages of the proposed method are as follows:

- Its advantage is that it allows us to detect a specific relationship between the SVNGS and its energy of λ_J-dominating. It means $E_D^{\lambda_J}(\zeta) = (E(P_D^{\lambda_{1J}}), E(P_D^{\lambda_{2J}}), E(P_D^{\lambda_{3J}}))$ for all J=1,2,…,k. This can be calculated by the energy of λ_J-dominating SVNGS ζ.
- Also in this study, we have found some properties of isomorphic and identical energy of λ_J-dominating for specific relationship and their advantages.

Some of the work limitations are as follows:

- The energy of λ_J-dominating SVNGS was the main goal of the investigation and related network systems.
- This approach is only applicable to the SVNGS in an environment of symmetric, irreflexive, and mutually disjoint relations.
- There is no significance to the SVNGS concept if the characters' membership values are given in disparate environments.
- It may not always be possible to get trustworthy results.

6. Conclusion and Future Works

The concept of λ_J-dominating SVNGS energy is elaborated by the authors in this study. Beyond conventional fuzzy graph energy and dominating properties, the concept of λ_J-dominating SVNGS energy offers even more flexibility in describing uncertainty. It is an extension of fuzzy graph energy and dominating fuzzy graph energy. It also provides definitions that are important for comprehending the main results. Further, the energy of λ_J-dominating SVNGS was also investigated, along with some of its properties and bounds. We also present the notion of isomorphic and identical λ_J-dominating SVNGS. There are many different directions that future research in this field could go if the adjacency matrix SVNGS is used. Utilizing SVNGS, determine the properties of the edge regular, connectivity index, and Wiener index. Further research is suggested in the following areas, which we intend to expand on: complex bipolar neutrosophic graph structures; complex q-rung orthopair fuzzy graph structures; and complex interval-valued spherical fuzzy graph structures.

Acknowledgments
The author is grateful to the editorial and reviewers, as well as the correspondent author, who offered assistance in the form of advice, assessment, and checking during the study period.

Author Contributions

All authors contributed equally to this research.

Data availability

The datasets generated during and/or analyzed during the current study are not publicly available due to the privacy-preserving nature of the data but are available from the corresponding author upon reasonable request.

Funding

This research was not supported by any funding agency or institute.

Conflict of interest

The authors declare that there is no conflict of interest in the research.

References

1. Gutman, I. (1978). The energy of a graph. Ber. Math. Stat. Sekt. Forsch. Graz. 103, 1–22.
2. Ivan Gutman, Bo Zhou,. (2006). Laplacian energy of a graph. Linear Algebra and its Applications. Volume 414, Issue 1, Pages 29-37, https://doi.org/10.1016/j.laa.2005.09.008.
3. Kinkar, C. D., Abdullah A., Milica, A. (2020). On energy and Laplacian energy of chain graphs. Discrete Applied Mathematics. Volume 284, 30, Pages 391-400. https://doi.org/10.1016/j.dam.2020.03.057.
4. Milica, A., Tamara, K., & Zoran, S. (2022). Signed graphs whose all Laplacian eigenvalues are main Linear and Multilinear Algebra. Volume 71, Issue 15 .https://doi.org/10.1080/03081087.2022.2105288.
5. Bilal, A. R., Hilal, A. G., Kinkar, C. D. (2024). The General Extended Adjacency Eigenvalues of Chain Graphs. Mathematics. 12(2), 192. https://doi.org/10.3390/math12020192.
6. Amir, H. G., Mohammad, A. H. (2024). Signless Laplacian spectrum of a graph. Linear Algebra and its Applications. Volume 682, 1, Pages 257-267. https://doi.org/10.1016/j.laa.2023.11.007.
7. Zadeh, L. A. (1965). Fuzzy sets. Inf. Control, 8: 338-353. https://doi.org/10.1016/S0019-9958(65)90241-X.
8. Atanassov, K.T. (1986). Intuitionistic fuzzy sets. Fuzzy Sets & Syst, 20(1), 87-96: https://doi.org/10.1016/S0165-0114(86)80034-3.
9. Yager, R.R. (1988) On ordered weighted averaging aggregation operators in multicriteria decisionmaking, IEEE Transactions on Systems, Man and Cybernetics, 18, 183-190. https://doi.org/10.1109/21.87068.
10. Z. Xu. (2007). Intuitionistic fuzzy aggregation operators, IEEE Trans. Fuzzy Syst. 15 (6) 1179–1187. DOI: 10.1109/TFUZZ.2006.890678.
11. F. Smarandache. Neutrosophic Graphs. in his book Symbolic Neutrosophic Theory, Europa, Nova
12. F. Smarandache. (2005). Neutrosophic set, a generalisation of the intuitionistic fuzzy sets. Inter. J.Pure Appl. Math. 24, 287-297.
13. F. Smarandache. (1999). A Unifying Field in Logics. Neutrosophy: Neutrosophic Probability. Set and Logic. Rehoboth: American Research Press.
14. F. Smarandache. Neutrosophy, Neutrosophic Probability, Set, and Logic. Amer. Res. Press, Rehoboth, USA, 105 pages, 1998; http://fs.gallup.unm.edu/eBookneutrosophics4.pdf(4th edition).
15. Xindong Peng, Jingguo Dai. (2018). A bibliometric analysis of neutrosophic set: two decadesreview from 1998 to 2017. Artificial Intelligence Review. https://doi.org/10.1007/s10462-018-9652-0.
16. A. Rosenfeld. (1975). Fuzzy graphs, L.A. Zadeh, K.S. Fu, M. Shimura (Eds.), Fuzzy Sets and their Applications. Academic Press, New York. pp.77-95.
17. Bhattacharya, P. (1987). Some remarks on fuzzy graphs, \em Pattern Recognition Letters. Volume 6, Issue 5, Pages 297-302. https://doi.org/10.1016/0167-8655(87)90012-2.
18. John N. Mordeson , Sunil Mathew, Davender S. Malik. Fuzzy Graph Theory with Applications to Human Trafficking. Studies in Fuzziness and Soft Computing Book 365.
19. Islam, S. R., M. Pal. (2023). Hyper-Connectivity Index for Fuzzy Graph with application. TWMS J. App. and Eng. Math. V.13, N.3, pp. 920-936.
20. Islam, S. R., M. Pal. (2021) Hyper-Wiener index for fuzzy graph and its application in share market. Journal of Intelligent & Fuzzy Systems, vol. 41, no. 1, pp. 2073-2083. DOI: 10.3233/JIFS-210736.
21. A. Somasundaram. (1998). Domination in fuzzy graphs – I. Pattern Recognition Letters. Volume 19, Issue 9, Pages 787-791. https://doi.org/10.1016/S0167-8655(98)00064-6.

22. A. Somasundaram. (2005). Domination in products of fuzzy graphs. International Journal of Uncertainty, Fuzziness and Knowledge-Based Systems. Vol. 13, No. 02, pp. 195-204. https://doi.org/10.1142/S0218488505003394.
23. rfan, N.,Tabasam, R., & Juan, L. G. G.(2021). Domination of Fuzzy Incidence Graphs with the Algorithm and Application for the Selection of a Medical Lab. Hindawi Mathematical Problems in Engineering. 2021, Article ID 6682502, 11 pageshttps://doi.org/10.1155/2021/6682502.
24. Gong, S., Hua, G. & Gao, W. (2021). Domination of Bipolar Fuzzy Graphs in Various Settings. Int J Comput Intell Syst 14, 162. https://doi.org/10.1007/s44196-021-00011-2.
25. Afsharmanesh, S., Borzooei, R.A. (2021). Domination in fuzzy incidence graphs based on valid edges. J. Appl. Math. Comput. https://doi.org/10.1007/s12190-021-01510-3.
26. Bera, S., Pal, M. (2022). A novel concept of domination in m-polar interval-valued fuzzy graph and its application. Neural Comput & Applic 34, 745–756. https://doi.org/10.1007/s00521-021-06405-9.
27. Amita Samanta Adhya, Sukumar Mondal, and Sambhu Charan Barman. (2024). Edge-vertex domination on interval graphs. Discrete Mathematics, Algorithms and Applications. Vol. 16, No. 02, 2350015. https://doi.org/10.1142/S1793830923500155.
28. Peng, Z., Abbaszadeh Sori, A., Nikbakht, M. et al. (2023). Computing constrained shortest path in a network with mixed fuzzy arc weights applied in wireless sensor networks. Soft Comput. https://doi.org/10.1007/s00500-023-09259-6.
29. Soumitra Poulik, Ganesh Ghorai. (2022). Applications of graph's complete degree with bipolar fuzzy information. Complex and Intelligent Systems. 8:1115–1127. https://doi.org/10.1007/s40747-021-00580-x.
30. Soumitra Poulik, Ganesh Ghorai. (2022). Estimation of most effected cycles and busiest network route based on complexity function of graph in fuzzy environment. Artificial Intelligence Review. 55:4557–4574. DOI: 10.1007/s10462-021-10111-2.
31. Soumitra Poulik, Ganesh Ghorai. (2022). Connectivity Concepts in Bipolar Fuzzy Incidence Graphs. Thai Journal of Mathematics. Volume 20 Number 4 Pages 1609–1619.
32. S. Mathew. (2013). Energy of a fuzzy graph. Annals of fuzzy mathematics and Informatics. 6(3), pp. 455–465.
33. Shabaf, S.R, Fayazi, F. (2014). Laplacian Energy of a Fuzzy Graph. Iran. J. Math. Chem. doi:2014, 5, 1–10. 10.22052/IJMC.2014.5214.
34. Akram, M., and Sumera N. (2018). Energy of Pythagorean Fuzzy Graphs with Applications. Mathematics. 6, 136; doi:10.3390/math6080136.
35. Akram, M., Sarwar, M., Dudek, W.A. (2021). Energy of Bipolar Fuzzy Graphs. In: Graphs for the Analysis of Bipolar Fuzzy Information. Studies in Fuzziness and Soft Computing. vol 401. https://doi.org/10.1007/978-981-15-8756-6_8.
36. Akram, M., Saleem, D. and Davvaz, B. (2019). Energy of double dominating bipolar fuzzy graphs. J. Appl. Math. Comput. 61, 219–234. %https://doi.org/10.1007/s12190-019-01248-z.
37. Mullai, M., Broumi, S. (2020). Dominating Energy in Neutrosophic graphs. International Journal of Neutrosophic Science. 2020 Vol. 5, No.1, PP. 38-58. DOI: 10.5281/zenodo.3789020.
38. Mohamad, S.N.F.; Hasni, R.; Smarandache, F.; Yusoff, B. (2021). Novel Concept of Energy in Bipolar Single-Valued Neutrosophic Graphs with Applications. Axioms. 10, 172. https://doi.org/10.3390/axioms10030172.
39. Mohamad, S.N.F., Hasni, R., Yusoff, B. (2023). On Dominating Energy in Bipolar Single-Valued Neutrosophic Graph. Neutrosophic Sets and Systems. Vol. 56. %https://digitalrepository.unm.edu/nss_journal/vol56/iss1/10.
40. E. Sampathkumar. (2006). Generalized graph structures. Bulletin of Kerala Mathematics Association. vol. 3, no. 2, pp. 65-123.
41. T.Dinesh, T.V.Ramakrishnan. (2011). Generalised Fuzzy Graph Structures. Applied Mathematical Sciences. Vol. 5, no. 4, 173 -180.
42. Muhammad Akram and Rabia Akmal. (2016). operations on Intuitionistic Fuzzy Graph Structures. Fuzzy Inf.Eng. 8,389-410. https://doi.org/10.1016/j.fiae.2017.01.001.
43. Muhammad Akram, Muzzamal Sitara. (2017). Single-Valued Neutrosophic Graph Structures, Applied Mathematics E-Notes. 17, 277-296.

44. Bathusha, S. N. S., Kavitha Raj, A. S. (2023). Climatic Analysis Based on Interval-Valued Complex Pythagorean Fuzzy Graph Structure. Annals of Mathematics and Computer Science. ISSN: 2789-7206 Vol 19, 10-33. https://doi.org/10.56947/amcs.v19.213.
45. Bathusha, S. N. S., Sowndharya, J., Kavitha Raj, A. S. (2024). The Energy of Interval-Valued Complex Neutrosophic Graph Structures: Framework, Application and Future Research Directions. Neutrosophic Systems with Applications. (2024), Vol. 13. https://doi.org/10.61356/j.nswa.2024.106.

Received: 28 Dec 2023, **Revised:** 07 Mar 2024,

Accepted: 03 Apr 2024, **Available online:** 06 Apr 2024.

NEUTROSOPHIC
SYSTEMS WITH APPLICATIONS

AN INTERNATIONAL JOURNAL ON INFORMATICS, DECISION SCIENCE, INTELLIGENT SYSTEMS APPLICATIONS

Sciences Force
Five Greentree Centre, 525 Route 73 North, STE 104 Marlton, New Jersey 08053.
www.sciencesforce.com

ISSN (ONLINE): 2993-7159
ISSN (PRINT): 2993-7140